Gene flow and models of avian speciation in tropical mountains

Ethan Linck

A dissertation
submitted in partial fulfillment of the
requirements for the degree of

Doctor of Philosophy

University of Washington

2019

Reading Committee:

John Klicka, Chair

Lorenz Hauser

Richard G. Olmstead

Program Authorized to Offer Degree:
Biology

University of Washington

Abstract

Gene flow and models of avian speciation in tropical mountains

Ethan Linck

Chair of the Supervisory Committee:
Dr. John Klicka
Department of Biology

Eight decades after the modern synthesis, the role of gene flow in speciation remains contentious. Because gene flow is a homogenizing force and sister species frequently occur in allopatry, geographic isolation was assumed to be a requirement for the majority of speciation events for most of the 20th century. More recently novel theory, genome-wide DNA sequence data and computational tools have provided evidence to challenge this assumption, demonstrating speciation with gene flow is both plausible and more common than previously thought. These results have prompted a shift in emphasis from the geography of diverging populations to the interplay of underlying evolutionary mechanisms. Yet convincing empirical examples remain rare, and imprecise language blurs the distinction between classical models of sympatric or parapatric speciation and allopatric speciation followed by extensive secondary contact and hybridization. When and where—if ever—is speciation with gene flow likely to occur? What, exactly, does "speciation with gene flow" indicate about the constancy and timing of migration? Can our tools distinguish even distinguish among these parameters? Tropical mountains are the most species-rich terrestrial environment on earth, with significant geographic complexity and strong, temporally stable environmental gradients to generate selection. These features provide a powerful natural laboratory to address fundamental questions in speciation, but research effort has historically lagged behind studies of temperate regions due to obstacles of access and cost.

In this dissertation I use empirical data, theory, and evolutionary simulations to explore the role of gene flow during speciation events in tropical mountains. In Chapter 1, I validate a method for collecting genome-wide DNA sequence data from historical museum specimens and develop a bioinformatic pipeline to assemble loci and call variants. I apply this approach to degraded DNA from historical museum samples of a poorly known New Guinea kingfisher species, *Syma torotoro*, inferring population genetic structure in contiguous forest habitats. This methodology allows me to overcome logistical difficulties inherent to work in remote tropical environments to achieve appropriate sample sizes. In Chapter 2, I combine these data with additional samples from its montane sister species, *Syma megarhyncha*, and test a hypothesis of speciation with gene flow across an elevational gradient in *Syma*. I find evidence of assortative mating the face of extensive historical and contemporary gene flow, suggesting selection across mountainsides can maintain species limits in the face of incomplete reproductive isolation. In Chapter 3, I use theory and evolutionary simulations to explore the probability and genomic signature of speciation with alternating periods of isolation and gene flow. I find speciation with even brief lulls in gene flow is significantly easier than speciation with gene flow every generation and difficult to distinguish by standard methods. However, I also find periodic gene flow leaves a distinctive signature in common population genetic summary statistics, potentially a promising method for evaluating the timing of migration events in speciation genomic studies. Together, these results suggest gene flow likely plays an underappreciated role in avian speciation in tropical mountains, highlighting the need to encompass increased complexity in verbal and quantitative models.

TABLE OF CONTENTS

LIST OF FIGURES

ACKNOWLEDGMENTS

How can science at once be so isolating and so profoundly social? In no particular order, I wish the acknowledge the following friends, mentors, and colleagues who have shaped this dissertation. First, I owe a huge debt to the scientific community at University of Washington who made this such an enjoyable five years in Seattle. Many thanks to my advisor John Klicka, for allowing me to pursue a highly independent research project and introducing me to the importance and wonder of museum collections. To my labmates Dr. C.J. Battey, Cooper French, and Dave Slager, for good humor and a fridge stocked with Vitamin R. To Kevin Epperly, for patience, diligence and skill at most things I am bad at. To Dr. Rebecca Harris (and Shane, and Stringer), Ana Maria Bedoya, and the rest of the evolution-minded students and faculty in the Department of Biology. To Dr. Kameron Harris, for help with math. To my committee, for both freedom and gentle skepticism when necessary.

Thanks are also due to the many collaborators and mentors outside of University of Washington who have shaped my career as a scientist. To Drs. Haldre Rogers and Kimberly Sheldon, for opening the door to research and providing my initial training as a tropical ecologist. (Maybe I still qualify as one, on a good day.) To Dr. Jack Dumbacher, for 7 years of opportunities, mentorship, and a shared joy of all things New Guinea. To. Dr. Sarah Schaack, with admiration. To Drs. Bob Kaplan and Keith Karoly—I miss Reed! And to Matt Chmielewski, for the shared misery and a couch in Portland.

This work would have been impossible to complete without outside funding. For grants in support of research expenses, I thank the Society of Systematic Biologists, the American Museum of Natural History, the National Science Foundation, and the Washington Research Foundation, John S. Edwards Endowed Fund in Biology, and Hoag Endowed Graduate Fel-

lowship. For supporting my stipend, I thank the National Defense Science and Engineering Graduate Fellowship and the Washington Research Foundation.

The road to a completed dissertation is rarely linear, and only a portion of the many projects I embarked on during graduate school (some ill-advised) appear within this document. In particular, I wish to acknowledge those who helped me with two seasons of fieldwork in New Guinea–with significant detours to Fiji and Solomon Islands—characterized by setbacks and surreal beauty in equal measure. To Dr. Elisabeth Holland, for endless generosity and rent-free accommodation for the longest 6 weeks I ever hope to spend in Suva. To Chris Filardi and David Boseto, for a very memorable trip to Guadalcanal and Western Province. To Nathan Whitmore, for significant help with logistics in Eastern Highlands and Chimbu and the best evening of company and whiskey I can imagine having in Goroka. To Toppy and Tresa Sundu, and the rest of Womkama; Kate and I will always remember our time in your magical village. To Drs. Francesca Dem and Vojtech Novotny, Salape Tulai, and Bulisa Iova; I hope to make it back to the Binatang Research Center in the future. To Stanley Jacob: we've been wantoks for over a decade now, and I don't see that changing soon.

No one has ever accused me of spending too much time indoors, and I wish to also acknowledge the landscapes of the Pacific Northwest and the many friends I've spent time in them with. To the Burke Gilman Trail, and to Snoqualmie Pass, for endless hours of asphalt and snow of wildly variable quality. To the North Cascades, ever beyond comprehension. To Jake Douglas, Erik Turner, Todd Kilcup, and Allen Taylor, for living that pass life. To Luke Distelhorst, Dave Swoish, Richard Kresser, Kevin Smythe, Greg Hanscom, and the rest of the group chat. And especially to Dr. Patrick Fink and Peter Innes, partners across time and space. I think we may be growing up

Finally, I wish to acknowledge the long-term support of my parents, who nurtured a love of nature and tolerated a concerning level of academic absent-mindedness in me as a child. I also express love and gratitude beyond measure to my wife, Kate Schimel, who gets it.

DEDICATION

This dissertation is dedicated to the memory of Shimona Najo Amet Anonga of Tamigidu Village, Nawaib District, Morobe.

Chapter 1

EVALUATING HYBRIDIZATION CAPTURE WITH RAD PROBES AS A TOOL FOR MUSEUM GENOMICS WITH HISTORICAL BIRD SPECIMENS

*Zachary R. Hanna, Anna Sellas, and John P. Dumbacher were coauthors on the version of this manuscript published in *Ecology and Evolution*: https://dx.doi.org/10.1002/ece3.3065

1.1 Abstract

Laboratory techniques for high-throughput sequencing have enhanced our ability to generate DNA sequence data from millions of natural history specimens collected prior to the molecular era, but remain poorly tested at shallower evolutionary time scales. Hybridization capture using restriction site-associated DNA probes (hyRAD) is a recently developed method for population genomics with museum specimens. The hyRAD method employs fragments produced in a restriction site-associated double digestion as the basis for probes that capture orthologous loci in samples of interest. While promising in that it does not require a reference genome, hyRAD has yet to be applied across study systems in independent laboratories. Here, we provide an independent assessment of the effectiveness of hyRAD on both fresh avian tissue and dried tissue from museum specimens up to 140 years old and investigate how variable quantities of input DNA affect sequencing, assembly, and population genetic inference. We present a modified bench protocol and bioinformatics pipeline, including three steps for detection and removal of microbial and mitochondrial DNA contaminants. We confirm that hyRAD is an effective tool for sampling thousands of orthologous SNPs from historic museum specimens to describe phylogeographic patterns. We find that modern DNA performs significantly better than historical DNA better during sequencing but that assembly performance is largely equivalent. We also find that the quantity of input DNA predicts %GC content of assembled contiguous sequences, suggesting PCR bias. We caution against sampling schemes that include taxonomic or geographic autocorrelation across modern and historic samples.

1.2 Introduction

Over the past three decades, novel laboratory techniques have enhanced our ability to generate DNA sequence data from millions of natural history specimens collected prior to the molecular era (Payne and Sorenson, 2002). The advent of ancient DNA methods has allowed researchers to obtain both nuclear and mitochondrial DNA (mtDNA) sequences from extinct taxa (Cooper et al., 1992; Fleischer et al., 2006), explore changes in genetic diversity and population genetic structure over time (Habel et al., 2014; Weber et al., 2000), incorporate threatened or difficult-to-collect taxa into population genetic or phylogenetic studies (Guschanski et al., 2013; Linck et al., 2016), and take advantage of extant biological collections to boost sample size and inferential power (Linck et al., 2016; Wójcik et al., 2010). Now, high-throughput sequencing has dramatically increased both the overall efficiency of data collection and the total amount of sequence data that it is possible to collect from museum specimens (Hofreiter et al., 2001; Rizzi et al., 2012) by overcoming scalability hurdles intrinsic to traditional Sanger sequencing methods (Soltis and Soltis, 1993; Wandeler et al., 2007).

Although high-throughput sequencing has already proved widely useful for incorporating museum specimens into phylogenomic studies (Besnard et al., 2016; Burbano et al., 2010; McCormack et al., 2012), its application for collecting genome-wide markers at the population level has lagged behind its use for addressing questions at deeper evolutionary time scales due to limitations in the most commonly employed library preparation methods for reduced-representation Illumina sequencing (Suchan et al., 2016). The limitations of historic museum samples include their high degree of fragmentation and low concentration of long DNA fragments, which reduces the amount of flanking sequence that can be captured using ultraconserved element probes (Faircloth et al., 2012) and lowers the likelihood that multiple restriction digest recognition sequences are retained in a given DNA fragment (Baird et al., 2008; Peterson et al., 2012). Only in the past few years have library preparation protocols suitable for population genomics become available (Bi et al., 2013; Jones and Good,

2016; McCormack et al., 2016), but their recent proliferation has meant that few have yet to be applied to multiple study systems in independent laboratories (McCormack et al., 2016). As a result, our understanding of the efficacy and biases of different approaches to reduced-representation genome sequencing from degraded DNA remains incomplete relative to either Sanger sequencing (Soltis and Soltis, 1993; Wandeler et al., 2007), or high-coverage, single-sample whole genome sequencing (Poinar et al., 2006).

One promising but under-tested approach to museum genomics suitable for population-level studies is hybridization capture of restriction site-associated DNA (RAD) probes (hyRAD) (Suchan et al., 2016). Briefly summarized, the hyRAD method uses fragments produced by a double digest RAD (ddRAD) protocol (Peterson et al., 2012; Suchan et al., 2016) as the basis for biotinylated probes that capture orthologous loci in other samples, allowing them to be enriched and indexed for pooled Illumina sequencing. Although the method requires a high molecular weight DNA sample to produce the probe set, hyRAD offers advantages over other targeted capture methods in requiring no prior knowledge of the organism's genome, such as transcriptome data or pre-existing sequences for probe design (Bi et al., 2013; McCormack et al., 2016). Additionally, because hyRAD relies on hybridization capture of orthologous regions across samples rather than retained restriction-site recognition sequences, the method mitigates the concerns of allelic dropout due to polymorphisms at restriction sites with increasing phylogenetic distance intrinsic to other RAD-based protocols (Gautier et al., 2013).

In their original paper, Suchan et al. (2016) validated their method by applying it to both fresh tissue and museum specimens of a butterfly (*Lycaena helle*) and grasshopper (*Oedaleus decorus*). They discussed the impact of library preparation, sample type, and bioinformatics pipeline on the number of SNPs produced. Here, we provide an independent assessment of the effectiveness of hyRAD using both fresh avian tissues and dried tissue taken from museum specimens up to 140 years old. We present a modified version of the hyRAD protocol aimed at increasing efficiency and minimizing reagent use and employ a custom bioinformatics pipeline with steps for detecting and removing microbial contamination in raw reads, contiguous

sequences, and SNPs. We utilize hyRAD data to describe phylogeographic patterns in a New Guinea forest kingfisher (*Syma torotoro*) and we expand the available description of hyRAD's performance by investigating how variable input DNA affects sequencing, assembly, and population genetic inferences.

1.3 Methods

1.3.1 Study species, sampling, and DNA extraction

A major promise of museum genomics is the ability to conduct population-level studies in regions that are too logistically difficult to be amenable to broad modern sampling programs. The island of New Guinea is an apt example of this scenario, with poorly known biodiversity, large historical collections, rugged terrain, and ongoing political instability (Mack and Dumbacher, 2007; Pratt and Beehler, 2015). Phylogeographic research in New Guinea has been limited (Deiner et al., 2011; Dumbacher and Fleischer, 2001), especially in the species inhabiting the island's ring of lowland tropical rainforest. To evaluate the efficacy of for use in a broader study of the phylogeography of lowland new Guinea, we sampled 21 individuals of forest interior resident *S. torotoro* (Yellow-billed Kingfisher), representing five named subspecies and the breadth of the species' range on the island of New Guinea (Table 1.1). For seven individuals, we extracted whole-genomic DNA from fresh tissue using a DNeasy tissue extraction kit (Qiagen, Valencia, CA, USA) following the manufacturer's protocol. For the remaining 14 individuals, we extracted DNA from the toepads of museum study skins in a dedicated ancient DNA laboratory at the California Academy of Sciences using a phenol-chloroform and centrifugal dialysis method described elsewhere (Dumbacher and Fleischer, 2001). No modern DNA or post-PCR products are handled in this laboratory, which is located on a separate floor from the main genetics facility.

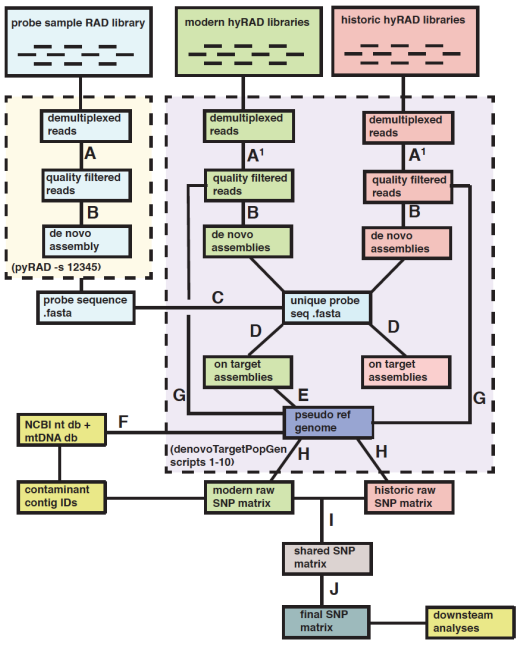

Figure 1.1: **Bioinformatics pipeline for *S. torotoro* hyRAD data.** We demultiplexed 100 bp paired-end reads from three genomic libraries and filtered for adapter contamination/quality scores (A), or adapter contamination/quality scores and *E. coli* contamination (A1). Reads were clustered (as consensus fasta files) (B), and repeat regions removed from probes (C). After determining which assembled clusters were orthologous with probe regions (D), we merged flanking regions from on-target loci in modern samples with the repeat-free probe sequence to create a pseudo-reference genome (E). To identify which contigs represented contamination in the original probe sample library from exogenous microbes or mitochondrial DNA, we BLAST searched against both the NCBI nt database and a full mitochondrial genome from *S. torotoro* relative *Halcyon sanctus* (F). We aligned quality filtered reads to this pseudo-reference (G), called SNPs to produce a raw.vcf file for historic and modern DNA libraries separately (H). After filtering SNPs for origin in contaminant contigs and then restricting our matrix to sites present in both sample types (I), we filtered SNPs by read depth, quality scores, probability of being variable sites, and minor allele frequencies (J) prior to downstream analyses.

Table 1.1: Sampling information, input DNA quantity, and sequencing and assembly performance statistics.

Specimen	Subspecies	Source	Locality	Date	# Cleaned Reads	% Duplicate Reads	Coverage (X)	Specificity	Enrichment (X)	Sensitivity	Loci	Mean locus length	# Long Contigs	DNA (ng/l)	%GC
KU:Birds:5215	*pseuestes*	Tissue	Ivimka Camp, Gulf Province, Papua New Guinea	2003	2,915,214	68.1	12.74	16.87	16.58	84.93	22,568	518	489	71.6	44.22
KU:Birds:5464	*pseuestes*	Tissue	Sapoa Camp, Gulf Province, Papua New Guinea	2003	2,512,928	68.2	11.2	16.65	16.36	79.43	19,880	499	340	51.8	44.69
KU:Birds:6927	meeki	Tissue	Mt. Suckling, Oro Province, Papua New Guinea	2011	3,103,912	73.2	14.46	17.37	17.07	85.02	23,162	510	494	37	44.53
KU:Birds:7131	*pseuestes*	Tissue	Dark End Camp, Gulf Province, Papua New Guinea	2002	1,154,541	60.4	5.87	17.29	16.99	65.44	12,725	434	157	31.8	45.01
CAS:ORN:626	*meeki*	Blood	Varirata National Park, Central Province, Papua New Guinea	2011	1,945,868	70.2	9.38	17.06	16.77	77.25	18,519	488	262	43	44.62
KU:Birds:9145	*torotoro*	Tissue	Gahom Camp, East Sepik Province, Papua New Guinea	2003	2,309,716	70.2	10.75	16.91	16.62	80.15	20,057	452	312	10.1	44.35
AMNH:Birds:637445	*torotoro*	Toe pad	Wasior, West Papua Province, Indonesia	1928	48,257	78.2	2.59	11.16	10.97	33.52	849	449	57	3.66	46.03
AMNH:Birds:329542	*ochracea*	Toe pad	Sewa Bay, Normanby Island, Papua New Guinea	1934	40,402	82.2	1.8	8.9	8.75	29.19	388	465	24	3.84	47.62
AMNH:Birds:637464	*tentelare*	Toe pad	Wannambai, Maluku Province, Indonesia	1896	139,248	59.9	9.2	11.07	10.88	50.24	3,197	449	154	10.2	44.98
AMNH:Birds:637450	*torotoro*	Toe pad	Humbolt Bay, Papua Province, Indonesia	1928	16,359	75.1	0.89	12.06	11.85	14.62	153	543	15	0.714	48.74
AMNH:Birds:637429	*torotoro*	Toe pad	Misool Island, West Papua Province, Indonesia	1900	35,925	79.8	2.13	9.46	9.30	30.09	412	448	26	2.54	46.44
AMNH:Birds:300723	*torotoro*	Toe pad	Waigeu Island, West Papua Province, Indonesia	1900	34,596	82.2	1.91	10.03	9.86	27.78	508	401	21	0.846	46.88
AMNH:Birds:637446	*torotoro*	Toe pad	Kepaur, West Papua Province, Indonesia	1897	36,627	84.1	2.15	8.02	7.88	23.19	177	600	22	1.07	48.18
NHMUK:ZOO: 1911.12.20.823	*pseuestes*	Toe pad	Mimika River, Papua Province, Indonesia	1913	19,115	50.9	1.55	10.85	10.66	20.44	239	611	40	1.49	47.28
NHMUK:ZOO: 1911.12.20.822	*pseuestes*	Toe pad	Satakwa River, Papua Province, Indonesia	1911	46,548	59.8	2.08	9.44	9.28	24.39	296	579	36	0.584	48.32
AMNH:Birds:437798	*torotoro*	Toe pad	Amberbaki, West Papua Province, Indonesia	1877	4,957	73.4	0.39	9.1	8.94	4.58	52	582	4	1.84	48.88
AMNH:Birds:637441	*torotoro*	Toe pad	Mt. Mori, West Papua Province, Indonesia	1899	19,623	76.9	1.3	9.5	9.34	21.38	157	512	11	7.36	47.89
AMNH:Birds:293741	*torotoro*	Toe pad	Ifaar, Papua Province, Indonesia	1928	49,786	91.1	2.14	12.48	12.27	23.84	493	447	28	0.124	50.41
AMNH:Birds:293715	*torotoro*	Toe pad	Kepaur, West Papua Province, Indonesia	1928	56,972	90.5	2.15	11.15	10.96	24.2	438	504	30	0.15	50.95

1.3.2 Library preparation, hybridization capture

We prepared samples for reduced-representation whole genome sequencing using a modified version (Hanna and Sellas, 2017) of Suchan et al.'s (2016) hyRAD method aimed at increasing efficiency of reactions and reducing reagent use. We present this protocol in a detailed bench-ready version online (`https://github.com/calacademy-research/hyRADccg`) and summarize it below.

To produce biotinylated probes, we performed a double restriction digest with enzymes MluCl and SphI (New England Biolabs) on 400 ng of high molecular weight DNA extracted from fresh tissue of a single *S. t. ochracea* individual. After ligation of adapters to fragments, we size-selected the resulting fragments on a Pippin Prep (Sage Science, Beverly, MA, USA) with a target peak at 270 bp and "tight" size selection range. We ran 16 cycles of real-time polymerase chain reaction (RT-PCR) and purified products by gel excision and a Zymoclean Gel Recovery Kit (Zymo Research). We preserved one aliquot of this product for sequencing while performing an additional MluCl/SphI double digest to remove adapters from a second aliquot. We labeled this deadapterized aliquot with biotin-14-dATP, using a BioNick DNA Labeling System (Thermofisher Scientific).

To produce whole genome libraries, we sheared high molecular weight DNA from modern tissue samples to 400 bp using a M-220 Focused-ultrasonicator (Covaris). DNA from museum specimen toepads was already fragmented as a product of natural degradation associated with the age of the samples and was therefore left untreated. For both modern and historic samples, we used a Kapa Hyper Prep Kit (Kapa Biosystems) to prepare dual-indexed libraries. We amplified libraries using 5-13 cycles of RT-PCR. After quantifying DNA content in each sample, we made standardized dilutions of each sample and combined equal amounts of these dilutions to create one pool of modern DNA samples (n=6) and two pools of ancient DNA samples (n=7 each). We used a 1-1.5x ratio of AmPure XP beads to remove small DNA fragments throughout the protocol and assessed DNA quantity and quality with a Qubit 2.0 fluorometer and an Agilent 2100 Bioanalyzer between all major

steps.

To perform hybridization capture reactions, we incubated each pool of samples with 250 ng of biotinylated probe for 72 hr at 55C in a solution containing 20x saline-sodium citrate (SSC), 50x Denhardt's Solution, 0.5 mol/L EDTA, 10% sodium dodecyl sulfate (SDS), and a blockers mix containing Chicken Hybloc (0.5 μg/μl), IDT's xGen Universal Blocking Oligo-TSHT-i5 (0.05 nmol/μl), and IDT's xGen Universal Blocking Oligo-TSHT-i7 (0.05 nmol/μl). Following hybridization, we prepared 50 l Dynabeads MyOne Streptavidin C1 beads for use by washing three times with 1x binding buffer containing 2 mol/L NaCl, 10 mmol/L Tris-HCl (pH 7.5), 0.5% Polysorbate 20 (Tween-20), and 1 mmol/L EDTA, and final resuspension in 70 μl 2x binding buffer. We then bound the probes to the beads by mixing and incubating at room temperature for 30 min. After performing three 500 μl washes of the bead-probe mixture using a prewarmed buffer containing 10% SDS with 0.1x SSC, we concentrated our final pooled libraries in 30 μl 10 mm Tris-HCl, 0.05% Tween-20 (pH 8-8.5). We next amplified these libraries using RT-PCR for 9-2 cycles, cleaned using 1.2x Ampure XP beads, and quantified using Qubit. We sent a single final pool with equimolar amounts of all three hybridized pools to University of California Bekeley's QB3 Vincent J. Coates Genomics Sequencing Laboratory (hereafter called "QB3") for sequencing with 100 bp paired-end sequence reads on a single lane of an Illumina HiSeq 4000.

1.3.3 Sequence read quality control, assembly, and alignment

To clean and quality filter reads, assemble reads into contigs, align sequences across samples, and map reads to merged alignments for SNP discovery, we used a custom pipeline combining in-house R scripts as well as pre-existing genomics tools and wrapper scripts from QB3's two de novo targeted capture bioinformatics pipelines (`https://github.com/CGRL-QB3-UCBerkeley`; "denovoTargetCapturePopGen" and "denovoTargetCapturePhylogenomics"). We present our full pipeline online as both a tutorial and a list of shell commands (`https://github.com/elinck/hyRAD/`) (Figure 1.1).

We first processed reads from our probe library with pyRAD version 2.17 (Eaton, 2014)

to create a pseudo-reference genome to use as the basis for aligning sequences from samples in our hybridization capture reactions. After quality filtering reads and trimming adapter contamination, pyRAD used the vsearch algorithm (Rognes et al., 2016) to cluster reads into loci within samples, cluster loci into stacks between samples, and aligned putatively orthologous loci using MUSCLE version 3.8 (Edgar, 2004). We implemented strict adapter filtering, retained reads longer than 70 bp after trimming, set a minimum sequence identity threshold of 97% for clustering, and kept four sites per cluster with a Phred Quality Score <20. (This strict identity threshold was selected to generate an estimate of the total number of fragments in our probe library.) We removed repetitive genomic regions and paralogs with the NCBI BLAST+ version 2.4 tool BLASTn (Boratyn et al., 2013) by aligning the output file of assembled clusters against itself and retained only cluster sequences that aligned uniquely to themselves using an *e*-value of 0.00001.

To remove reads that failed to pass Illumina quality control filters, trim reads for quality and adapter contamination, merge overlapping reads, remove PCR duplicates, and remove endogenous *E. coli* contamination, we used QB3's denovoTargetCapturePopGen "2-ScrubReads" wrapper around the Trimmomatic version 0.36 (Bolger et al., 2014), Bowtie 2 (Langmead, 2010), Cutadapt (Martin, 2011), Cope (Liu et al., 2012), FastQC (`http://www.bioinformatics.babraham.ac.uk/projects/fastqc/`), and FLASh (Mago and Salzberg, 2011) tools. We assembled cleaned and filtered reads for each sample using QB3's denovoTargetCapturePhylogenomics wrapper script "2-GenerateAssembliesPhylo" around the SPAdes version 3.8.1 genome assembler (Bankevich et al., 2012), which automatically selects a k-mer value based on read length and dataset type. To determine which contigs from our capture libraries were orthologous with probe regions, we used the denovoTargetCapturePopGen wrapper "5-FindingTargets" around the BLAST+ (Boratyn et al., 2013) and cd-hit-est (Fu et al., 2012) tools. Analyzing samples from modern and historical DNA separately, we used a clustering identity threshold of 95% and permitted 100 bp of sequencing flanking the core probe region. After determining matches, we collapsed overlapping, orthologous contigs from all modern samples with the probe library to generate

an extended pseudo-reference genome to which we aligned cleaned reads using QB3's denovoTargetCapturePopGen wrapper "7-Alignment" around the Novoalign version 3.04.06 tool (`http://www.novocraft.com/products/novoalign/`). We ran Novoalign with an average library insert size of 235 and a maximum alignment score of 90.

1.3.4 SNP discovery

Traditional SNP calling algorithms based on allele counting and quality scores are characterized by high degrees of uncertainty with low-coverage sequence data (Korneliussen et al., 2014). We incorporated uncertainty into genotype estimation by calling SNPs and estimating allele frequencies using an empirical Bayesian framework implemented in the software ANGSD version 0.913 (`http://www.popgen.dk/angsd/index.php/ANGSD`). ANGSD uses the likelihood of all 10 possible genotypic configurations for each site passing quality filters in all individuals to estimate a site frequency spectrum, which is then used as a prior to estimate the posterior probabilities for all possible allele frequencies at each site in each sample. Using these estimates, we called SNPs with a 95% probability of being variable and a minimum minor allele frequency of 5%.

1.3.5 Contamination control and data filtering

In order to identify if any contigs in our assemblies represented off-target mtDNA captures, we performed a BLAST+ (Boratyn et al., 2013) nucleotide search with each of our assemblies as a query against a database of the full mitochondrial genome of *S. torotoro* relative *Halcyon santcus*. We then removed all matching contigs from each sample's assembly fasta with in-house R scripts ("excerptcontigIDs.R" and "cutcontigsbatch.R") and used these mtDNA-free sequences for all subsequent assembly performance calculations. To prepare our sequence alignment in .sam/.bam format for SNP calling, we followed Bi et al. (2013) in hierarchically filtering out individuals, contigs, and sites that appeared to be quality outliers and implemented additional steps for regions derived from microbial contamination or mtDNA. We determined no individuals had abnormal coverage (defined as <1/3 or >3x the average

coverage across all individuals) and we created merged, sorted BAM files and generated raw variant call format files (.vcf) with samtools version 1.3 (Li et al., 2009) and bcftools version 1.3.1 (Narasimhan et al., 2016), processing modern and historical DNA samples separately.

Because our SNP matrix was derived independently from our assemblies, we performed a second step of contamination filtering by removing SNPs originating from read alignments to regions of exogenous microbial DNA and/or mtDNA present in the original probe sample RAD library. We used our full pseudo-reference genome as the query in a search of the entire BLAST+ (Boratyn et al., 2013) nucleotide database and our *H. sanctus* mtDNA BLAST+ database. We then used Henderson and Hanna's Henderson and Hanna (2016) "GItaxidIsVert.py" script to identify sequences that were potentially microbial in origin and performed a second BLAST+ search with this subset to further select only the subset of contigs that had their best or only alignment with nonvertebrate reference genomes. To exclude such sequences as well as those aligning with mtDNA sequence, we used the vcftools version 0.1.11 "-not-chr" flag and removed indels in the same step with the "-remove-indels" flag.

We estimated independent empirical gene coverage and site depth distributions using QB3's denovoTargetCapturePopGen "9-preFiltering" script and used these distributions as input to the QB3 "10-SNPcleaner" script. Run separately for modern and historical samples, this script removed all sites with coverage below 6x, sites missing in more than half of our samples, and sites with variant identity biases associated with quality score, mapping quality, or distance of alleles from the ends of reads. Because hydrolytic deamination of cytosine (C) to uracil (U) residues is the most common form postmortem nucleotide damage present in historic museum specimens, which may result in misincorporation of thymines (Ts) instead of uracil during PCR amplification and bias population genetic inference, this script also eliminated all C to T and G to A SNPs (Axelsson et al., 2008; Briggs et al., 2007; Hofreiter et al., 2001). Finally, we used the BEDtools version 2.26.0 "intersect" function (Quinlan and Hall, 2010) to retain only the sites that passed all filters for both historic and modern specimens.

1.3.6 Statistical analyses

To assess the differences in sequencing and assembly performance between modern and historical samples, we implemented Wright's two-sample t tests in the R (Team, 2018). We evaluated differences between groups in the mean percentage of duplicate reads, the mean number of on-target contigs, the mean length of on-target contigs, and the percentage of sequenced reads successfully mapping to our pseudo-reference genome. Because some commonly used polymerases bias against amplification of targeted DNA in favor of the GC-rich microbial contamination common to extracts from museum specimens (Dabney and Meyer, 2012), we assessed differences in GC content present in assembled on-target contigs. In order to determine whether sample age, initial sample DNA concentration, or sequencing effort were significant predictors of %GC content among historical samples and mean number or length of on-target contigs, we used simple linear regression. We used stepwise model selection with corrected Akaike information criterion (AIC) scores to determine best-fit models and did not include interaction terms to avoid over-parameterization given our small sample size.

1.3.7 Population genetic clustering and discriminant analysis of principal components

Although accurate estimation of population genetic structure in *S. torotoro* was not the primary goal of our study, we were nonetheless interested in assessing hyRAD's ability to produce biologically meaningful results by testing whether our data reflected the signature of phylogeographic processes such as isolation by distance (IBD) and vicariance, rather than the signature of DNA degradation, contamination, or other artifacts of library preparation and sequencing. We implemented k-means clustering and discriminant analysis of principal components (DAPC) in the R package adegenet (Jombart, 2008), using 100% complete data matrix (1,690 SNPs) to avoid biasing inferences with nonrandom patterns of missing data. We retained all principal component (PC) axes for k-means clustering and inspected both population assignments and change in Bayesian information criterion (BIC) scores

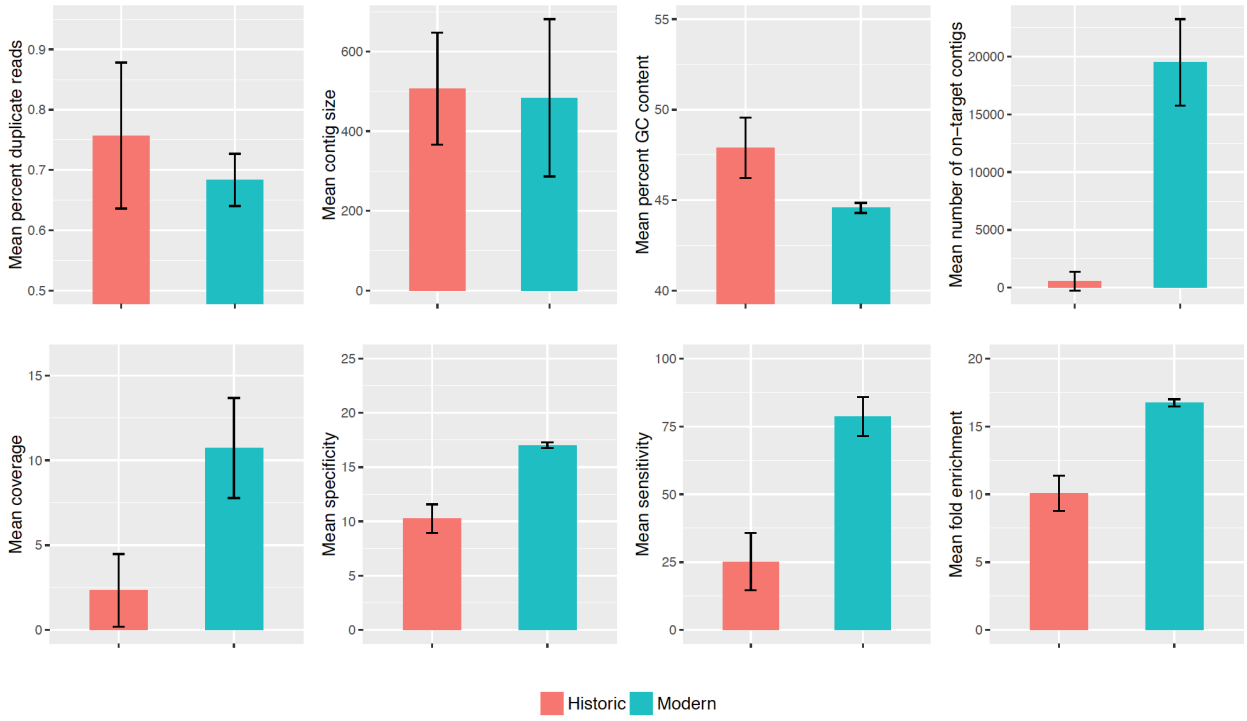

Figure 1.2: **Differences in sequencing and assembly performance between historical and modern DNA extractions**. We observed significantly higher specificity (t = 17.711, df = 14.015, p <.001), sensitivity (t = -12.928, df = 14.014, p <.001), fold enrichment (t = 17.711, df = 14.015, p <.001), and average coverage (t = 6.248, df = 7.555, p <.001) in modern samples. We recovered a significantly higher total number of on-target loci in modern samples (t = 12.239, df = 5.221, p <.001), but significantly higher mean %GC content in historic samples (t = 6.997, df = 13.368, p <.001). We observed no significant differences between modern and historic samples for mean contig size or mean percentage of duplicate reads.

across multiple values of K to select an optimal partitioning scheme. To maximize among-population variation and calculate ancestral population membership probabilities for each sample, we performed DAPC on the first six PCs using two discriminant axes. We then chose to retain these six PCs to optimize the a-score value for our data, which is the difference between the proportion of successful reassignment of the analysis and values obtained using random groups. However, because the change in BIC scores failed to clearly indicate any "true" value of K, we repeated our analysis with clustering assignments for K values of 1-8. To explore correlations between our three retained PCs and variables expected to differ between modern and historic samples (specificity, sensitivity, fold enrichment, age, initial concentration), we again performed simple linear regressions. Finally, to test for patterns of IBD across our samples, we performed a Mantel test among all individuals based on 999 simulated replicates using the R package ade4 (Thioulouse and Dray, 2007).

1.4 Results

1.4.1 Hybridization capture experiments and sequencing

We obtained a total of 397 million sequence reads for the probe and hybridization capture libraries, successfully demultiplexing 20/21 samples, with one sample failing due to barcode error. The total reads per sample ranged from 1.6 million to 30.7 million, and the average number of reads per sample did not vary significantly between modern and historical samples ($t = 0.946$, $df = 14.6$, $p = .359$). Of the original 397 million reads, 19.8% passed initial Illumina quality filters, contamination checks, adapter trimming, and removal of PCR duplicates (Table 1.1). The resulting number of cleaned reads per sample ranged from approximately 16,000 to 3.1 million, with an average count of 766,662, and significantly fewer reads for historic samples ($t = 3.185$, $df = 13.088$, $p = .007$). Most reads lost to quality control were PCR duplicates, with a range of 50.9%-91.1% duplicate reads per sample. 2,455 reads were removed as *E. coli* contamination from 12 of 20 individuals (range 1-2,318 reads per individual) (Table 1.2). The average depth of read coverage per sample, calculated as

Table 1.2: Results of microbial and mitochondrial contamination removal at three distinct steps. Raw reads were filtered for *E. coli* contamination; assemblied contigs were filtered for mitochondrial DNA; SNP matrices were filtered for both microbial DNA and mitochondrial DNA.

Contamination filtering step	Source	Total count	Count removed	Percent removed
Raw reads	Modern	13,942,179	4	<0.001
	Historic	548,415	2,451	0.44
Assembled contigs	Modern	296,828	8	<0.001
	Historic	36,109	53	0.15
SNP matrix	Modern	6,915,902	6,620	<0.001
	Historic	749,091	3,945	0.53

the read depth per base averaged across the length of the pseudo-reference genome, ranged from 7.6 to 26.4, and was significantly lower in historic samples (t = 3.754, df = 12.632, p = .002).

1.4.2 Assembly and alignment results

Assembly of our probe library in pyRAD resulted in a total of 554,048 contigs and 61.9 million nucleotides (nt), which was reduced to 160,014 unique contigs and 16.1 million nt after excluding repetitive regions. We captured orthologous loci from all successfully sequenced samples, and after merging the probe library with flanking regions from assemblies of other modern tissue samples our extended pseudo-reference genome contained 29,297 loci. The number of contigs per sample that was orthologous to our probe library ranged from 55 to 23,155 and was significantly higher in modern samples (Table 1.2, Figure 1.2).

Across all samples, we discarded 55%-92% of the total number of assembled clusters as off-target loci, losing significantly more from historic samples (t = 6.6035, df = 16.889, p <.001). We removed an additional eight contigs from the modern samples and 53 contigs

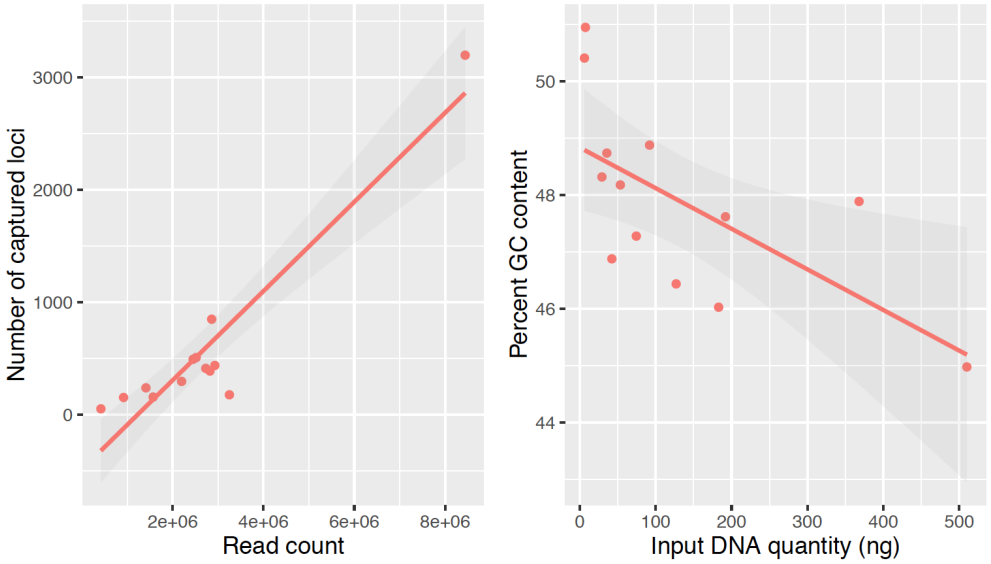

Figure 1.3: Among historic samples, the number of trimmed reads was a significant predictor of the number of captured loci (R^2 = .872, p <.001) and the initial sample DNA input quantity was a significant predictor of percent GC content in on-target assembled contigs (R^2 = .370, p = .016).

from the historic samples due to their mitochondrial origin (Table 1.2). Mean contig size ranged from 401 to 611 nt and did not differ significantly between modern and historic samples. However, the historic samples had significantly fewer contigs exceeding 1 knt in length (t = -3.181, df = 5.004, p = .025). The percentage of reads passing quality filters that successfully mapped to the pseudo-reference genome (also known as specificity) ranged from 51.8% to 57.7% and was significantly higher on average for modern samples (Figure 1.2). Additionally, %GC content was significantly higher in historic than modern samples (Figure 1.2). Among historic samples, the number of cleaned reads was a significant predictor of the number of captured loci and sample input DNA quantity was a significant predictor of %GC content in on-target assembled contigs (Figure 1.3).

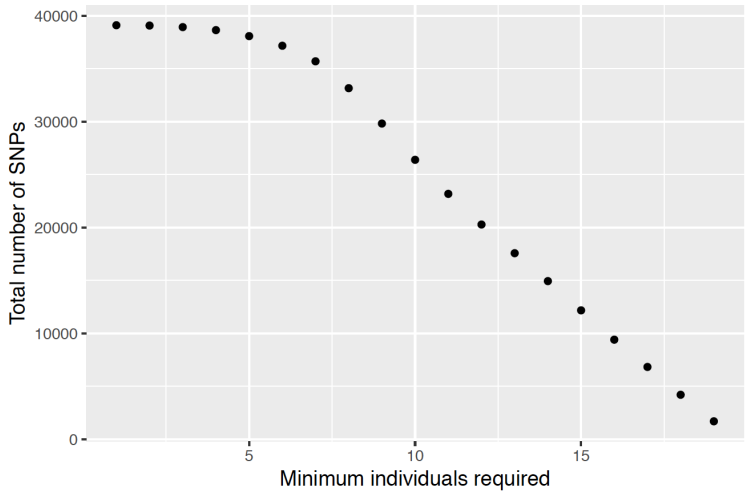

Figure 1.4: This displays the relationship between the cutoff for the minimum number of genotyped individuals required for a given SNP to be included in the data matrix and the total number of SNPs included in the resulting matrix.

1.4.3 SNP discovery and filtering

We identified two contigs of mitochondrial origin and eight contigs of potential nonvertebrate origin in our pseudo-reference genome and excluded all sites from these contigs in our alignment prior to SNP calling (Table 2.1). Using ANGSD, we identified 39,105 high-quality SNPs with at least a 95% probability of being variable from 3,206 loci, for a matrix completeness of 62.8% (or 37.2% missing data across all individuals). Per individual, the proportion of missing sites ranged from 5.6% to 90.6%, with a significantly higher mean percentage missing data for historic samples (54.5%) than modern samples (28.3%) ($t = 6.727$, $df = 14.594$, $p > .001$). The total number of SNPs in our data matrix decreased linearly after the first 10 individuals when we increased the minimum number of individuals successfully genotyped to retain each SNP (Figure 1.4).

1.4.4 Population genetic clustering and discriminant analysis of principal components

Discriminant analysis of principal components analysis of our 100% complete data matrix revealed a linear pattern of increase in the total amount of genetic variation explained when retaining additional PCs. Replicate attempts to optimize *a*-score values alternatively suggested retaining either five or six PCs to maximize discrimination ability without overfitting the model. Similarly, BIC scores from DAPC decreased in an approximately linear fashion as more clusters were added and did not indicate a clear shift to a slower rate of BIC change. Therefore, we repeated our analysis for values of K from 1 to 8, which revealed patterns of increasingly fine, geographically coherent structure from $K = 1$ to $K = 5$ (Figure 1.5). At $K = 2$, DAPC separated individuals from mainland Papua New Guinea (PNG) from individuals in western New Guinea and Normanby Island in PNG, which also reflected the break between modern and historic samples. At $K = 3$, DAPC identified an additional cluster from West Papua that included individuals from the southwest New Guinea Coast and the Aru Islands. At $K = 4$, DAPC isolated an individual from the northern slope of the Arfak Mountains in Western New Guinea, which, collected in 1877, was also the oldest sample included in our study. A fifth cluster distinguished the single individual from Normanby Island, PNG. At $K = 6$ and greater, DAPC began subdividing individuals into additional clusters without a shared geographic basis. Our Mantel test did not find statistically significant correlation between geographic and genetic distance ($p = .251$). Linear regression analyses showed significant correlations between all variables and PC1 but no other PC and sample variable pairs (Table 1.3).

1.5 Discussion

1.5.1 HyRAD is an effective tool for sampling thousands of orthologous SNPs from historic museum specimens

In their description of hyRAD, Suchan et al. (2016) suggest that it allows "sequencing of orthologous loci even from highly degraded DNA samples" and can be used to retrieve

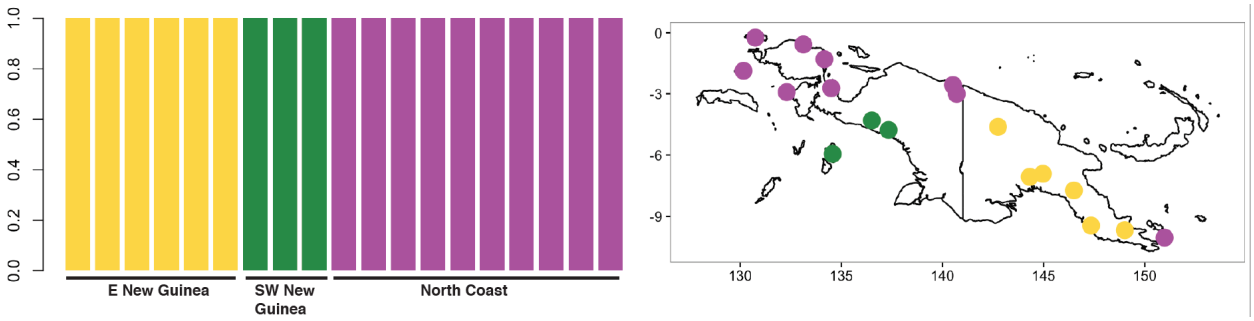

Figure 1.5: Individual membership probabilities for $K = 3$ ancestral populations inferred from analyzing 1,690 SNPs (100% complete data matrix) using discriminant analysis of principal components and retaining six principal component axes with two discriminant axes. Individual sampling locations are color coded accordingly.

Table 1.3: P values for simple linear regression between PC axes and sample variables.

	Specificity	Sensitivity	Fold enrichment	Age	Initial concentration
PC1	<.001	<.001	<.001	<.001	<.001
PC2	.076	.534	.076	.242	.253
PC3	.437	.335	.437	.466	.552

sequence data using museum samples up to 100 years old.

Our hybridization capture experiments in an independent laboratory with an independent study organism (*S. torotoro*) largely support this conclusion. Assessed by the total number assembled contigs, orthologous loci, SNPs collected, and number of SNPs recovered across multiple individuals (Table 1.1; Figure 1.4), our modified version of Suchan et al.'s hyRAD protocol generated sufficient quantities of genome-wide data for a wide range of phylogenetic and population genetic questions. In particular, we note that our application of standard library preparation methods for both modern and historic libraries (as opposed to protocols optimized for degraded DNA, as in Suchan et al. (2016)) does not appear to have negatively affected data recovery rates. We believe this reflects the relative robustness of the approach to different taxa, laboratory conditions, specimen preparation conditions, and bioinformatics pipelines. Even with stringent filtering for quality and postmortem damage, our 100% complete data matrix of 1,690 SNPs is similar to the number of orthologous SNPs collected in similar studies of museum genomics that used UCE capture (McCormack et al., 2016), exon sequence capture (Bi et al., 2013), or even ddRAD methods with fresh tissues (Shultz et al., 2016), with the caveat that differences in starting material, evolutionary timescale, and experimental design preclude direct comparisons across studies. For phylogenetic or population genetic analyses methods that correct for nonrandom patterns of missing data, our full matrix of 39,105 SNPs potentially offers significant power to resolve rapid, recent divergences, detect fine scale patterns of population structure, infer historical effective population sizes with high accuracy, and reveal histories of drift, selection, and migration (Toews et al., 2015).

Suchan et al. (2016) included historical museum specimens up to 58 years old in their validation experiment and up to 100 years old in their pilot study. We successfully captured 55 on-target loci, including four contigs exceeding 1 knt in length, from a specimen collected in 1877, and as many as 508 loci from specimens collected from 1896 to 1934 (Table 1.1). Moreover, and contrary to similar analyses by Suchan et al. (2016) and McCormack et al. (2016), we found no significant linear relationship between age and assembly or sequencing

success metrics across historical samples. While this is possibly an artifact of small sample size relative to both previous studies, it may also suggest a relatively shallow trend of degradation during a period when many bird specimens in natural history museums were originally collected. This is an encouraging result for researchers looking to make use of these specimens as a genomic resource.

1.5.2 Variation in sequencing and assembly performance across sample types reduces efficiency

Our small sample size prevents us from making broad conclusions about factors affecting variation in enrichment, sequencing, and assembly performance. However, preliminary statistical analyses revealed variation between modern and ancient DNA libraries across numerous metrics. Modern DNA samples had significantly higher specificity (% mapped cleaned reads), sensitivity (% of probe sequence with at least 1x coverage), and fold enrichment (the fold increase in % mapped reads over baseline random expectations) (Figure 1.2). While initially intuitive, our findings contrast with the results of Bi et al. (2013) and Suchan et al. (2016), who found improved capture efficiency with historic samples, potentially related to smaller fragment size. We encourage future studies to explore how variation in hybridization capture protocols affects relative performance of different sample DNA sources.

Encouragingly, there were no significant differences between the two sample populations for the overall percentage of duplicate reads. However, we wish to highlight the high percentage of duplicate reads present in all samples (50.9%-91.1%). This may be due to combination of the relatively high number of amplification cycles used to amplify libraries with low input DNA prior to pooling. While high duplicate read percentages have also been reported in RADseq studies with fresh tissue (Andrews et al., 2016), this inefficiency is important to consider when working with valuable, low-quality historical samples, as increased sequencing effort may be required to generate sufficient read depth for variant detection and accurate assembly of contiguous sequences.

Lastly, following assembly, the total number of captured on-target loci was higher among

modern samples, likely reflecting higher copy number and limited degradation of DNA from fresh tissues. In contrast, mean contig length did not vary significantly among samples, indicating similar assembly performance relative to the amount of high-quality data for each sample type. While we believe this result will prove robust to different assembly methods, we encourage future studies to explore their influence on resulting assemblies and downstream analyses.

1.5.3 Input DNA quantity predicts GC content, suggesting PCR bias

Although inferences are similarly limited by sample size, our regression analyses largely failed to reveal significant correlations between input DNA/sequencing variables and assembly performance except in two comparisons (Figure 1.2). First, an increase in the number of filtered reads was positively correlated with the total number of assembled on-target contigs, which matches a standard expectation of increased recovery with greater sampling of a genomic library with an uneven distribution of fragments, suggested for our libraries by the high levels of duplication (Table 1.1). Second, the initial quantity of input DNA in a sample was negatively correlated with %GC content in resulting assemblies, for example, the two samples in our study that with the lowest input DNA quantity also the highest percentage of GC content across all assembled contigs (Table 1.1). This finding may reflect biased PCR enrichment of GC-rich exogenous microbial contamination in samples with low initial input DNA quantity (Dabney and Meyer, 2012) and explain the significantly higher GC content of historic samples overall. While our SNP calling pipeline and data filtering removed sites potentially originating from nonvertebrate sequences (although see further discussion below), we nonetheless recommend researchers interested in applying hyRAD to historical specimens heed the recommendations of recent empirical studies (Gamba et al., 2016) to select an extraction protocol suited to degraded DNA and maximize input tissue quantity whenever possible.

1.5.4 Geographic and/or taxonomic autocorrelation with input DNA type is potentially problematic with hyRAD studies

We implemented rigorous and conservative laboratory and bioinformatic protocols to reduce the influence of exogenous DNA contamination and postmortem DNA degradation, the results of which we summarize as a reference for future studies in Table 1.2. Despite these precautions, repeated DAPC with different parameters failed to change a basic pattern where all modern DNA samples ($n = 6$) clustered until the chosen K value of ancestral populations was seven or more (Figure 1.5). Unfortunately, as the close geographic proximity of modern DNA samples would also lead to this pattern, we could not easily determine from our sampling scheme if this pattern reflected biological reality or whether factors correlated with sample type, such as undetected microbial contamination, DNA degradation, and/or library amplification artifacts, were affecting population genetic inference. We first attempted to disentangle its potential drivers during PCA and DAPC analyses by examining histograms of %GC content per read for anomalous distributions, but failed to detect a significant second peak indicative of contamination with exogenous GC-rich microbes. We next performed linear regressions with specificity, sensitivity, fold enrichment, specimen age, and input DNA quantity as predictors for each of our first three retained PCs. From these regression analyses, we found significant correlations of all variables with PC1, but no other PCs (Table 1.3). While these results are consistent with the possibility that biased sequencing performance affected population genetic inference, the exact mechanism responsible remains unclear. To avoid artifacts related to the separate treatment of different sample types, we suggest randomizing individuals from both modern and historic DNA sources throughout library preparation, hybridization capture, and sequencing. Additionally, we suggest researchers intending to use hyRAD in studies with both modern and historic tissue attempt to avoid geographic and taxonomic autocorrelation wherever possible and include a control in their sampling scheme to indicate potential DNA input quality problems.

1.5.5 The phylogeography of S. torotoro reflects biogeographic barriers in New Guinea

Our DAPC results are consistent with previous studies of lowland avian phylogeography in New Guinea, and we interpret them as independent confirmation the ability of hyRAD to reveal biologically meaningful patterns. K-means clusters recovered for three ancestral populations reflect broad trends in codistributed taxa and expected patterns of genetic variation given geographic barriers and the geologic history of New Guinea (Figure 1.5) (Deiner et al., 2011; Dumbacher and Fleischer, 2001). Although IBD across all samples was not significant (see Results for details), the initial division of samples into mainland eastern and western clusters is consistent with both the primary latitudinal axis of the island and the barriers to gene flow in lowland forest taxa presented by the Bewani Mountains and Trans-Fly savannah region (Deiner et al., 2011; Mack and Dumbacher, 2007). Inclusion of Normanby Island subspecies *S. t. ochracea* in the western New Guinea cluster is consistent with previous studies that have reported genetic similarity between other taxa in far eastern and far western New Guinea, such as birds of the genus *Pitohui* (Dumbacher and Fleischer, 2001). Samples from southwest New Guinea clustered with those from the Aru Islands, suggesting shared ancestry among these currently allopatric populations. This is potentially explained by both the linkage of these landmasses during the Pleistocene via the Sahul Shelf (Voris, 2000) and the subsequent emergence of previously identified barriers to avian gene flow to the north, east, and west in the form of the Central Ranges, the Trans-Fly Savannah, and Aetna Bay, respectively (Dumbacher and Fleischer, 2001; Deiner et al., 2011) Our analysis reveals broad similarities between the phylogeography of *S. torotoro* and the codistributed lowland bird species *Colluricincla megarhyncha* (Deiner et al., 2011), albeit with lower resolution due to the inherent limitations of our sampling. We believe that future studies of resident lowland forest species with similar ranges that use hyRAD or other means of capturing nuclear DNA markers will continue to aid in building a cohesive picture of the comparative phylogeography of this biodiverse region.

1.6 Acknowledgements

This material is based upon work supported by the National Science Foundation under DBE Grant No. 1601515 [to Z.R.H.]. Any opinions, findings, and conclusions or recommendations expressed in this material are those of the authors and do not necessarily reflect the views of the National Science Foundation. Additional support for this research was provided by NDSEG and WRF-Hall Fellowships, a Society of Systematic Biology GRSA [to E.B.L.] and a gift from M. and K. Simon [to J.P.D.]. For tissue loans, we thank R. Moyle and M. Robbins at KUMNH, P. Sweet at AMNH, and Robert Prys-Jones at NHMUK-Tring. For field assistance, we thank T. Bozic, A. Mack, D. Mindell, J. Fuchs, M.A.C. Dodge, and Bruno and Carmen Montel. For laboratory assistance, we thank L. Wilkinson and M. Flannery. For comments on the manuscript, we thank J. Klicka, C.J. Battery, D. Slager, C. French, and R. Harris. We performed all laboratory work at the Center for Comparative Genomics, California Academy of Sciences, and all sequencing at the Vincent J. Coates Genomics Sequencing Laboratory at UC Berkeley, supported by NIH Instrumentation Grant S10 OD018174. In PNG, we thank the Institute of Biological Research, the National Museum and Art Gallery, the National Research Institute, and the Department of Conservation. We add special thanks to the many New Guineans who provided field and logistical assistance, especially Bulisa Iova and tribal leaders of the villages that participated in and allowed our work.

1.7 Data availability

Raw sequence data are available from the NCBI SRA: SRR5451181-SRR5451200 (BioProject PRJNA383002). SNP matrices, contig assemblies, and other data available from DRYAD: `https://doi.org/10.5061/dryad.r7q86`. Custom R scripts, shell commands, and a bioinformatics tutorial are available at `https://github.com/elinck/hyRAD`.

Chapter 2

SPECIATION WITH GENE FLOW ACROSS AN ELEVATIONAL GRADIENT IN NEW GUINEA KINGFISHERS

*Ben G. Freeman and John P. Dumbacher were coauthors on a preprint version of this manuscript posted to *bioRxiv*: https://dx.doi.org/10.1101/589044

2.1 Abstract

The role of environmental gradients in speciation remains contentious. Theory suggests speciation without geographic isolation is plausible if divergent natural selection is strong enough to counteract gene flow, but empirical examples are elusive. Tropical mountains provide strong and temporally stable environmental gradients that can promote local adaptation and population genetic structure. Pairs of closely related species with adjacent but divergent elevational ranges are common in these environments, a pattern that suggests parapatric speciation (i.e., speciation with moderate gene flow), but have rarely been studied in a speciation genomics framework. Here we use genomic data from modern and historical museum specimens to provide evidence for speciation with gene flow across an elevational gradient in a pair of New Guinea kingfishers. We find that the lowland species *Syma torotoro* and montane species *S. megarhyncha* form discrete genotypic clusters with bimodal variance in phenotypic traits. Nevertheless, demographic inference, *D*-statistics, and phylogenetic networks indicate range-wide gene flow over long time periods, with divergence concentrated in small regions of the genome shaped by positive selection. We propose these data can be explained by a "magic trait" model of ecological speciation where selection on body size also affects mate choice. Our results provide a rare validation of theoretical models of adaptive speciation and are consistent with a strong influence of tropical thermal stability on diversification. We suggest selection across elevational gradients can effectively maintain species boundaries in the face of incomplete reproductive isolation, a mechanism contibuting to high tropical biodiversity.

2.2 Introduction

Adaptation across environmental gradients is ubiquitous in nature (Turesson, 1925; McCormack and Smith, 2008; Cheviron and Brumfield, 2009), but its role in promoting speciation remains contentious (Coyne and Orr, 2004; Mallet, 2005; Fitzpatrick et al., 2008; Mallet, 2008). Disruptive natural selection can lead to local adaptation that restricts gene flow between populations in different environments if it becomes paired with a mechanism to promote nonrandom mating such as a pleiotropic "magic trait," linkage disequilibrium between separate loci involved with local adaptation and assortative mating, or habitat preference leading to ecogeographic isolation (Rundle and Nosil, 2005; Via, 2009; Nosil, 2012). A robust body of theory suggests this process is possible under a range of circumstances (Smith, 1966; Endler, 1977; Kirkpatrick and Ravigné, 2002; Doebeli and Dieckmann, 2003; Doebeli et al., 2005; Hua Xia, 2016). However, many evolutionary biologists dismiss its relevance in natural systems as it is unlikely compared to models of speciation without gene flow and because there are few obvious empirical examples (Coyne and Orr, 2004). Despite a recent shift from the traditional emphasis on the geography of diverging populations to a focus on measuring relative rates of gene flow (Fitzpatrick et al., 2008; Mallet, 2008; Butlin et al., 2008), intermediate values of migration only imprecisely map on to conceptual models. Perhaps as a result, the most compelling studies of speciation without geographic isolation have focused on a single, relatively compact deme (Schliewen et al., 1994; Savolainen et al., 2006; Ryan et al., 2007). Yet if speciation with some degree of gene flow is common, as Nosil has argued (Nosil, 2008b), it is likely parapatric divergence that predominates. Testing for its occurrence in a diverse range taxa will help clarify when it is likely to occur and spur the development of more accurate models.

Both the emphasis on the geography of speciation and skepticism towards speciation with gene flow were deeply seeded by the writings German-American zoologist Ernst Mayr (Mayr, 1942, 1963; Coyne, 1994), a prominent architect of the Modern Synthesis. Mayr's theory of "geographic" (or allopatric) speciation was rooted in his detailed study of the birds of the

island of New Guinea and nearby islands in Northern Melanesia (Mayr, 1942, 1963). Mayr observed that putative sister species or geographically differentiated races nearly always had non-overlapping geographic ranges on separate islands, isolated mountains, or in lowland basins separated by mountain ranges. Consequently, he suggested geographic differentiation in isolation was nearly always a better explanation for speciation than divergence in sympatry, in part because it allowed Bateson-Dobzhansky-Muller Incompatibilities (Dobzhansky, 1937) or other isolating factors to accumulate in the absence of the homogenizing influence of gene flow. Initially implicating drift as the primary evolutionary force driving speciation, his views later shifted to emphasize founder effects (Provine, 2004) while conceding a role for natural selection (Nosil, 2008a).

Recent theory and empirical work has undermined the generality of Mayr's intuitive central assumption, which held that contemporary distribution of species can be used to infer their arrangement at the time of divergence. Models of speciation that invoke biotic interactions between diverging populations suggest suggest that reproductive isolation may evolve more readily in the presence of competition and an environmental gradient than in strict allopatry (Doebeli and Dieckmann, 2003). Phylogenetic comparative approaches have been applied to evaluate the frequency of alternate modes of speciation, but are hampered by the lability of species ranges over evolutionary time scales and their limited information on underlying mechanisms (Losos and Glor, 2003). Demographic modeling using genomic data from multiple young species pairs has similarly found that the arrangement of current species ranges fails to predict inferred rates of ancestral gene flow (Penalba et al., 2017). Moreover, genome-wide DNA sequence data has profoundly altered our understanding of the speciation process. We now understand speciation is far more dynamic than previously assumed: reticulation of lineages is common across the tree of life and may be a generative force for adaptive variation or even speciation itself, while species limits can be maintained by selection in the face of significant gene flow (Brelsford et al., 2011; Kumar et al., 2017; Schumer et al., 2018b; Edelman et al., 2018).

Ironically, Melanesia, the very region that was so important to Mayr's theory and ecology

and evolution more broadly (Wilson, 1959; Diamond, 1972b, 1973), has seen comparatively little modern research in the emerging discipline of speciation genomics (but see Stryjewski and Sorenson (2017)), in part due to logistical difficulties facing fieldworkers. While allopatric divergence following dispersal or vicariance is doubtless an important factor in the origin of species in tropical areas like New Guinea (Smith et al., 2014), the importance of abiotic and biotic ecological variables in driving evolutionary processes agnostic to geography is increasingly recognized (Polato et al., 2018). Ecologists have long known that reduced seasonal variation in temperature drives strong thermal stratification across tropical mountainsides (Polato et al., 2018; Janzen, 1967; Sheldon et al., 2018), a pattern correlated with high beta diversity (Jankowski et al., 2009; Cadena et al., 2012), especially among closely related species (Terborgh and Weske, 1975; Freeman and Freeman, 2014). Because many tropical taxa are residents that appear to show low rates of dispersal and have a "slow pace of life" (Wiersma et al., 2007; Harvey et al., 2017a; Smith et al., 2017), strong disruptive selection could plausibly counteract migration to drive adaptive divergence.

Local adaptation across tropical elevational gradients has been documented by clines in functional genes and intraspecific population genetic structure (Cheviron and Brumfield, 2009; DuBay and Witt, 2014; Funk et al., 2016; Gadek et al., 2018). This has been shown theoretically to "scale up" to speciation under a scenario of niche expansion (Hua Xia, 2016), but empirical evidence remains mixed. Phylogenetic and phylogeographic comparative studies suggest this process has occurred in *Ithioma* butterflies (Elias et al., 2009) and Andean amphibians and reptiles (Arteaga et al., 2016). In Andean birds, a broad consensus holds that elevational replacements primarily form through divergence in allopatry followed by secondary contact and displacement (Cadena et al., 2012; DuBay and Witt, 2014; Caro et al., 2013; Cadena and Céspedes), despite equivocal results in some tests. Yet we are aware of only one study that has used population genomics to evaluate speciation across elevational gradients, which found strong evidence that adaptation to altitude drives speciation in *Senecio* ragwort plants in temperate Italy (Chapman et al., 2013; Osborne et al., 2013). The question of the relative contribution of adaptation in the presence of gene flow across elevational

Table 2.1: Alternate speciation hypotheses with predicted patterns from different data types and their associated references in the literature.

Hypothesis	Description	Genomic Predictions	Phenotypic Predictions	Geographic Predictions
H_0	Null hypothesis: not distinct species	No population genetic structure congruent with species limits (De Queiroz, 2007)	*S. megarhyncha* larger and has lower call (Freeman, 2017); variation clinally distributed (Cadena et al., 2018)	No prediction
H_1	Single parapatric speciation event followed by range expansion	Reciprocal monophyly of *megarhyncha* and *torotoro* (De Queiroz, 2007); support for isolation-with-migration model (10); widespread introgression (Behm et al., 2010; Seehausen et al., 2008); extensive reticulation in phylogenetic network (Martin et al., 2019)	*S. megarhyncha* larger and has lower call (Freeman, 2017); bimodal distribution of morphological and bioacoustic traits (Cadena et al., 2018)	Limited elevational range overlap in areas of allopatry (Schluter and McPhail, 1992)
H_2	Parallel parapatric speciation events	Isolated *megarhyncha* populations nested within clade of *torotoro* (Nosil, 2012); two species demographic model poorly supported (Nosil, 2012); widespread introgression (Behm et al., 2010; Seehausen et al., 2008); extensive reticulation in phylogenetic network (Martin et al., 2019)	Polyphyletic high elevation lineages larger and have lower call (Freeman, 2017); bimodal distribution of morphological and bioacoustic traits not aligned with current species limits (Cadena et al., 2018)	Limited elevational range overlap in areas of allopatry (Schluter and McPhail, 1992)
H_3	Allopatric speciation event followed by range expansion	Reciprocal monophyly of *megarhyncha* and *torotoro* (De Queiroz, 2007); support for strict isolation or secondary contact model (Nosil, 2012); limited introgression (Behm et al., 2010; Seehausen et al., 2008); limited reticulation in phylogenetic network (Martin et al., 2019)	*S. megarhyncha* larger and has lower call (Freeman, 2017); bimodal distribution of morphological and bioacoustic traits (Cadena et al., 2018)	Elevational range overlap in areas of allopatry (if niche displacement) (Schluter and McPhail, 1992)

gradients to speciation and broader patterns of tropical biodiversity remains open.

The Yellow-billed and Mountain Kingfishers *Syma torotoro* and *S. megarhyncha* (Aves: Alcedinidae) are putative sister taxa that segregate by elevation and vary only subtly in phenotype (Mayr, 1942; Pratt and Beehler, 2015; Diamond, 1972a). The lowland species *S. torotoro* is reportedly smaller with a higher-pitched call, and primarily found below 700 m, above which it is replaced by the slightly larger, deeper-voiced *S. megarhyncha* (Pratt and Beehler, 2015) in at least two discontinuous mountain ranges. Among New Guinea's many elevational series, the distribution and morphological conservatism of *Syma* has led systematists to suggest speciation driven by colonization of montane forest (Rand, 1936),

though Mayr discounted this possibility in New Guinea mountain birds generally (Mayr, 1942). However, species limits and range-wide variation have never been quantitatively assessed, and observed differences might instead reflect phenotypic plasticity or clinal variation of a single widespread lineage (Caro et al., 2013).

Here we use genome-wide DNA sequences, bioacoustic data, and morphometric analyses to infer the mode of speciation in *Syma* kingfishers. We developed predictions for alternate speciation hypotheses that could explain the current distribution of these species (Table 2.1; Figure 2.1), and looked for the genomic signatures of gene flow and natural selection. Multiple lines of evidence support a scenario of parapatric speciation across an elevational gradient followed by range expansion into currently discontinuous montane forest habitat. Our data provide a rare empirical validation of models of adaptive speciation, and highlight how selection across elevational gradients can maintain species boundaries in the face of incomplete reproductive isolation, a mechanism for generating high tropical biodiversity.

2.3 Methods

2.3.1 Study system

Yellow-billed Kingfisher *Syma torotoro* and Mountain Kingfisher *Syma megarhyncha* (Aves: Alcedinidae) are the sole members of their genus. Tree kingfishers (subfamily Halcyoninae), they are endemic to New Guinea, its satellite islands, and the Cape York Peninsula of Australia. *S. torotoro* is found in tropical lowland forest and savannah from sea level to 500 m elevation, or less commonly to 1100 m (Pratt and Beehler, 2015). *S. megarhyncha* is found from 600 m to 2700 m or higher (Pratt and Beehler, 2015). Though cited as a classic example of congeneric elevational replacements occurring in parapatry (Diamond, 1972a), their elevational ranges have also been reported to either overlap (Gregory, 2017) or be separated by a substantial gap (Freeman and Freeman, 2014; Sam et al., 2014). Both species are omnivorous territorial interior forest residents and differ only in *S. megarhyncha's* larger body size, deeper call, and the extent of black on the top of its bill in one subspecies

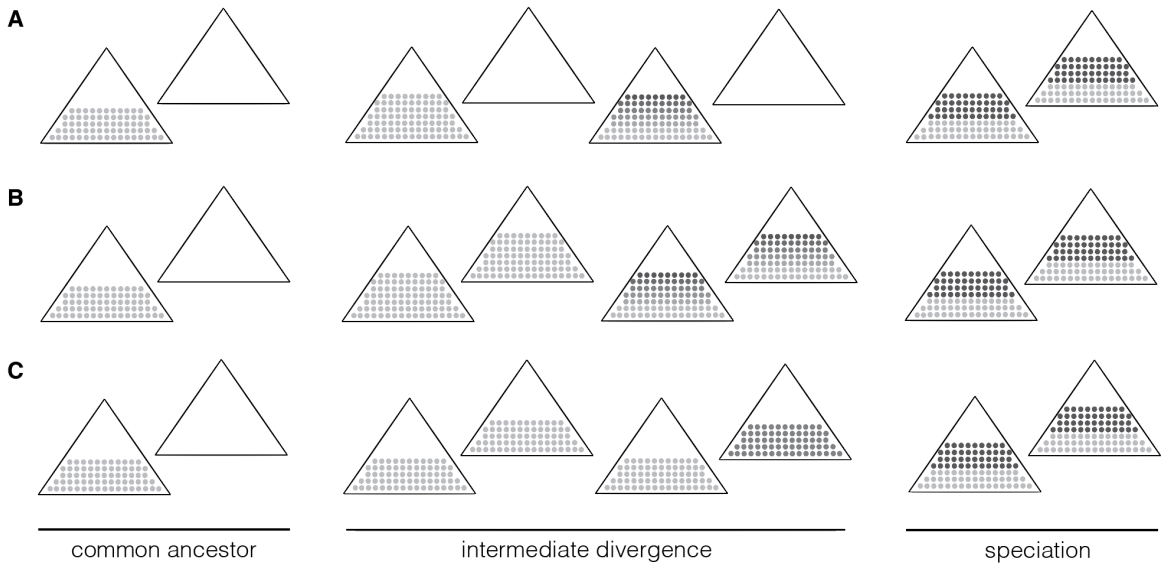

Figure 2.1: **Simplified hypotheses for the origin of elevational elevational series.** A) Range expansion across a local elevational gradient exposes a population to disruptive natural selection, leading to local adaptation that restricts migration across the gradient until reproductive isolation develops as a byproduct. Dispersal to other mountain ranges occurs after speciation (H_1 in Table 1). B) Parallel speciation events driven by local adaptation across two elevational gradients (H_2). C) A single population splits following a dispersal event or vicariance and develops reproductive isolation in allopatry. Following range expansion and secondary contact in multiple mountain granges, niche displacement leads to separate elevational distributions (H_3).

(Pratt and Beehler, 2015). Insular *S. torotoro* subspecies *S. t. ochracea* differs substantially from its conspecifics and *S. megarhyncha* in call, and is intermediate in size.

2.3.2 Morphological and bioacoustic data

We measured bill length, bill depth, tarsus, wing chord, and tail length from 72 museum specimens of *Syma torotoro* (n=40) and *S. megarhyncha* (n=32) at the American Museum of Natural History, representing all described subspecies. Using these data, we performed principal component analyses in R (Team, 2018) with normalized variables, and used PC1 to build mixture models using the R package mclust v. 5.4.1, which we evaluated with a maximum likelihood classification approach (Scrucca et al., 2016). We downloaded all available vocalizations from *S. torotoro* (n = 34) and *S. megarhyncha* (n = 14) from xeno-canto and Cornell's Macaulay Library. We filtered these data for quality and quantified a suite of bioacoustic variables using the warbleR package v. 1.1.14 in R (Araya-Salas and Smith-Vidaurre, 2017), analyzing 278 distinct vocalizations from *S. torotoro* and 106 from *S. megarhyncha* in total. We ran PCA with normalized variables on the output, and used these data to alternate species delimitation models using the same approach as with our morphological data.

2.3.3 Sampling, library preparation, and DNA sequencing

We extracted DNA from fresh tissues (n=6) and toepad samples from historical museum specimens (n=34) from 30 individuals of *S. torotoro* (n=30) and 10 individuals of *S. megarhyncha* (n=10). These individuals represented the full extent of both species' ranges in New Guinea and Australia (Table 2.2), and included all described subspecies. These are: *S. t. flavirostris* in southern New Guinea, northern Australia, *S. t. ochracea* in the D'Entrecasteaux Archipelago, oceanic islands off the southeastern peninsula of Papua New Guinea; *S. t. meeki* in southeastern Papua New Guinea; *S. t. pseuestes* in south-central New Guinea; *S. t. tentelare* of the Aru Islands; *S. m. megarhyncha* of the eastern Central

Ranges; *S. m. wellsi* of the western Central Ranges; and *S. m. sellamontis* of the mountains of the Huon Peninsula.

We extracted DNA from fresh tissues using a Qiagen DNAeasy kit and the manufacturer's recommended protocol. For historical toepad samples (collected 1877-1977), we extracted DNA using either a using a phenol-chloroform and centrifugal dialysis method (Dumbacher and Fleischer, 2001) (for reduced representation sequencing) or a standard salt extraction protocol (for whole genome resequencing). Due to constraints of cost and time, we employed two complementary sequencing approaches. On a subset of samples (n=20), we performed reduced representation genome sequencing using a hybridization capture with RAD probes (hyRAD) approach, described in detail elsewhere (Linck et al., 2017). We sent the remaining samples to the UC Berkeley's Vincent J. Coates Genomic Sequencing Laboratory, where laboratory staff prepared genomic libraries for low coverage whole genome sequencing (WGS) using Illumina TruSeq Nano kits and a modified protocol that skipped sonication and enzymatically repaired fragments with RNAse. They then pooled (n=20) and sequenced these samples with 150 base pair paired-end reads on a single lane of an Illumina HiSeq 4000.

2.3.4 Sequence assembly and variant calling

We processed demultiplexed reads with a custom bioinformatic pipeline optimized for handling degraded DNA data and available at `https://github.com/elinck/syma_speciation/`. Briefly, we trimmed raw reads for adapters and low quality bases using bbduk from BBTools version 38.06 suite of bioinformatics tools. We aligned these reads to an unpublished draft genome of Woodland Kingfisher *Halcyon senegalensis* from the Bird 10K Genome Project using bbmap with a k-mer value of 12, a maximum indel length of 200 bp, and a minimum sequence identity of 0.65. We used PicardTools v. 2.17.8 and GATK v. 3.6.0 (McKenna et al., 2010) to append read groups and perform local realignment on .bam files. We then used mapDamage 2.0.9 to account for postmortem damage to DNA from historical museum specimens by rescaling quality scores (Jónsson et al., 2013). We performed multisample variant calling using the UnifiedGenotyper tool in GATK v. 3.6.0, and filtered our

variant calls for missing data, coverage, and quality with VCFtools 0.1.16 (Danecek et al., 2011). To complement our nuclear DNA sequences, we assembled near-complete mitochondrial genomes from a majority of individuals using a baiting and iterative mapping approach implemented MITObim v 1.9.1. (Hahn et al., 2013), which we ran for 10 cycles using a complete mtDNA genome from close relative *Todiramphus sanctus* as a reference (Andersen et al., 2015).

2.3.5 Population structure inference

We evaluated population genetic structure within and between species using both nonparametric and model-based clustering approaches. We performed principal component analysis of genotypes (PCA) and identified putative genetic clusters for K=2 through K=4 using adegenet v. 2.1.1 and a 95% complete dataset with 66,917 SNPs from all individuals passing quality filters and a minimum minor allele frequency of 0.05. After first determining that small sample sizes made unsupervised inference inappropriate for our data and resulted in extremely high cross validation error (Puechmaille, 2016), we implemented model-based clustering using ADMIXTURE v. 1.3.0 (Alexander et al., 2009) and population priors from the K=3 K-means clustering result.

2.3.6 Phylogenetic inference

We constructed a consensus neighbor joining tree in the R package ape v. 5.1 (Paradis et al., 2004), implementing Sanderson's nonparametric rate smoothing with λ=1 using a 22,226 SNP dataset of all individuals passing quality filters with no more than 5% missing data per site, a minimum minor allele frequency of 0.05, and a minimum depth of coverage of 3x. To evaluate and visualize gene tree variance, we generated 500 additional neighbor joining trees by resampling 10,000 SNPs from the matrix with replacement, and plotted them on the consensus tree using the densiTree() function in ape. We used the same underlying distance matrix to compute a phylogenetic network using the Neighbor-Net approach (Bryant and Moulton, 2004) implemented in SplitsTree (Huson and Bryant, 2006) with default parame-

ters. We inferred a maximum likelihood tree with an alignment of mtDNA genomes from the majority of individuals using RAxML through the CIPRES portal (Miller et al., 2010) with default parameters.

2.3.7 Demographic inference

We calculated the joint site frequency spectrum (JSFS) using a SNP dataset with a minimum per site depth of 3x and a minimum quality of Q=30, thinned to 1 site for every 50 kbp to reduce the influence of linkage disequilibrium. We then defined four nested models which differed by level and timing of gene flow (Figure 2.5): isolation with migration (IM), isolation with initial migration (IIM), secondary contact (SC), and strict isolation (SI). All models featured a split of an ancestral population into two daughter lineages of arbitrary size, followed by a second time period allowing population growth. After initially optimizing parameters using the "optimize_log" method, we ran 25 additional optimizations, allowing a 1-fold random perturbation of parameter values each time. We selected the model with the maximum log-likelihood and estimated parameter uncertainty using 100 bootstrapped frequency spectra and the Godambe Information Matrix. We converted parameter values to real units using a genome-wide mutation rate of $2.3x10^{-9}$ (Smeds et al., 2016), an effective sequence length scaled to reflect our LD-thinned SNP dataset, and a generation time estimate of two years, and generated parameter uncertainty estimates using a Godambe Information Matrix. To evaluate changes in historical effective population size through time in greater detail, we used SMC++ (Terhorst et al., 2017), which accounts for the distribution of variation across the genome. We masked continuous stretches of homozygosity greater than 30 kb, included all contigs longer than $1x10^6$ bp, assumed a generation time of 2 years, and again assumed mutation rate of $2.3x10^{-9}$. We visualized uncertainty by refitting models to 10 bootstrap replicates per population, resampling both individuals and contigs with replacement.

2.3.8 Introgression

We explicitly tested for introgression between lineages using a four taxon test implemented in ANGSD with the "doAbbababa" function, described in detail elsewhere (Korneliussen et al., 2014; Green et al., 2010). We calculated D for each combination of individuals conforming to the topology (mega,ochr),toro), and assessed significance by block jackknife over 1 mbp windows. We summarized results by collapsing individual tests representing the same geographic comparisons and calculating median Z scores and the proportion of individual tests that were significant given a cutoff of Z=3.59, which is equivalent to p=0.005 after performing a Bonferroni correction for multiple comparisons (n=31). These comparisons included *S. torotoro*, insular *S. t. ochracea* and three *S. megarhyncha* populations: *S. megarhyncha* in the mountains of the Huon Peninsula, *S. megarhyncha* in the eastern Central Ranges, and *S. megarhyncha* in the far western Central Ranges.

2.3.9 Genome scans and tests for positive selection

We assessed levels of divergence across the genome by calculating Wright's F_{ST}, D_{XY}, and π for each species in 50 kbp windows with a 10 kbp step size using scripts written by Simon Martin (`https://github.com/simonhmartin/genomics_general`), using a VCF file filtered for a minimum Q score of 30 and a minimum depth of 3x with a total of 1,858,764 SNPs and 102,606,487 total sites. To assign chromosome identity to scaffolds and windows, we aligned the *H. senegalensis* draft genome to the chromosome-level genome assembly of *Taenopygia guttata* (Warren et al., 2010) using NUCmer in MUMmer v. 3.1 (Delcher et al., 1999), allowing a maximum gap of 1000 bp and using a minimum sequence identity threshold of 10 kbp per contig. We evaluated correlations among summary statistics using simple linear models implemented in R (R Core Team, 2018). To formally test for the signature of positive selection in the genomes of both species, we used the program RAiSD (Alachiotis and Pavlidis, 2018). We calculated Wright's F_{ST}, D_{XY}, and π for each species in nonoverlapping 50 kbp windows, and used these statistics to identify a set of scaffolds hosting F_{ST} outlier

windows at the $P = 0.005$ threshold. We then created an identically sized set non-F_{ST} outlier windows using random sampling without replacement, and ran RAiSD on species-specific .vcf files including only these scaffolds. To establish a value of composite selective sweep summary statistic to use as a threshold for a false positive rate of 0.05, we used the program SFS_CODE (Hernandez, 2008) to simulate data similar to our own but under the influence of purifying selection, outputting a .vcf file to analyze with RAiSD using the "-k 0.05" option.

2.4 Results

2.4.1 DNA sequencing from historical specimens

We extracted DNA and generated genome-wide sequence data from all historic toepad samples across both species' relatively inaccessible distributions, with collection dates ranging from 1896 to 1973 and including 3 individuals collected by Ernst Mayr himself in 1929. We present a detailed description of reduced representation hyRAD data elsewhere (Linck et al., 2017). On average we were able to align 83.3% of reads to the draft *Halcyon senegalensis* genome, ranging from 35.5% to 92.37% across individuals; this broad range likely reflects high DNA degradation in a handful of samples. Whole genome resequencing data had an average depth of coverage of 5.38x per individual, ranging from 1.92x to 12.12x. Following variant calling and filtering for depth of coverage and quality, a 95% complete data matrix including 37 individuals and both WGS and hyRAD data had 66,917 SNPs, which was further reduced to 10,351 SNPs after thinning to 1 site for every 50 kbp to reduce the influence of linkage disequilibrium. A second matrix of whole genome resequencing data alone had 78,882,912 SNPs, which was reduced to 1,858,764 SNPs after filtering for a minimum depth of coverage of 3x and a minimum quality score of 30.

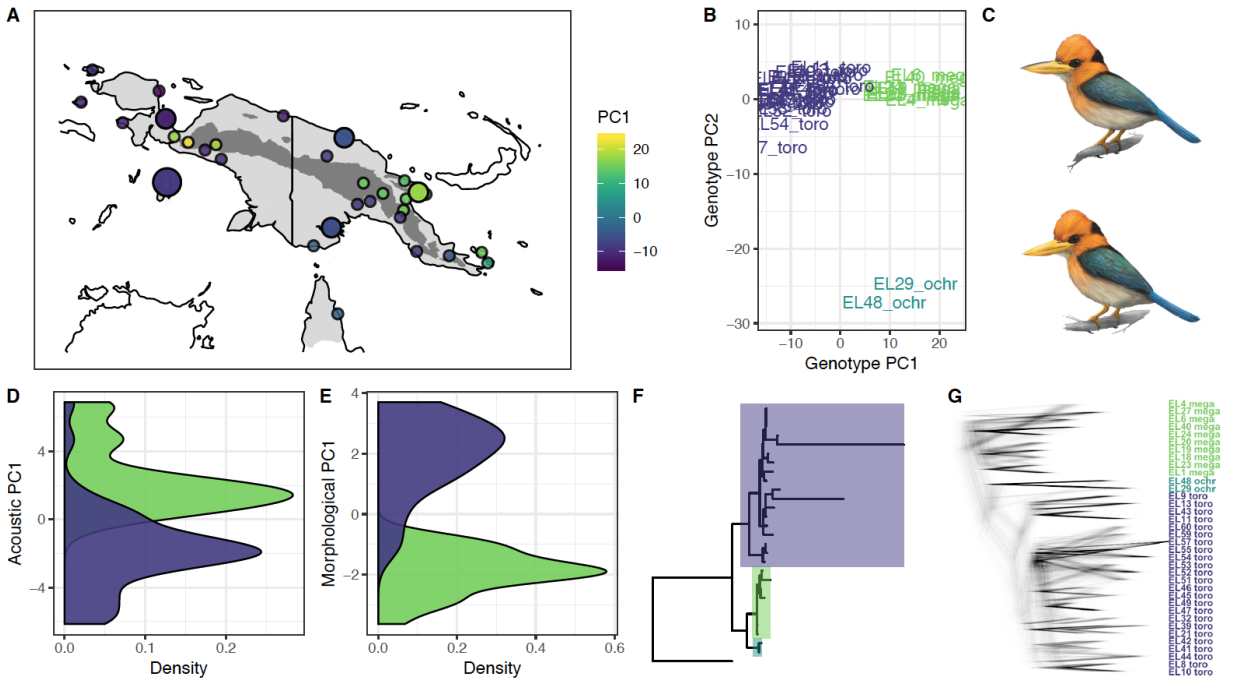

Figure 2.2: **Genomic and phenotypic data provide evidence of assortative mating.** A) Sampling localities for *Syma* kingfishers across New Guinea and Australia, color-coded by genotype PC1 and scaled by number of individuals. B) Principal component analysis of genotypes, colorcoded by the best fit k-means clustering result (K=3). C) Illustration of *S. megarhyncha* (top) and *S. torotoro* (bottom), by Kevin Epperly. D) The first principal component of bioacoustic parameters measured from vocalizations is bimodally distributed by species. E) The first principal component of morphological data is bimodally distributed by species. F) A maximum likelihood phylogeny from near-complete mitochondrial genomes supports reciprocal monophyly of *S. torotoro* and a clade with *S. megarhyncha* and *S. t. ochracea*. Highlighted clades have full bootstrap support. Note *S. t. ochracea* occurs on oceanic islands off southeastern Papua New Guinea. G) A consensus neighbor-joining tree overlaid with trees bootstrapped from 10,000 loci is concordant with relationships revealed by mitochondrial data.

2.4.2 Species limits and phylogeny

Analysis of genome-wide DNA sequence data, morphometrics, and calls supported Syma torotoro and *S. megarhyncha* as distinct, assortatively mating lineages (Figure 2.2). Principal component analysis of genotypes identified elevation (and by extension current species limits) as the primary axis of genetic differentiation, with PC1 explaining 17.02% of total variance and separating *S. torotoro* and *S. megarhyncha* into discrete clusters (Figure 2.2A; Figure 2.2B) with little evidence of hybrid genotypes. PC1 explained 6.31% of total variance and separated insular subspecies *S. t. ochracea* into a third discrete cluster. The best-fit model from a k-means clustering analysis (as identified by BIC scores) perfectly recovered these groups (Figure 2.2B). Using assignments from this best-fit model as population priors, supervised inference of population structure in ADMIXTURE (Alexander et al., 2009) recovered identical clusters (log-likelihood= -104066.81; cross validation error: 0.5974) with no evidence of recent hybridization (Figure 2.5). Unsupervised inference of population structure for K=2 through K=5 assigned clusters that were discordant with both species identity and geography, with high cross-validation error (0.6822-1.113), suggesting the analysis was inappropriate due to uneven sampling (Puechmaille, 2016) or small total sample size.

Analyses of phenotypic data formed discrete clusters concordant with genomic results and consistent with morphological differentiation by elevation. Bill width and depth, tarsus, wing chord, and tail length were significantly larger in *Syma megarhyncha* after correcting for multiple comparisons in Welch's two sample T-tests (all comparisons $p < 1x10^{-7}$), and species was a significant predictor of PC1 in a linear model ($p < 1x10^{-14}$). Following principal component analysis, PC1 explained 81.47% of variance across all five traits. Bayesian Information Criterion (BIC) selected two distinct normal distributions out of normal mixture models (NMMs) fit to PC1 (log-likelihood= -378.0914) (Figure 2.2D). Calls of *S. torotoro* had a significantly higher frequency ($p < 1x10^{-5}$) but did not differ in duration. Species was a significant predictor $p < 1x10^{-5}$) of PC1 in a principal component analysis of the 24 bioacoustic variables quantified in warbleR (Araya-Salas and Smith-Vidaurre, 2017), and

explained 35.72% of total variance. Because NMMs assume independence of observations, we did not perform formal model fitting for bioacoustic data, but a frequency distribution strongly suggests values are bimodally distributed by species identity (Figure 2.2E).

A maximum likelihood phylogeny (Stamatakis, 2014) from near-complete mtDNA genomes further supported the distinctiveness of *S. megarhyncha* and *S. torotoro*, but unexpectedly recovered mainland *S. torotoro* as sister with a clade containing *S. megarhyncha* and insular endemic subspecies *S. t. ochracea* (Figure 2.2F). Within *S. torotoro*, a clade of four individuals with full bootstrap support from the southeast peninsula of Papua New Guinea was separated from the remaining individuals, but with little other apparent geographic structure across the tree. Because we expected the assumption of strict bifurcation underpinning many methods of phylogenetic inference to be explicitly violated by recent gene flow between species, we evaluated evolutionary relationships using resampled neighbor joining trees. Neighbor-joining trees are an empirical description of the distance matrix among individuals, and their behavior under admixture has been described (Kopelman et al., 2013). We recovered the same four major clades as in our mtDNA phylogeny in a consensus neighbor joining tree using a 95% complete data matrix from all individuals passing quality filters. Neighbor joining trees estimated from resampling a subset of these data with replacement indicated substantial discordance within species. Nodes in the consensus tree separating *S. torotoro* from *S. megarhyncha* and *S. t. ochracea*, and *S. megarhyncha* from *S. t. ochracea*, were present in all 500 resampled trees. The bipartition separating four *S. torotoro* individuals from the southeast peninsula from the remainder of the clade was present in 469/500 trees.

2.4.3 Demographic history and introgression

A formal test for introgression, a phylogenetic network analysis, and demographic inference indicate a long history of gene flow between *S. torotoro* and *S. megarhyncha*. We performed ABBA-BABA tests between *S. torotoro* and the three subspecies of *S. megarhyncha* in isolated mountain ranges, and between *S. t. ochracea* and these taxa. These tests can

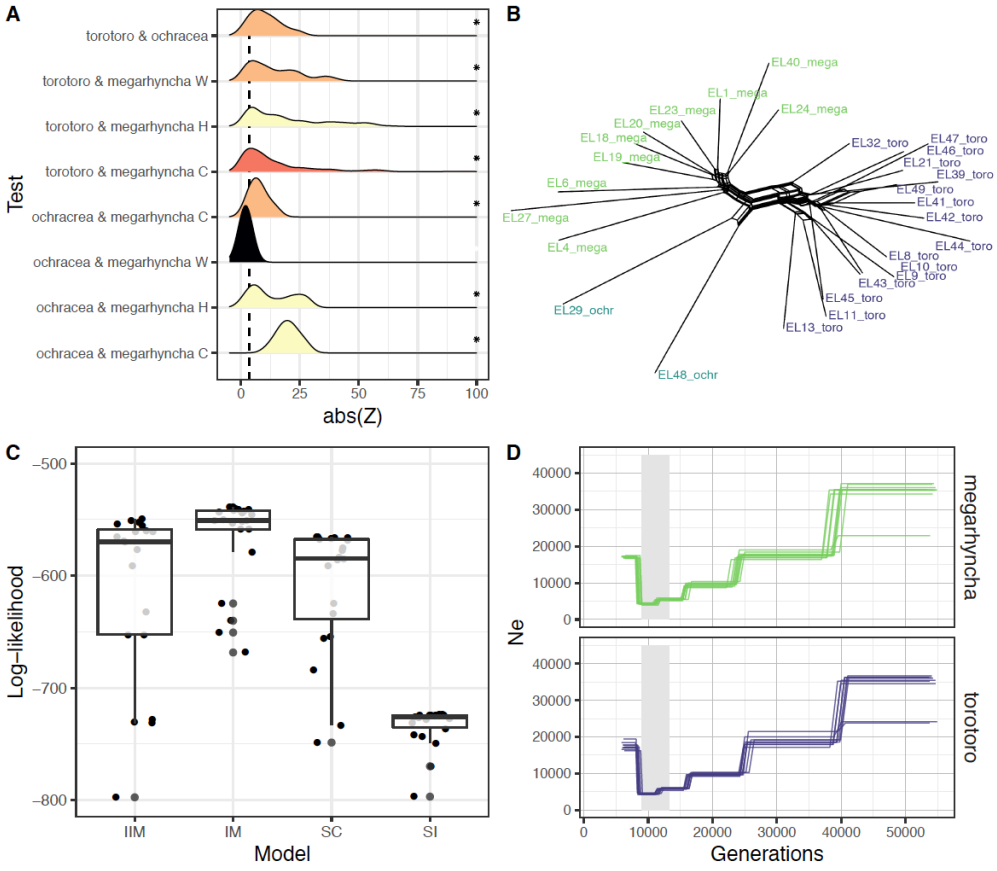

Figure 2.3: **Evidence for long-term introgression between species.** A) Median values for Z-scores from D-statistics ("ABBA-BABA tests") in pairwise comparisons between *S. torotoro* and allopatric *S. megarhyncha* and *S. t. ochracea* populations. Comparisons are color-coded by the proportion of individual combinations in each test that were significant, ranging from 0 to 1.0 and from black (low) to off-white (high). B) A phylogenetic network supported previously inferred species limits but revealed extensive reticulation. C) Demographic inference from the joint site frequency spectrum supported a model of isolation with migration, but with broad uncertainty across replicate parameter optimizations. Models (IIM, IM, SC, and SI) are defined in Methods. D) Trajectories of ancestral population sizes for indicate a bottleneck at the last glacial maximum, and are likely biased by gene flow.

distinguish gene flow from incomplete lineage sorting in discordant genealogies (Green et al., 2010). We found evidence of widespread introgression, with each tested pairwise comparison revealing significant median Z scores, even after correction for multiple comparisons (Figure 2.3A). Of these, the proportion of individual tests that were significant ranged from 0.74-1.0. Intriguingly, there was also evidence of introgression between *S. t. ochracea* and mainland *S. torotoro*, and *S. t. ochracea* and two out of three *S. megarhyncha* populations (Figure 3A). There was no evidence of gene flow between the far western population of *S. megarhyncha* and far eastern *S. t. ochracea*. These results were mirrored by a distance-based phylogenetic network analysis (Figure 2.3B), which showed clear distinctions among the three lineages shaped by large reticulations, a pattern consistent with introgression over long time periods (Martin et al., 2019).

We formally evaluated alternate demographic hypotheses by fitting the empirical joint site frequency spectrum (JSFS) to the its expected distribution using moments v. 1.0.0, which uses ordinary differential equations to model the evolution of allele frequencies (Jouganous et al., 2017). We tested models that shared growth in the most recent of two time periods following an initial divergence but differed in which of the two time periods migration was allowed in, if any (Figure 2.6). Across all parameter optimizations, a model of isolation with migration (IM; e.g., parapatric speciation with incomplete reproductive isolation) had the highest log-likelihood (-538.72), followed by a model of initial isolation with migration (IIM; parapatric speciation leading to strong reproductive isolation), with a maximum log-likelihood of -552.46, and then a model of secondary contact, with a maximum log-likelihood of -565.69 (Figure 2.3C). An allopatric speciation ("strict isolation"; SI) model was poorly supported (maximum log-likelihood -723.79). Both the wide range of likelihoods across runs and large standard deviations associated with parameter values for all models (Table 2.2) indicated difficulty reaching a global optima and / or poor fits for a more complex scenario involving selection.

Parameter estimates varied widely across models, but broadly agreed in indicating greater ancestral than contemporary population sizes, larger populations in lowland species *S. toro-*

toro, and greater gene flow from *S. torotoro* to *S. megarhyncha* than the reverse (approximately 2-17 migrants per generation versus 0-2, respectively). Historical effective population size trajectories inferred in SMC++ (Terhorst et al., 2017) were nearly identical in both species (Figure 2.3D), likely due to the confounding effects of gene flow, but agreed with results from moments in indicating large ancestral effective population sizes and a pronounced bottleneck at the last glacial maximum assuming a two-year generation time (Clark et al., 2009).

2.4.4 Natural selection and genomic divergence

Analysis of WGS data suggests *S. torotoro* and *S. megarhyncha* diverge primarily in small regions of the genome shaped by positive selection. Genome scans of divergence in 50 kb sliding windows were broadly consistent with expectations of speciation with gene flow driven by disruptive natural selection, revealing globally low to moderate genetic divergence (mean F_{ST}=0.0947) defined by 21 autosomal F_{ST} peaks (Figure 2.4A; Figure 2.7A). The Z chromosome showed low interspecific divergence, suggesting a limited role in speciation (Irwin, 2018), though this may represent an artifact of high intraspecific diversity due to misincorporation of reads from the W chromosome in unsexed females. Correlations between summary statistics suggested a role for both structural reductions in recombination and positive selection in shaping F_{ST} peaks. F_{ST} was negatively but weakly correlated with D_{XY} ($p < 1x10^{-15}$, $R^2 = 0.1271$), $\pi_{torotoro}$ ($p < 1x10^{-15}$, $R^2 = 0.2427$), and $\pi_{megarhyncha}$ ($p < 1x10^{-15}, R^2 = 0.3785$) (Figure S3B). D_{XY} was positively and strongly correlated with $\pi_{torotoro}$ ($p < 1x10^{-15}$, $R^2 = 0.9214$) and $\pi_{megarhyncha}$ ($p < 1x10^{-15}$, $R^2 = 0.8495$) (Figure 2.7B). F_{ST} was approximately exponentially distributed, while D_{XY}, $\pi_{torotoro}$, and $\pi_{megarhyncha}$ showed higher median values (Figure 2.7C). However, a method for detecting selective sweeps based on multiple signatures (Alachiotis and Pavlidis, 2018) indicated a strong role for positive selection in generating F_{ST} outliers. First, the value of the composite selective sweep summary statistic μ was significantly greater within peaks than without (Wilcox-Mann-Whitney U test; $p < 2x10^{-15}$) (Figure 2.4B). Second, the total number of

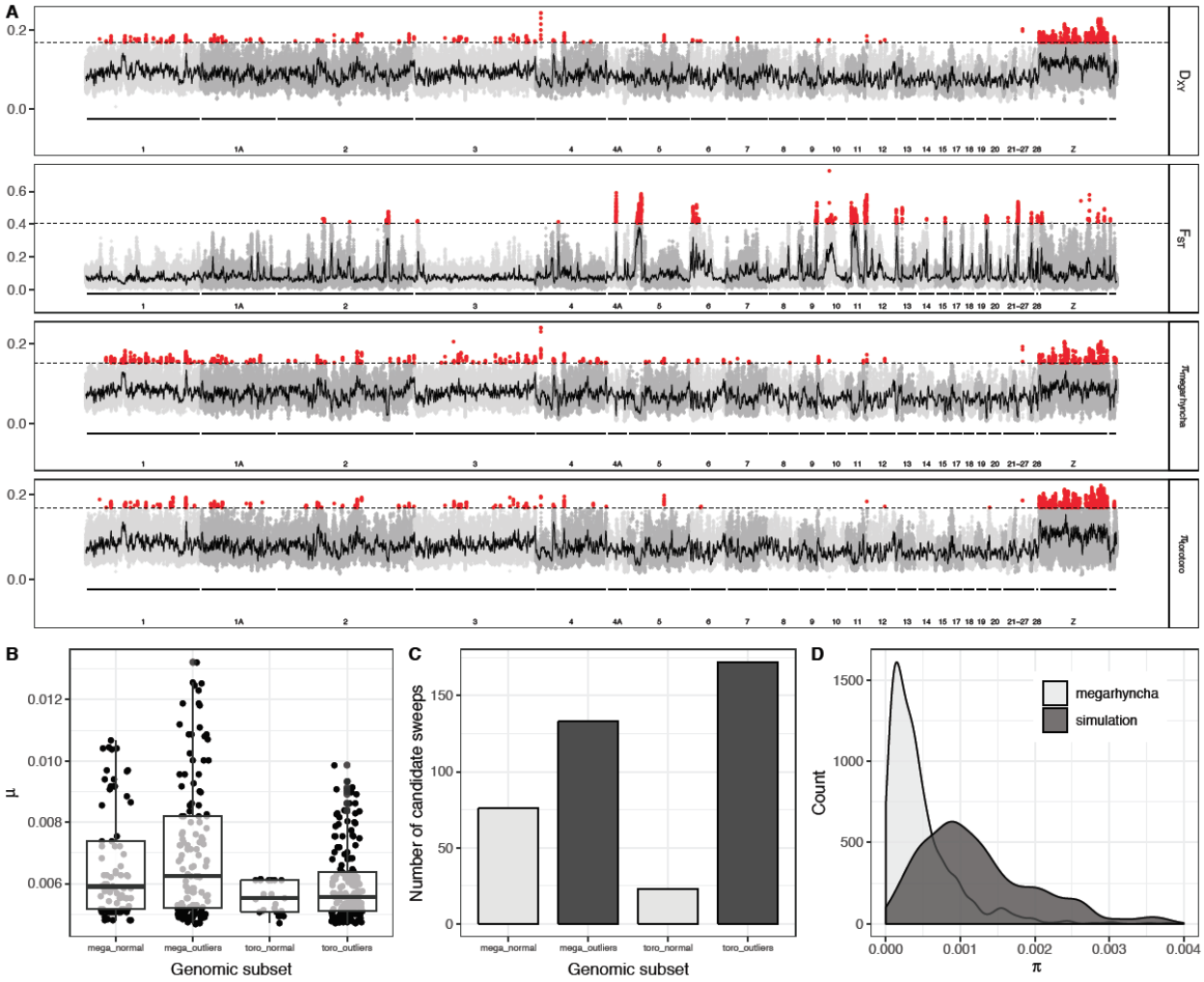

Figure 2.4: **Heterogeneous genomic divergence shaped by positive selection.** A) Relative divergence (F_{ST}), absolute divergence (D_{XY}), and intraspecific diversity ($\pi_{torotoro}$ and $\pi_{megarhyncha}$) in 50 kb sliding windows across the genome. B) Significantly higher values of selective sweep summary statistic μ in F_{ST} peaks relative to a random sample of windows. C) F_{ST} peaks are enriched for the total number of candidate sweeps relative to non-outlier windows. D) Values of π on *S. megarhyncha* chromosome 5 are reduced below expectations from purifying selection alone

candidate selective sweeps within F_{ST} outlier regions was enriched relative to a random subset of nonoutlier windows, given a false positive rate of 0.05 (Figure 2.7C). Lastly, empirical values for $\pi_{megarhyncha}$ on chromosome 5 were significantly lower than expected under purifying selection alone (Wilcox-Mann-Whitney U test; $p < 2x10^{-15}$), based on values generated by forward-time simulations (Hernandez, 2008) (Figure 2.7C).

2.5 Discussion

Speciation across environmental gradients is commonly invoked in explanations of high tropical species richness and the latitudinal biodiversity gradient (Caro et al., 2013; Schneider et al., 1999; Portik et al., 2017; Beheregaray et al., 2015). Tropical elevational gradients have high levels of temporally stable thermal stratification (Janzen, 1967) that has been linked to selection for narrow thermal physiologies (Sheldon et al., 2018), reduced upslope or downslope dispersal (Polato et al., 2018), and high beta diversity (Jankowski et al., 2009). As a result, they have frequently been studied as a stage for this process (Mayr, 1942; Cadena et al., 2012; Funk et al., 2016; Arteaga et al., 2016; Caro et al., 2013; Moyle et al., 2017). Yet previous comparative phylogenetic studies have overwhelmingly supported models of divergence in allopatry followed by secondary contact and range displacement, particularly in vertebrates (Arteaga et al., 2016; Caro et al., 2013; Moyle et al., 2017). Our finding of well-defined species limits (Figure 2.2) in the face of extensive historical and contemporary introgression (Figure 2.3) suggests that selection across elevational gradients is sufficient to maintain species boundaries with little evidence of strong postzygotic isolation. This result provides rare validation of an intuitive and widely cited but poorly buttressed theory: that selection across environmental gradients can serve as a motor for tropical diversification, either as the primary driver of speciation (e.g., in ecological speciation models) or as a force for reinforcement and disruptive selection after the build-up of partial reproductive isolation in allopatry.

We believe *Syma* provides a rare example of speciation with gene flow driven by niche expansion and disruptive selection across an elevational gradient (Hua Xia, 2016), rather

than allopatric speciation by another mechanism. Multiple lines of evidence are difficult to reconcile with an extensive period of isolation followed by secondary contact and niche displacement. Divergence in morphometric traits, the most visible phenotypic difference between *S. torotoro* and *S. megarhyncha* (Figures 2.2D, 2.2E), is largely thought to reflect ecological adaptation in allopatric populations (Ricklefs and Bermingham, 2007; Winger and Bates, 2015). While this may arise as a result of character displacement from competition in populations experiencing secondary contact (Diamond et al., 1989), it presumes sufficient reproductive isolation has developed to permit coexistence without genetic homogenization and the fusion of lineages. In *Syma*, *D*-statistics in replicated pairwise comparisons across both species' full range, (Figure 2.3A), demographic inference (Figure 2.3C), and a phylogenetic network analysis (Figure 2.2B) refute this with evidence for extensive gene flow between species. Further, several lines of evidence suggest gene flow has occurred since nearly their initial divergence. Extensive reticulation in a phylogenetic network paired with an apparent absence of individuals with recent hybrid ancestry in our dataset is consistent with low rates of hybridization over long time periods (Martin et al., 2019), as expected if interspecies mating occurs in the limited area of contact between parapatric ranges (Figure 2.3B). Though this reticulation may also be shaped by incomplete lineage sorting, the relatively old divergence date and small effective population size of *S. megarhyncha* (Table 2.2) suggests introgression is at least partly responsible for this pattern. Similarly, support for an isolation-with-migration model (Figure 2.3C) over a model of secondary contact indicates historical as well as contemporary gene flow. Finally, significant introgression between mainland *S. torotoro* and insular endemic *S. t. ochracea* can be most easily explained by the sorting of introgressed loci following its split with *S. megarhyncha*, which would indicate gene flow between mainland lineages. (We note our data indicate *S. t. ochracea* deserves species status, to be formally proposed in a future manuscript.)

However, we emphasize that for most cases, parapatric speciation (and its vaguer, spatially agnostic variant "speciation with gene flow") are overly simplified models of what is likely a highly dynamic process over evolutionary time scales. Nor are genomic data ever

likely to completely eliminate the possibility of a period of allopatry in the history of diverging lineages (Strasburg and Rieseberg, 2011; Martin et al., 2013). A more likely scenario with similar signatures might consist of numerous interdigitated periods of gene flow and isolation, driven by fluctuating local population sizes or by Pleistocene glacial cycling and its compression of elevational zones throughout New Guinea Hope (2014). Indeed, recent surveys on Mt. Wilhelm and Mt. Karimui in Papua New Guinea found a large gaps in the elevational ranges of *S. torotoro* and *S. megarhyncha* (Freeman and Freeman, 2014; Sam et al., 2014), in contrast to earlier studies (Diamond, 1972a), suggesting that populations are effectively allopatric at short horizontal distances. We suspect periodic gene flow is difficult to distinguish using data from site frequency spectra alone, but may be detected using other summary statistics, a process to be elaborated on elsewhere.

Though we did not identify the targets of selection, our data suggest disruptive positive selection has led to high divergence in small regions of the genome against a background of long-term introgression. These genomic "islands" have become a hallmark of the high throughput sequencing era and have been shown in wide range of nonmodel organisms (Nosil, 2012; Bay and Ruegg, 2017). Early interpretations of the pattern as a clear signature of speciation with gene flow—where F_{ST} peaks correlate to genes for traits under disruptive selection while low F_{ST} regions remain susceptible to introgression—have been complicated by evidence numerous processes can produce similar distributions, including selective sweeps in allopatry or recombination rate variation (Cruickshank and Hahn, 2014; Bay and Ruegg, 2017; Irwin et al., 2018; Via, 2012; Burri, 2017). Using multiple signatures of selective sweeps paired with simulations to establish a false positive threshold, we found F_{ST} peaks were enriched for candidate sweeps in both species (Figure 2.4B, Figure 2.4C), with values of π on *S. megarhyncha* chromosome 5 (the site of one major peak) reduced below expectations under purifying selection alone. Evidence from multiple summary statistics across the same genomic windows can also help tease apart underlying mechanisms in some cases (Irwin et al., 2018): for instance, low absolute differentiation (D_{XY}) in genomic islands can indicate F_{ST} values are inflated by low intraspecific diversity due to reduced recombination, casting

doubt on models of divergence with gene flow (Cruickshank and Hahn, 2014). Here, our data defy easy description, highlighting the limits of this approach. A handful of major F_{ST} peaks stand out against a background of low F_{ST} windows, with a global average of 0.0947 (Figure 2.4A; Figure 2.7A). However, D_{XY} shows only a weak correlation with F_{ST} values (Figure 2.7B): low in some F_{ST} peaks and high in others, consistent with the likely hypothesis that recombination rate, selection against hybrid ancestry, disruptive selection, and gene flow have interacted to form a complex mosaic in the genomes of *S. torotoro* and *S. megarhyncha.* (Given the limitations of short-read sequencing data, we concede these patterns may be influenced by either an undetected structural rearrangement or alignment artifacts.)

As adaptive differentiation in morphology appears to have occurred during the initial stages of lineage divergence (either in the presence of gene flow or accompanied by it shortly afterwards), *Syma* is plausibly a case of ecological speciation *sensu* Nosil and Schluter (Rundle and Nosil, 2005; Nosil, 2012; Schluter, 2009). We propose this may have been facilitated by a so-called "magic trait", or trait under environmentally-mediated selection that also influences reproductive isolation (Servedio et al., 2011). Magic trait models are among the easiest ways to explain speciation with gene flow (Nosil, 2012), and perhaps especially apply to birds, where intrinsic incompatibilities are rare and prezygotic isolation is thought to play a major role in speciation (Edwards et al., 2005; Price, 2008). While we lack strong evidence for a target of disruptive selection or a specific mechanism to link it to reproductive isolation, we speculate selection on body size may also affect mate choice. Morphometric data from *Syma* are consistent with Bergmann's rule and its prediction of larger body size in the higher elevation cooler climate species, *S. megarhyncha* (but see Freeman (2017)). As one of only three kingfisher species found above 2000 m in New Guinea and the only regional kingfisher that is a high elevation specialist, *Syma megarhyncha* is likely to have a thermal physiology under stronger selective constraint for warm environments, requiring greater adaptive divergence in body size to colonize montane environments. An increase in body size might directly lower frequency calls as a biproduct of morphological divergence,

and assortative mating might act on either trait individually or in tandem (Derryberry et al., 2018; Slabbekoorn and Smith, 2002; Zhen et al., 2017).

What does *Syma* reveal about the origin of elevational series of congeners and by extension their significant contribution to tropical montane biodiversity (Freeman and Freeman, 2014)? First, our results suggest disruptive selection across elevational gradients can effectively maintain species limits in the absence of strong postzygotic reproductive isolation, a finding with broad relevance to speciation in tropical mountains regardless of the geographic mode of divergence or levels of gene flow. In a scenario of secondary contact without adaptation to divergent elevational niches, *Syma* lineages would likely have fused. This suggests allopatric divergence in isolation may not be sufficient to drive many speciation events in tropical mountains. Second, aspects of *Syma's* natural history may serve as a guide to where to expect speciation with gene flow in birds: species that are vocal nonlearners, have a conserved climatic niche, and have a small realized range and total area of suitable habitat. While New Guinea is large and geologically complex, it is dwarfed by other tropical montane regions, which potentially have increased odds for speciation in allopatry (Pratt and Beehler, 2015; Price, 2008). Yet even if speciation across elevational gradients remain a rare exception among birds, the conditions that make it possible in *Syma* are more common in other taxa. Indeed, preliminary studies suggest it may be a much more common mechanism in amphibians, insects, and plants (Funk et al., 2016; Elias et al., 2009; Arteaga et al., 2016; Chapman et al., 2013). We highlight the importance of natural history studies of poorly known tropical organisms in establishing candidates for further investigation with genomic and experimental approaches.

Ernst Mayr's emphasis on geographic isolation profoundly shaped the study of speciation and diversification, establishing the primacy of divergence in allopatry and highlighting the significance of coexistence in sympatry to species concepts and speciation theory (Coyne, 1994; Nosil, 2008a) Though famously a skeptic of sympatric speciation and its relatives (Mayr, 1963), he retained an appreciation of ecological factors in population divergence (Nosil, 2008a)—contrasting perspectives shaped by his foundational experience as an or-

nithologist, natural historian and systematist in New Guinea. Yet contemporary speciation research integrating genomic data with traditional analyses of phenotype and distributional data has only recently been applied to the New Guinea birds Mayr knew so well (Stryjewski and Sorenson, 2017), and continues to be difficult to implement due to massive logistical hurdles. Much as the study of ancient DNA has revolutionized our understanding of human prehistory (Green et al., 2010), widespread use of whole genome sequences from historic museum specimens has the potential to reshape our understanding of the speciation process in understudied tropical regions with few contemporary data and pressing conservation challenges. As this occurs, we expect much of Mayr's seminal work to gain new significance, as case studies like *Syma* highlight the continued relevance of the spatial organization of populations while enriching previously simple narratives of the role of selection and gene flow in the origin of species.

2.6 Acknowledgements

We thank generations of New Guinean field assistants—traditional landowners and stewards of the island's birdlife—without whose help this paper would have been impossible to write. For tissue loans, we thank L. Josef at ANWC, K. Zykowski at YPM, R. Moyle and M. Robbins at KUMNH, P. Sweet at AMNH, and R. Prys-Jones at NHMUK-Tring. For help arranging fieldwork, we thank A. Mack, G. Kapui, J. Robbins, N. Gowep, B. Beehler, L. Dabek, N. Whitmore, F. Dem, S. Tulai, B. Iova., and V. Novotny. We thank Alex Wiebe for assistance measuring specimens, and thank C.J. Battey for many discussions, help with analyses, and inspiration for data visualization. This work was supported by NSF Doctoral Dissertation Improvement Grant #1701224 to J. Klicka and E.B.L, a NDSEG Fellowship to E.B.L., and by NSF DEB #0108247 to J.P.D.

2.7 Data availability

All code written for this study, all processed data matrices, and supplemental material can be found at `https://github.com/elinck/syma_speciation/`.

2.8 Supplemental Material

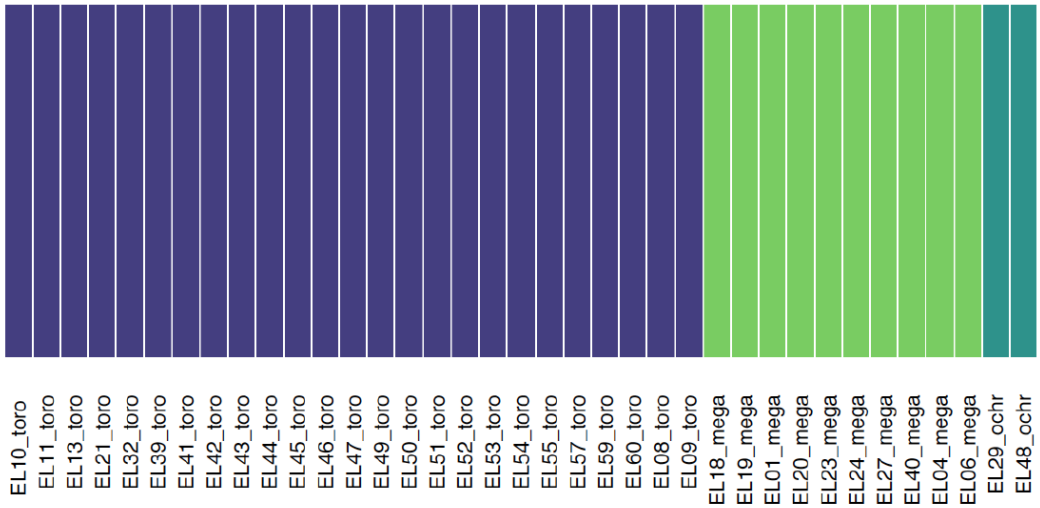

Figure 2.5: Supervised population assignments from ADMIXTURE for K=3.

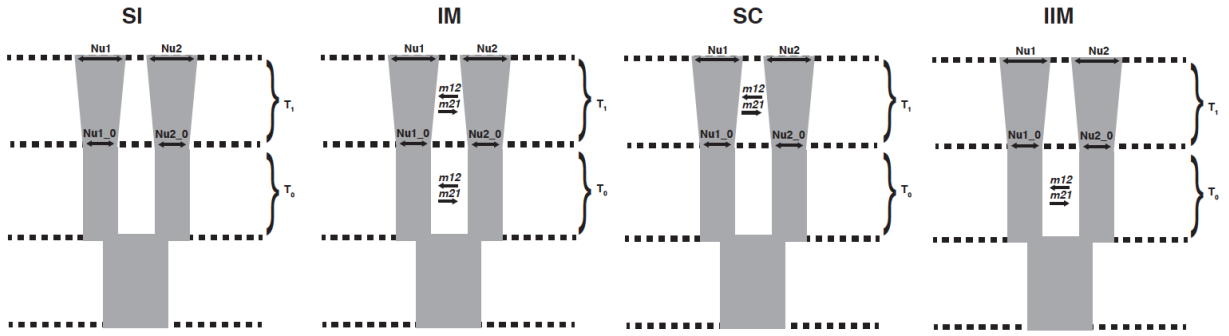

Figure 2.6: Diagrams of demographic models implemented in moments.

Table 2.2: Time scaled parameter values and standard deviations for the maximum likelihood optimization of each model tested with joint site frequency spectrum-based demographic inference in moments.

Parameter	IM (SD)	IIM (SD)	SC (SD)	SI (SD
N_{meg}	106049278.19 (10594095899.99)	60579620.96 (27780976.82)	1000897.40 (4239177.62)	9238.85 (43846.68)
N_{tor}	159173.09 (86403707.39)	2545587.85 (10952902.31)	22683700.58 (1101240437.82)	36584.85 (205321.52)
N_{meg}	19815.13 (1630633.17)	54725.12 (302722.54)	11001.51 (2176.37)	3241053.20 (18733219.57)
N_{tor}	12292.60 (363945.45)	149968.18 (733993.96)	29232.10 (72528.20)	5745.92 (35692.55)
T_0	2136554.73 (969702508.95)	93825473.64 (57666506.07)	17630682.86 (903397204.23)	1270.08 (6066.55)
T_0	77060.64 (4003285.38)	60728.46 (295712.88)	66475.59 (377322.25)	1209.56 (7760.79)
m_{meg_tor}	0.28 (106.22)	0.14 (0.01)	1.81 (2.62)	NA
m_{tor_meg}	2.03 (15.98)	17.62 (25.08)	3.14 (0.09)	NA

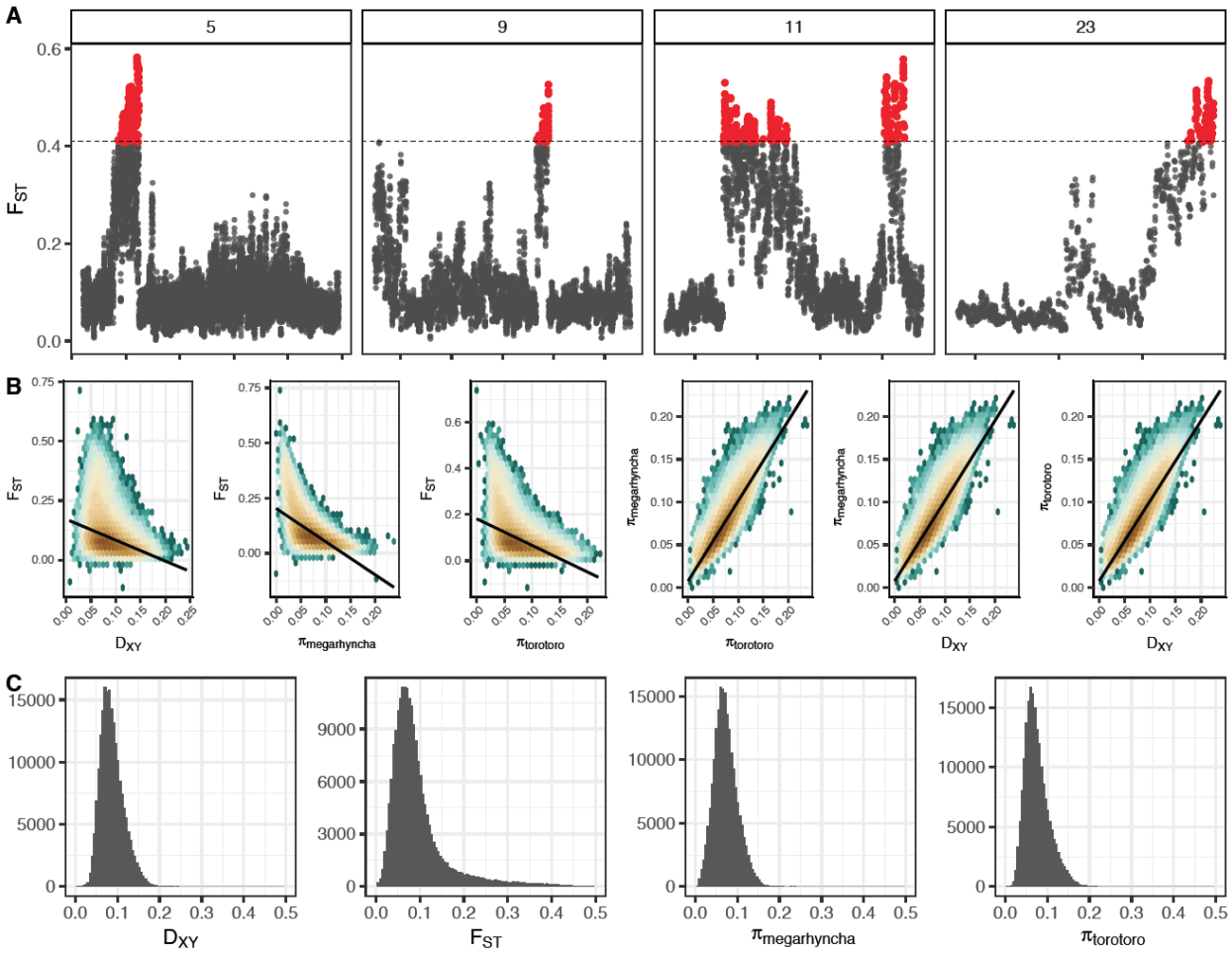

Figure 2.7: A) Pronounced peaks of relative genomic divergence on four chromosomes. B) Correlations between summary statistics of genomic diversity and divergence. C) Distributions of summary statistics.

Chapter 3

ON THE RELATIVE EASE OF SPECIATION WITH PERIODIC GENE FLOW

*C.J. Battey is a coauthor on a version of this manuscript in preparation for publication.

3.1 Abstract

Population genetic theory and genomic data from a wide range of taxa suggest speciation with gene flow between incipient lineages is common. However, in most cases it is unknown whether gene flow occurs throughout the process of speciation or if current patterns of diversity reflect admixture on secondary contact after partial reproductive isolation has evolved in allopatry. Though cycles of isolation and contact are thought to have played a major role in shaping extant biodiversity, the genomic consequences of this process have been rarely studied. Here we develop a simple model of speciation through Bateson-Dobzhansky-Muller incompatibilities in the face of periodic gene flow, and validate our model with forward time simulations. We additionally use empirical atmospheric CO_2 concentration data from the Vostok Ice Cores to simulate cycles of isolation and secondary contact in a tropical montane landscape, and ask whether they can be distinguished from a standard isolation-with-migration model by summary statistics or joint site frequency spectrum-based demographic inference. We find speciation is more likely under periodic migration rather than constant gene flow given equivalent effective migration (Nm), and that this process leaves a distinct signature in common population genetic summary statistics. In contrast, demographic inference from the site frequency spectrum fails to distinguish between periodic migration and isolation-with-migration. Our results suggest speciation with periodic gene flow may be a common force in generating species diversity through Pleistocene climate cycles, and highlight the limits of simple models of speciation with gene flow.

3.2 Introduction

Eight decades after the modern synthesis, the relative roles of gene flow, geography, and natural selection in speciation elude easy synthesis. For most of the 20th century, divergence in strict allopatry was assumed to be the dominant, if not the only, mode of speciation in most taxa, leading to an emphasis on the geography of diverging populations and an implicit suggestion of a major role for genetic drift (Dobzhansky, 1937; Mayr, 1942, 1963; Coyne and Orr, 2004; Provine, 2004). While a burgeoning body of theory demonstrated the plausibility of speciation with gene flow in a range of circumstances (Smith, 1966; Felsenstein, 1981; Gavrilets, 2003), a lack of clear empirical examples and the related difficulty of disproving a null hypothesis of allopatric speciation did little to contest this paradigm.

More recently, a renewed emphasis on the role of natural selection in speciation in the context of adaptive radiations and "ecological" speciation has questioned the requirement of strict isolation (Schluter, 2001; Via, 2009; Nosil, 2012). The rise of genomic datasets from a wide array of model and nonmodel organisms and the concordant development of sophisticated statistical tools for demographic inference has further complicated previous assumptions (Nosil, 2008b). Coalescent theory and genome-wide genetic markers provide the basis for simultaneous model selection and inference of parameter values, now implemented in a range of computational tools (Nielsen and Wakeley, 2001) (Hey and Nielsen, 2007; Gutenkunst et al., 2009; Hey, 2010; Jouganous et al., 2017). As much as an early consensus from the current proliferation of studies applying these methods can be gleaned, it appears that gene flow between lineages at various points in the speciation continuum is more common than previously assumed (Mallet, 2008; Nosil, 2008b; Strasburg and Rieseberg, 2008; Cui et al., 2013; Martin et al., 2013; Kumar et al., 2017; Linck et al., 2019).

While more complex models of speciation dynamics can be applied using these methods, e.g., by allowing parameter values to vary at different loci across the genome (Rougeux et al., 2017), model selection has largely treated migration (m; the probability a given allele is an immigrant) as an average rate in one of a maximum of two time periods (Figure 3.1) (Sousa

and Hey, 2013). Traditional isolation with migration models are therefore distinguished from secondary contact by the presence of a time period (T_1 to T_2) where m=0. Even this relatively sophisticated model is clearly a dramatic simplification of speciation dynamics in most systems, however, where alternative assumptions of continuous gene flow (recurrent migration every generation) or strict isolation are unrealistic in most cases. For example, divergence in allopatry is widely believed to be the dominant mode of speciation in birds (Mayr, 1963; Price, 2008). Yet the extreme vagility of many bird taxa poses the question of how readily geographic classifications of speciation map on to realized rates of gene flow, leading some workers to strongly advocate for strictly process-based definitions (Fitzpatrick et al., 2008; Mallet, 2008). Further complications arise from the imprecise, redundant language associated with the study of speciation itself (Harrison, 2012).

An alternative to either divergence in strict isolation or in the face of recurrent migration involves alternating phases of interbreeding and isolation, i.e., speciation with intermittent (or "cyclical" / "periodic") gene flow. Cyclical processes are common over geologic, evolutionary, and ecological time scales, and include predator-prey dynamics (Elton and Nicholson, 1942), glacial cycling (Roy et al., 1996), ecological succession (Levin and Paine, 1974), and fluctuating population sizes (Vucetich et al., 1997). Yet the role of cyclical processes in generating or retarding evolutionary change has seen relatively little attention (Duckworth and Semenov, 2017). Ehrendorfer (1959) proposed that "differentiation-hybridization" cycles were responsible for evolutionary patterns in the flowering plant genus Achillea, viewing hybridization as a strictly homogenizing force, an idea further developed by Rattenbury (1962) as an explanation for the diversity and persistence of the New Zealand flora. In phylogeography, Pleistocene glacial cycles in Boreal regions and the Amazon have been invoked to explain both diversification (Lovette, 2005) and patterns of genetic diversity and population genetic structure (Klicka and Zink, 1999), though the link between population subdivision and speciation remains unclear (Harvey et al., 2017b).

Recently, He et al. (2019) proposed that cycles of gene flow and isolation constituted a new model of speciation, which they term mixing-isolation-mixing (or MIM), and suggest it

can lead to accelerated rates of diversification. Given its relaxed requirements and flexible application to a range of potentially stochastic histories, speciation with periodic gene flow is plausibly more common than either speciation in strict allopatry or with continuous gene flow. Furthermore, recent studies on hybridization as a generative force in evolution, through either homoploid hybrid speciation (Gompert et al., 2006; Brelsford et al., 2011; Schumer et al., 2014, 2018a) or adaptive introgression (Delmore et al., 2015; Norris et al., 2015; Racimo et al., 2015; Irwin et al., 2018) suggest the interaction of gene flow and isolation could promote accelerated speciation under some circumstances.

If the MIM model (hereafter "speciation with periodic gene flow") is indeed common and a more realistic description of speciation dynamics in many circumstances, a more explicit description of its features and assessment of its likely consequences and genomic signature will be useful for a broad range of evolutionary biologists. Here, we use theory and simulations to ask 1) if speciation is indeed easier to achieve under periodic migration rather than continuous migration given equivalent effective migration (Nm); 2) how time between migration pulses scales with waiting time to speciation; 3) whether periodic gene flow determined by a realistic scenario of glacial cycling leaves a distinct signature in commonly applied summary statistics; and 4) if joint site frequency-based approaches to demographic inference can distinguish divergence with periodic migration from traditional models of speciation with gene flow.

3.3 Methods

3.3.1 Analytical model

To evaluate the relative ease of speciation with periodic gene flow compared to speciation with continuous gene flow, we compare waiting times to speciation (average time until reproductive isolation develops between two diverging populations) using simple analytical models. First, we develop a general expectation of waiting time given two constant speciation rates. Consider a scenario of alternating periods of migration (at a constant rate $m>0$) and isolation ($m = 0$) between populations K_1 and K_2, which we model as n alternating

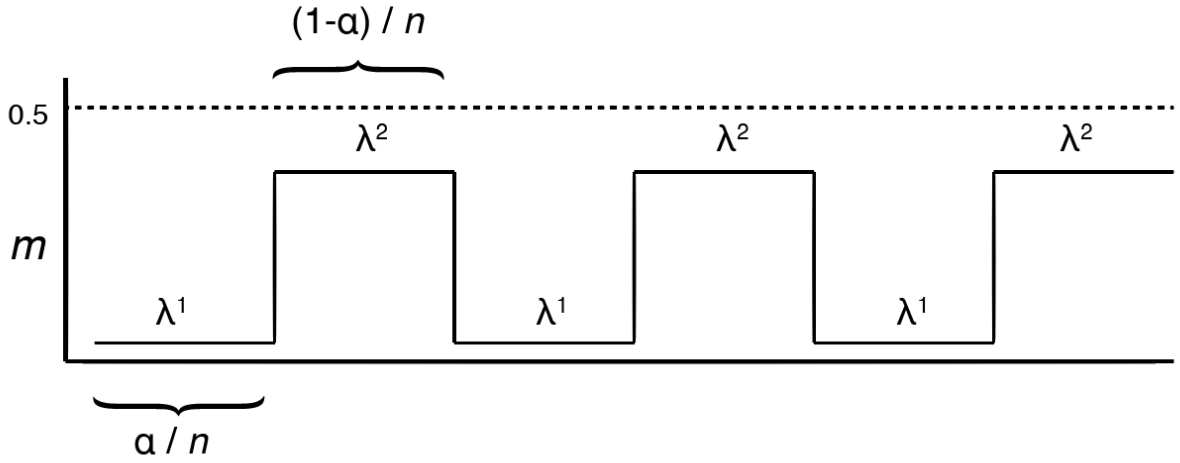

Figure 3.1: **A simple model of speciation with periodic gene flow**. Parameter values: m=probability an allele represents a migrant in a given generation; α= total time spent in isolation; $1 - \alpha$= total time spent exchanging migrants; n=total number of time periods; λ^1= speciation rate in isolation; λ^2= speciation rate with gene flow.

states of equal length , characterized by their different expected times to speciation (Figure 3.1). Let the rate of speciation (i.e., the probability of speciation occurring in a given time period τ) equal the reciprocal of the waiting time to speciation (either T^a, meaning the waiting time to speciation in isolation, or T^p, meaning the waiting time to speciation with recurrent migration), which we denote λ^1 and λ^2,respectively. The mean expected waiting time to speciation is the reciprocal of the weighted sum of the speciation rates under isolation and under migration:

$$T^t = \frac{n}{\sum_{i=1}^{n} \tau\lambda^1 + \tau\lambda^2} \quad (1)$$

To explore the behavior of Equation 1 under different regimes of migration and isolation, we input speciation rates determined by Gavrilets' neutral Bateson-Dobzhansky-Muller icompatibility (BDMI) model of the evolution of genetic incompatibilities on a holey adaptive landscape (Dobzhansky, 1936; Gavrilets, 2003). Full formulae and justification are provided elsewhere (Gavrilets et al., 1998; Gavrilets, 1999, 2003); a brief description of the model follows:

Consider a panmictic ancestral population of diploid organisms fixed for genotype $AABB$ without recombination and then split into two completely isolated daughter populations, K_1 and K_2. In K_1, let A mutate to a and B mutate to b unidirectionally at an equal rate of μ per generation. The combination of alleles a and B result in a single genotype is lethal or otherwise precludes hybrid viability; A and b remain compatible. Speciation is inevitably complete with when the genotype $aabb$ is fixed in the only population with mutation (by drift alone). We define T as the time to speciation, or average waiting period in generations to go from the ancestral state to complete reproductive isolation. In the absence of positive selection or gene flow, i.e., a scenario of allopatric speciation by mutation and drift alone, the average waiting time to speciation will be the time to fixation of two neutral alleles (a and b), which is approximately two times the reciprocal of its mutation rate and unrelated to effective population size (Nei, 1976):

$$T^a = 2 * \frac{1}{\mu} = \frac{2}{\mu} \text{ (2)}$$

We next use Gavrilet's (2003) extension of this model to describe parapatric speciation, i.e., speciation with limited gene flow ($0<m<0.5$) between two demes. Following subdivision of K_1 and K_2, a portion m of K_1 each generation is supplied by immigrants from K_2 with ancestral genotype $AABB$. Again assuming divergence in K_1 is driven only by neutral mutation at a per generation rate of μ for both alleles, and assuming that m is much larger than the mutation rate, the average waiting time to speciation is given by:

$$T^p = \left(2 + \frac{m}{\mu}\right)\frac{1}{\mu} \approx \frac{m}{\mu^2} \quad (3)$$

Given equal time is spent exchanging migrants as in allopatry, we calculate the arithmetic mean of these speciation rates (λ^t) :

$$\lambda^t = \frac{1}{2} \times \frac{\mu}{2} + \frac{1}{2} \times \frac{\mu^2}{m} = \frac{\mu}{4}\left(\frac{m}{m}\right) + \frac{\mu^2}{2m} = \frac{2\mu m + 4\mu^2}{8m} = \frac{2\mu(m+2\mu)}{8m} \text{ (4)}$$

The average waiting time across all time periods is given by its reciprocal:

$$T^t = \frac{8m}{2\mu(m+2\mu)} \text{ (5)}$$

We now consider speciation with periodic gene flow if n time periods τ are unequal. Let α equal the proportion of time spent in isolation and $1-\alpha$ equal the proportion of time exchanging migrants at a constant rate $m>0$, and let the rate of speciation equal the reciprocal of the expected times to speciation T^a and T^a, given by λ^1 and λ^2. The total expected waiting time to speciation is again simply the reciprocal of the weighted sum of the speciation rates:

$$T^t = \frac{n}{\sum_{i=1}^{n} \alpha\lambda^1 + (1-\alpha)\lambda^2} \text{ (6)}$$

Given Equations 2 and 3, total expected waiting time to speciation can be calculated by:

$$T^t = \frac{n}{\sum_{i=1}^{n} \alpha \left(\frac{\mu}{2}\right) + (1-\alpha)\left(\frac{\mu^2}{m}\right)} \text{ (7).}$$

3.3.2 Simulating cyclical speciation

We validated our simple models using forward-time evolutionary simulations implemented in SLiM v. 3.1 (Haller and Messer, 2019), with diploid genotypes, constant population size, and non-overlapping generations. All parameters were chosen to closely approximate the model in Gavrilets (2003). For all simulations, we set a mutation rate of $1x10^{-6}$ and a recombination rate of $1x10^{-8}$. We modeled BDMI loci as two sites 1 bp in length on either end of a 100 bp long chromosome; each of the three genomic "regions" (BDMI locus A, BDMI locus B, and a 98 bp intron) on this chromosome had a specific mutation type, and both BDMI loci had a fitness coefficient of 0.5 to reduce computational time. While this selective advantage violates the assumption of neutrality behind Equations 2 and 3 (Nei, 1976; Gavrilets, 2003) and therefore precludes direct comparison with analytical values, relative expected waiting times to speciation should remain valid assuming a constant fitness coefficient. We considered speciation complete when mutations were fixed in both BDMI loci in population K_2, and did not end the simulation until this occurs; mutations were prevented from occurring on BDMI loci in population K_1, which solely used as a donor of ancestral alleles in simulations involving gene flow. Outputting the final generation (i.e., waiting time to speciation) each time, we ran 25 replicates of all models. To simulate allopatric speciation, we used a single population of size n=50. To simulate parapatric speciation, we established two populations of size n=50 each, and set unidirectional migration from population K_1 to population K_2. We simulated speciation under periodic gene flow using three different values of α (the proportion of time spent in allopatry): 0.50, 0.1, and 0.01. We modified the migration rate parameter m across each value of α to fix the total effective migration (Nm) across the entire simulation, and initiated periods of allopatry every other generation, every 10 generations, and every 100 generations respectively. We again considered speciation

complete with the fixation of both BDMI loci in K_1. SLiM scripts for all simulations are available at `https://github.com/elinck/speciation_periodic_migration`.

3.3.3 Simulating glacial cycles of isolation and contact

As a distinct goal from our analytic model of speciation and our forward time simulations to validate it, we were interested in whether cycles of gene flow and isolation between diverging populations would leave unique genomic signatures given biologically realistic parameter values. To test this, we simulated population divergence and secondary contact both 1) mediated by Pleistocene glacial cycles and 2) under a standard isolation-with-migration model using the coalescent simulator msprime v. 0.7.1 (Kelleher et al., 2016). We determined the timing and duration of gene flow between populations using empirical atmospheric CO_2 concentration values from the Vostok Ice Core dataset (Petit et al., 1999). A collaborative drilling project in East Antarctica, the Vostok Ice Cores provide direct records of historical variation in atmospheric trace-gas composition through entrapped air inclusions, and cover four glacial cycles from 417,160 to 2,342 years before present (Petit et al., 1999).

We simulated a $5x10^7$ bp region for two populations of size $n = 1x10^5$, using a recombination rate of $1x10^{-8}$, mutation rate $1x10^{-8}$, and allowing 10 migrants per generation (i.e., m=0.0001) when atmospheric CO_2 fell below 250 ppm (Figure 3.2). This configuration effectively mimics connectivity dynamics in a tropical montane landscape, where cooler temperatures allow the expansion of forest habitat between adjacent peaks. We started and concluded the simulation with periods of isolation, allowing 8 periods of migration of varying duration in total. After completing each simulation, we calculated Wright's F_{ST} between populations, and then used the approximation $F_{ST} \approx \frac{1}{4mN\left(\frac{n}{n-1}\right)^2+1}$ (Wang, 2004) to determine a constant migration rate resulting in equivalent equilibrium F_{ST} for a paired simulation under a standard isolation with migration model (i.e., a model with continuous gene flow). We otherwise used identical parameters as our periodic migration simulation. In total, we ran 100 replicates of each scenario. We compared patterns of genetic variation between simulations by calculating a range of standard summary statistics both between and within popula-

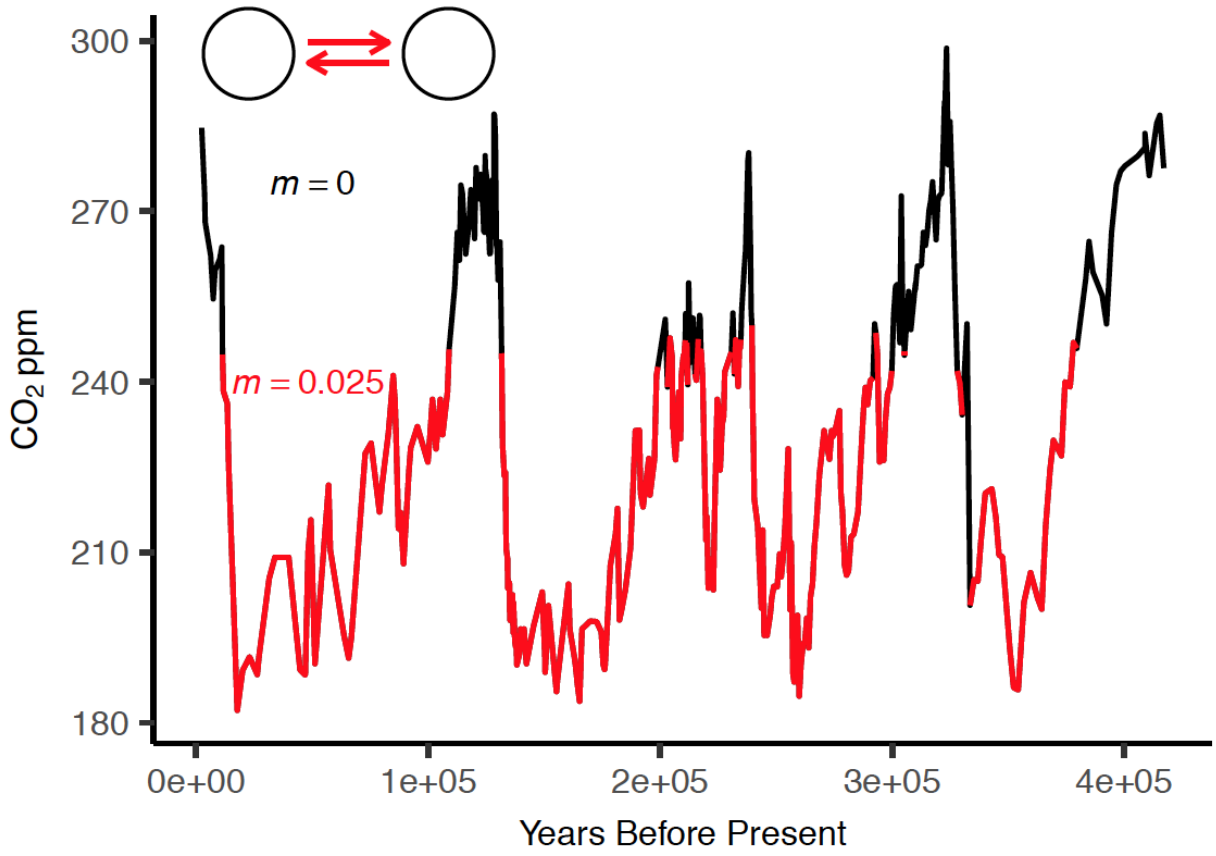

Figure 3.2: Atmospheric CO_2 concentration data from the Vostok Ice Cores, color coded by migration rate in msprime simulations of populations diverging with periodic gene flow.

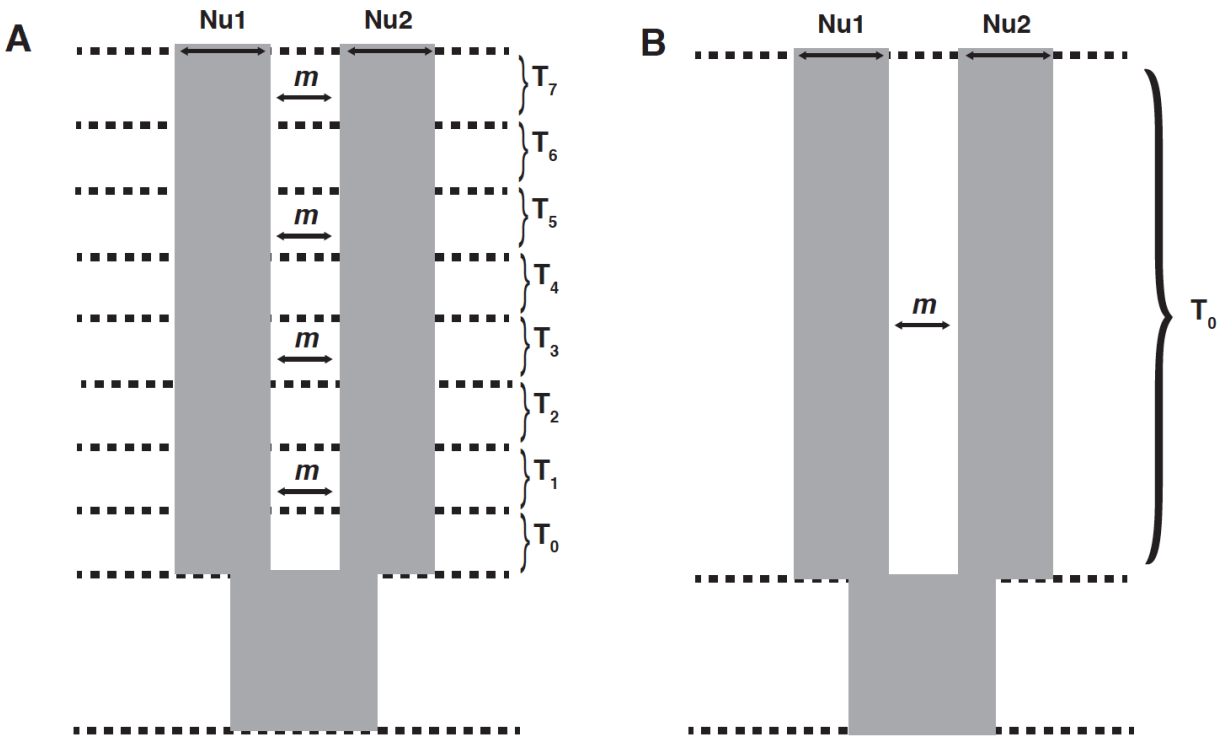

Figure 3.3: Demographic model parameters implemented in moments for A) periodic gene flow and B) constant gene flow (i.e., isolation-with-migration). Nu_1 and Nu_2 are parameters for the effective population size of populations 1 and 2, respectively; m is the symmetrical migration rate during a given time period T_0 through T_7.

tions using scikit-allel (Miles et al., 2019) implemented in custom Python scripts (available at `https://github.com/elinck/speciation_periodic_migration`). These statistics are: the number of segregating sites (SNPs); mean pairwise genetic distance (π); Tajima's D; Watterson's θ; observed heterozygosity; Weir & Cockerham's F_{ST}; D_{XY}, the average length of identical-by-state haplotype blocks; and the skew of identical-by-state haplotype blocks.

3.3.4 Demographic inference

As speciation processes are often studied using joint site frequency spectrum-based (JSFS) demographic inference, we were used our coalescent simulations to see whether this family of methods could distinguish between a model of periodic gene flow and a standard isolation-with-migration model using moments v. 1.0.0 (Jouganous et al., 2017). To model the evolution of allele frequencies under different demographic scenarios, moments analytically solves for the expected site frequency spectrum using numerical solutions of an appropriate diffusion approximation of allele frequencies (Jouganous et al., 2017). We defined two models which closely mimicked the demographic history of our msprime simulations: a periodic migration model, which allowed four time periods of migration interdigitated with periods of isolation, for a total of 8 time periods following population divergence; and an isolation with migration model (Figure 3.3). Both models featured symmetrical migration and independent effective population sizes (parameters m, $Nu1$, and $Nu2$). We initially optimized parameters using the "optimize_log" method, and ran 25 additional replicates with a 1-fold perturbation of parameter values to ensure convergence. As model complexity made a likelihood ratio test inappropriate, we compared the distribution of log-likelihood values between models using a Wilcox-Mann-Whitney U test.

3.4 Results

3.4.1 Analytical model

We plot T^t against μ for different values of α in Figure 3.4, generated by Gavrilet's models of speciation by BDM incompatibilities. Though simplified, these equations capture the intuitive relationship between allopatric and parapatric speciation, e.g., that moderate gene flow erodes differences between diverging populations and results in a longer average waiting time to speciation. For example, assuming a mutation rate of $\mu = 1x10^{-8}$ and a migration rate of $m = 0.1$, $T^a = 2x10^8$ generations under a model of allopatric speciation and $T^p = 1x10^{15}$ in a under a model of parapatric speciation—i.e., parapatric speciation takes five

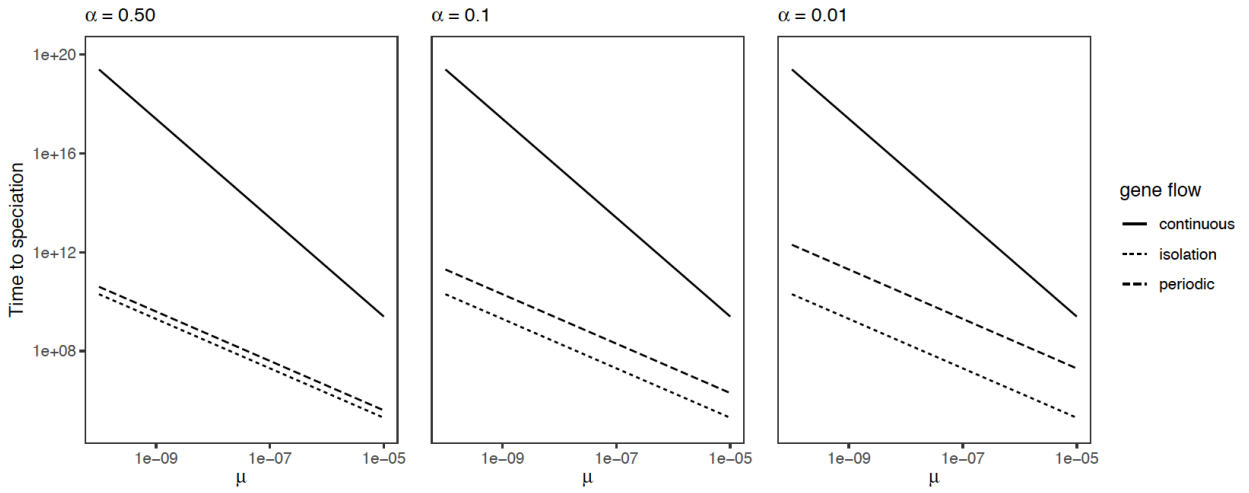

Figure 3.4: Analytical results for the relationship between BDM loci mutation rate and waiting time to speciation under alternate models of speciation, by proportion of total divergence time spent in allopatry (α).

million times longer. (In the absence of positive selection, speciation is clearly unlikely in both scenarios.) Notably, speciation is more likely under a model of periodic gene flow than continuous gene flow given a constant number of migrants across the entire divergence period for all three values of α. Further, as α approaches $1 - \alpha$ in value, the average waiting time to speciation with period migration approaches its value under strict isolation.

3.4.2 Simulating cyclical speciation

Our simulation of speciation by BDM incompatibilities broadly supported the predictions of our analytical model. The median time to speciation was lowest in isolation, highest under constant migration, and intermediate under periodic migration becoming increasingly longer as the proportion of time spent in allopatry was decreased (Figure 3.5). Interestingly, despite the expected trend in median waiting time, the outlier lowest waiting time values across all simulations occurred under periodic migration. These data hint at a bimodal distribution; given our limited number of replicates, we suggest it is an artifact of sampling.

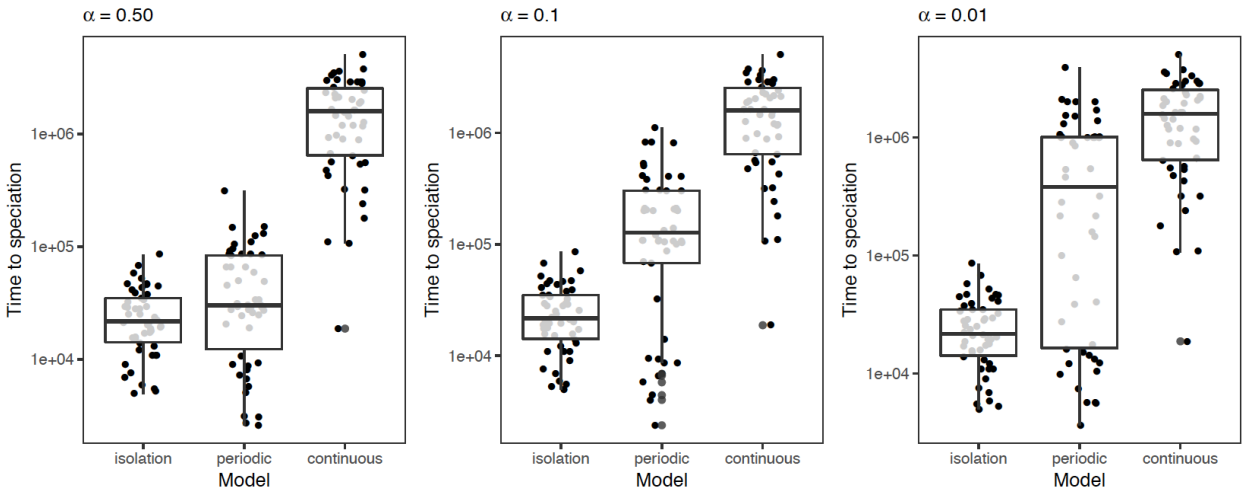

Figure 3.5: Forward time simulations of the waiting time to speciation by BDM incompatibilities under alternate models of speciation and different proportions of total divergence time spent in allopatry (α).

The interquartile range (IQR) was greatest when $\alpha = 0.01$ and lowest when $\alpha = 1$. However, the distribution of waiting time values for $\alpha = 0.01$ is bimodal with right skew, suggesting its low IQR may be an artifact of sample size and that variance is negatively correlated with α, reflecting stochasticity in the waiting time to fixation in isolation.

3.4.3 Simulating glacial cycles of isolation and contact

Despite controlling for equilibrium F_{ST} (which was identical between periodic and continuous migration scenarios; Wilcox-Mann-Whitney U test, $p = 0.89$), summary statistics could easily distinguish simulations of periodic and continuous migration (Figure 3.6). The total number of SNPs, π, Watterson's θ, Tajima's D, observed heterozygosity, and D_{XY} were all significantly higher in continuous migration simulations (Wilcox-Mann-Whitney U test, $p < 2.2x10^{-16}$). Identical-by-state haplotype blocks both between and within populations were significantly longer under periodic migration ($p < 2.2x10^{-16}$). The skew of identical-by-state haplotype blocks was greater within populations under periodic migration ($p < 2.2x10^{-16}$)

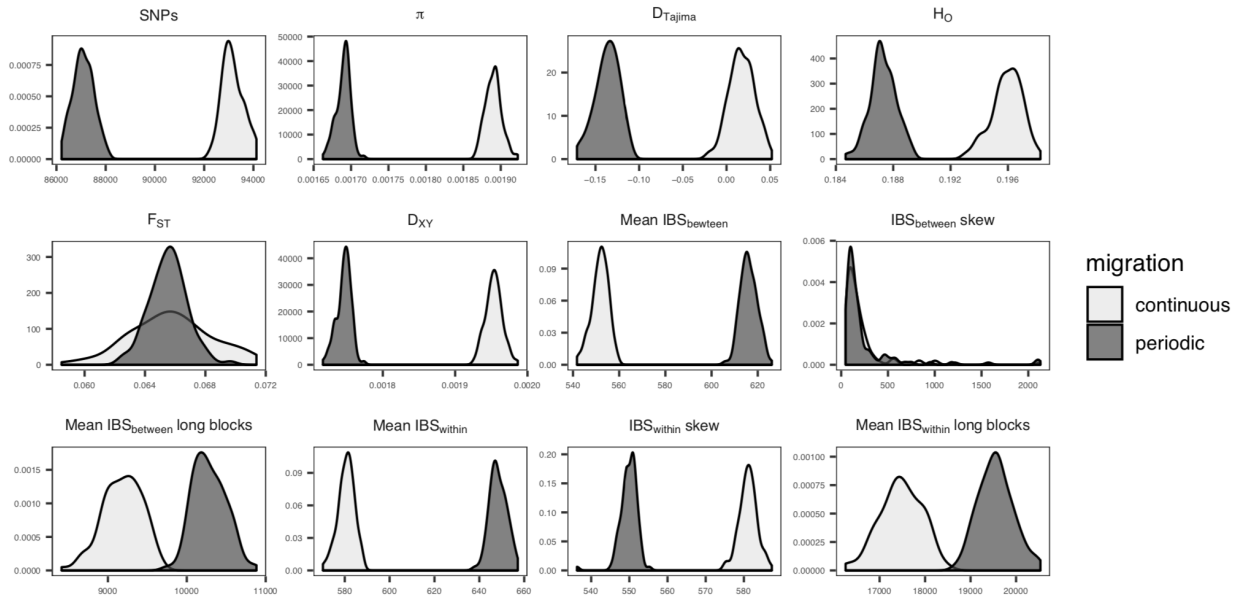

Figure 3.6: The distribution of summary statistics from simulations of periodic gene flow determined by Vostok Ice Core atmospheric CO_2 concentrations ("periodic") and a standard isolation-with-migration model ("continuous").

and between populations under continuous migration, though distributions were broadly overlapping ($p = 0.04978$). There was no difference in the distribution of identical-by-state haplotype blocks over 100,000 bp in length ($p > 0.05$).

3.4.4 Demographic inference

Across all parameter optimization replicates run in moments, the periodic migration model had the single highest log-likelihood (-2008.240), while the maximum log-likelihood for a model of continuous migration was -2763.830. However, the distribution of likelihoods for both models was broadly overlapping (Figure 3.7), and did not differ significantly (Wilcox-Mann-Whitney U test, $p = 0.7005$).

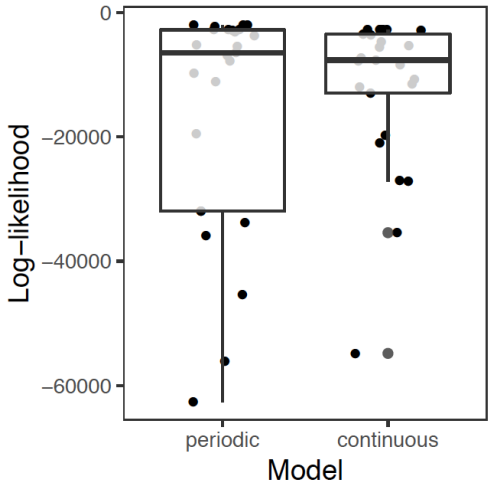

Figure 3.7: Log-likelihood values for 25 replicate parameter optimizations of demographic inference of population genomic data simulated under a model of periodic gene flow and under a model of continuous gene flow.

3.5 Discussion

3.5.1 Speciation with periodic gene flow

Since the inception of the field, speciation research has grappled with the question of whether reproductive isolation can develop while diverging populations exchange migrants (Darwin, 1859; Wagner, 1873; Mayr, 1963; Smith, 1966; Coyne and Orr, 2004; Fitzpatrick et al., 2008; Mallet, 2010). The inherent limitations of biogeographic definitions of speciation have lead to newer, more precise models, based on underlying processes (Schluter, 2009; Nosil, 2012) and / or the presence or absence of gene flow (Pinho and Hey, 2010). Our study of divergence with periodic gene flow found that genetic isolation is relatively more likely to occur compared to a model of continuous migration but difficult to distinguish by commonly applied methods for testing alternate speciation hypotheses with genomic data. These results suggest periodic gene flow between isolated populations may be an underappreciated force in generating species diversity under realistic conditions, and indicate gene flow-based definitions

are themselves a broad category containing related but distinct speciation processes.

Our analytical model describes the expected waiting time to speciation given alternating periods of isolation and migration of specific durations and specific speciation rates (Figure 3.1; Equations 2 and 6). By using speciation rates determined by Gavrilets' models of allopatric and parapatric speciation by BDM incompatibilities (Gavrilets et al., 1998; Gavrilets, 1999, 2003), we demonstrate that speciation with periodic gene flow can be nearly as likely (i.e., has a similar expected waiting time) as allopatric speciation when an equal amount of time is spent in isolation as exchanging migrants (Figure 3.4). Further, speciation with periodic gene flow remains substantially easier to achieve than speciation with constant migration even when as little as 1% of the total period of divergence is spent in isolation (Figure 3.4). This reflects an important property of our model, which is that total expected waiting time to speciation is equivalent to the harmonic mean of expected waiting times under alternate migration regimes. We thus know the average waiting time to speciation given periodic gene flow will always be less than or equal to its value given constant migration with equivalent effective migration (Nm). Intuitively, this application of the harmonic mean mirrors its use in estimating effective population size in the face of recurrent bottlenecks (Vucetich et al., 1997), and highlights the relationship between effective population size and effective migration rate ($4Nm$). These parameters together shape the time-averaged coalescent rate.

As it represents a specialized case of speciation in the face of periodic gene flow, we highlight several potential limitations of our simple model. First, while our validations with forward time simulations reflect the expected relative median waiting time to speciation for different modes of speciation and different values of α, they are not intended to exactly mimic the speciation rates of Gavrilets (2003). We therefore cannot perform a direct comparison of values or examine whether the waiting time to speciation holds constant across a wide range of mutation rates. Second, we model alternating periods of isolation and gene flow as independent, "memoryless" units: partial reproductive isolation developing in one time period is unrelated to the probability of reproductive isolation developing in the next pe-

riod, instead contributing to an average across the entire history of divergence. This might alternately lead to an underestimate (if migration substantially reduces the frequency of a BDM locus allele) or overestimate (if the frequency of the BDM locus allele is little reduced by migration after progressing substantially towards fixation) of waiting time to speciation. Third, we ignore the possibility that reinforcement, adaptive introgression, or many other evolutionary processes might interact with modeled dynamics (though these will be discussed below). Finally, we explore only a single model for evolving reproductive isolation between diverging populations. Could other isolating barriers—e.g., the evolution of a phenotype used in mate choice—have unique behavior under periodic gene flow? We encourage others to explore this interesting question with further theory and simulations.

3.5.2 Cycles of isolation and contact leave distinct genomic signatures

Repeated periods of isolation and migration between diverging populations are commonly cited in discussions of the impact of Pleistocene glacial cycles on extant biodiversity (Klicka and Zink, 1997; Avise and Walker, 1998; Klicka and Zink, 1999; Ayoub and Riechert, 2004; Lovette, 2005; He et al., 2019). Pleistocene glacial cycles and their effects on global climate (e.g., forest refugia in a drier Amazon) have been invoked as a mechanism for explaining both extant species richness and phylogeographic diversity in birds (Klicka and Zink, 1997, 1999; Weir and Schluter, 2004; Lovette, 2005; Lamb et al., 2019), plants (Vuilleumier, 1971; Bonaccorso et al., 2006; He et al., 2019), insects (Knowles, 2000; Ayoub and Riechert, 2004), fish (April et al., 2013), and mammals (Hundertmark et al., 2002). These studies have primarily evaluated a hypothesis of a Pleistocene effect by comparing molecular clock divergence time estimates between phylogroups to the timing of the last glacial maximum, sometimes to the point of controversy (Arbogast and Slowinski, 1998).

Our simulations using empirical atmospheric CO_2 concentration data from the Vostok Ice Cores provide data that may be useful in more rigorously evaluating hypotheses of the role of glacial cycles. We were surprised to find that periodic gene flow was readily distinguishable from continuous gene flow by multiple summary statistics commonly applied to genomic

data (Figure 3.6). These data suggest that neutral evolutionary processes have profoundly different effects in two scenarios that are often treated under the umbrella of "divergence with gene flow." For example, metrics reflecting genetic diversity and effective population size (e.g., D_{XY}, observed heterozygosity, π, Watterson's θ) are reduced under periodic migration given equivalent equilibruim F_{ST}, likely reflecting the increased strength of genetic drift during periods of isolation, when the effective population size of both lineages is reduced in the absence of recurrent migration and its input of novel genetic diversity. For similar reasons, the mean length of identical-by-state haplotype blocks is greater under periodic migration: the average population-scaled recombination rate ($\rho = 4Ner$) is reduced across the entire timeline of divergence, preventing rapid breakdown of uniparentally inherited chromosomal regions. While our study necessarily reflects a narrow window of parameter space, we believe these statistics provide a useful starting point for detecting gene flow pulses at deeper time scales (Harris and Nielsen, 2013).

3.5.3 Inferring speciation with demographic modeling

Joint site frequency spectrum based demographic model testing–conducted by comparing empirical data with the expected JSFS, as calculated by diffusion approximation (Gutenkunst et al., 2009), differential equations (Jouganous et al., 2017), or other approaches (Gronau et al., 2011)—is widely used to evaluate alternate speciation hypotheses (Hey, 2010; Nosil, 2012; Rougeux et al., 2017). These studies have provided much of the recent evidence for speciation with gene flow (Butlin et al., 2008; Jónsson et al., 2013; Filatov et al., 2016; Rougeux et al., 2017) and led Nosil to suggest the process might be common (Nosil, 2008b). Our finding that a realistic model of periodic gene flow is difficult to distinguish from an isolation with migration model using JSFS-based model testing sounds a cautionary note, at least insofar as "speciation with gene flow" and its analogs are used to refer to traditional models of parapatric or sympatric speciation without any period of allopatry. Given its reduced waiting time compared to these processes (Figure 3.4), we suggest studies claiming that initial population divergence occurred in the face of gene flow argue for its plausible

selective driver rather than relying on imprecise estimates of the timing of migration alone (Strasburg and Rieseberg, 2011). However, we highlight that many studies that use "speciation with gene flow" apply it broadly, including cases of secondary contact prior to the development of complete reproductive isolation (Rougeux et al., 2017). While we remain agnostic to its appropriate context, this ambiguity seems to be a continuation of a problem of language usage in speciation research more broadly (Harrison, 2012).

3.5.4 Complexity in speciation and future directions

The advent of affordable genome-wide DNA sequence data for nonmodel organisms and concurrent leaps in theory and computational methods have spurred a renaissance in speciation research (Nielsen and Wakeley, 2001; Fitzpatrick et al., 2008; Mallet, 2008; Nosil, 2008b; Rougeux et al., 2017). This new work has transformed our understanding of speciation, suggesting it is profoundly shaped by selection and frequently characterized by extensive introgression between diverging lineages (Mallet, 2008; Cui et al., 2013; Toews et al., 2016; Kumar et al., 2017). Our study highlights another dimension of complexity in speciation theory and research, and indicate temporal heterogeneity in rates of gene flow deserves increased scrutiny.

Beyond the findings reported in this paper, we believe several aspects of speciation with periodic gene flow provide promising research directions. First, hybridization is increasingly recognized as a generative force in evolution; adaptive introgression can increase fitness across population and species boundaries (Norris et al., 2015; Racimo et al., 2015), and occasionally lead to the evolution of reproductive isolation itself (Gompert et al., 2006; Brelsford et al., 2011; Schumer et al., 2014, 2018a; Barrera-Guzmn et al., 2018). Periodic gene flow could provide raw material for these processes, increase the efficacy of selection by boosting Ne, or facilitate reinforcement (Coyne and Orr, 2004), accelerating speciation. Second, while the constancy and timing of gene flow between diverging populations is an important parameter and connects the historical emphasis on biogeography with the population genomic era, the selective pressures driving speciation are likely more useful for the long-term goal of devel-

oping general predictions for when and where it will occur (Kumar et al., 2017). Though difficult to identify from genomic data alone, we believe the underlying mechanisms generating reproductive isolation form the most useful framework for classifying modes of speciation, and encourage the development of new methods to identify them (Schluter, 2009). Finally, demographic inference based on the site frequency spectrum will likely remain an important tool in speciation research, but it is limited by its lack of haplotype information. Machine learning approaches approaches based on realistic forward-time simulations and multiple summaries of genetic data (e.g., Schrider and Kern (2018)) or even raw genotype matrices (Flagel et al., 2019) represent a largely untapped frontier in our quest to understand the mechanisms underlying biological diversity.

3.6 Acknowledgements

We thank Kameron Harris for helpful discussions on modelling. E.B.L. was supported by a NDSEG Fellowship.

3.7 Data availability

All code and processed data for this study are available at `https://github.com/elinck/speciation_periodic_migration`.

BIBLIOGRAPHY

N. Alachiotis and P. Pavlidis. RAiSD detects positive selection based on multiple signatures of a selective sweep and SNP vectors. *Communications Biology*, 1(1):79, 2018. ISSN 2399-3642. doi: 10.1038/s42003-018-0085-8.

D. H. Alexander, J. Novembre, and K. Lange. Fast model-based estimation of ancestry in unrelated individuals. *Genome Research*, 19(9):1655–1664, 2009. ISSN 1088-9051, 1549-5469. doi: 10.1101/gr.094052.109.

M. J. Andersen, H. T. Shult, A. Cibois, J.-C. Thibault, C. E. Filardi, and R. G. Moyle. Rapid diversification and secondary sympatry in Australo-Pacific kingfishers (Aves: Alcedinidae: Todiramphus). *Royal Society Open Science*, 2(2), 2015. ISSN 2054-5703. doi: 10.1098/rsos.140375.

K. R. Andrews, J. M. Good, M. R. Miller, G. Luikart, and P. A. Hohenlohe. Harnessing the power of RADseq for ecological and evolutionary genomics. *Nature Reviews Genetics*, 17 (2):81–92, 2016. ISSN 1471-0064. doi: 10.1038/nrg.2015.28.

J. April, R. H. Hanner, A.-M. Dion-Côté, and L. Bernatchez. Glacial cycles as an allopatric speciation pump in north-eastern American freshwater fishes. *Molecular Ecology*, 22(2): 409–422, 2013. ISSN 1365-294X. doi: 10.1111/mec.12116.

M. Araya-Salas and G. Smith-Vidaurre. warbleR: an r package to streamline analysis of animal acoustic signals. *Methods in Ecology and Evolution*, 8(2):184–191, 2017. ISSN 2041-210X. doi: 10.1111/2041-210X.12624.

B. S. Arbogast and J. B. Slowinski. Pleistocene Speciation and the Mitochondrial DNA

Clock. *Science*, 282(5396):1955–1955, 1998. ISSN 0036-8075, 1095-9203. doi: 10.1126/science.282.5396.1955a.

A. Arteaga, R. A. Pyron, N. Peafiel, P. Romero-Barreto, J. Culebras, L. Bustamante, M. H. Ynez-Muoz, and J. M. Guayasamin. Comparative Phylogeography Reveals Cryptic Diversity and Repeated Patterns of Cladogenesis for Amphibians and Reptiles in Northwestern Ecuador. *PLOS ONE*, 11(4):e0151746, 2016. ISSN 1932-6203. doi: 10.1371/journal.pone.0151746.

J. C. Avise and D. Walker. Pleistocene phylogeographic effects on avian populations and the speciation process. *Proceedings of the Royal Society B: Biological Sciences*, 265(1395): 457–463, 1998. ISSN 0962-8452.

E. Axelsson, E. Willerslev, M. T. P. Gilbert, and R. Nielsen. The effect of ancient DNA damage on inferences of demographic histories. *Molecular Biology and Evolution*, 25(10): 2181–2187, 2008. ISSN 1537-1719. doi: 10.1093/molbev/msn163.

N. A. Ayoub and S. E. Riechert. Molecular evidence for Pleistocene glacial cycles driving diversification of a North American desert spider, Agelenopsis aperta. *Molecular Ecology*, 13(11):3453–3465, 2004. ISSN 1365-294X. doi: 10.1111/j.1365-294X.2004.02335.x.

N. A. Baird, P. D. Etter, T. S. Atwood, M. C. Currey, A. L. Shiver, Z. A. Lewis, E. U. Selker, W. A. Cresko, and E. A. Johnson. Rapid SNP Discovery and Genetic Mapping Using Sequenced RAD Markers. *PLOS ONE*, 3(10):e3376, 2008. ISSN 1932-6203. doi: 10.1371/journal.pone.0003376.

A. Bankevich, S. Nurk, D. Antipov, A. A. Gurevich, M. Dvorkin, A. S. Kulikov, V. M. Lesin, S. I. Nikolenko, S. Pham, A. D. Prjibelski, A. V. Pyshkin, A. V. Sirotkin, N. Vyahhi, G. Tesler, M. A. Alekseyev, and P. A. Pevzner. SPAdes: A New Genome Assembly Algorithm and Its Applications to Single-Cell Sequencing. *Journal of Computational Biology*, 19(5):455–477, 2012. ISSN 1066-5277. doi: 10.1089/cmb.2012.0021.

A. O. Barrera-Guzmn, A. Aleixo, M. D. Shawkey, and J. T. Weir. Hybrid speciation leads to novel male secondary sexual ornamentation of an Amazonian bird. *Proceedings of the National Academy of Sciences*, 115(2):E218–E225, 2018. ISSN 0027-8424, 1091-6490. doi: 10.1073/pnas.1717319115.

R. A. Bay and K. Ruegg. Genomic islands of divergence or opportunities for introgression? *Proceedings of the Royal Society B: Biological Sciences*, 284(1850):20162414, 2017. ISSN 0962-8452, 1471-2954. doi: 10.1098/rspb.2016.2414.

L. B. Beheregaray, G. M. Cooke, N. L. Chao, and E. L. Landguth. Ecological speciation in the tropics: insights from comparative genetic studies in Amazonia. *Frontiers in Genetics*, 5, 2015. ISSN 1664-8021. doi: 10.3389/fgene.2014.00477.

J. E. Behm, A. R. Ives, and J. W. Boughman. Breakdown in postmating isolation and the collapse of a species pair through hybridization. *The American Naturalist*, 175(1):11–26, 2010. ISSN 1537-5323. doi: 10.1086/648559.

G. Besnard, J. A. M. Bertrand, B. Delahaie, Y. X. C. Bourgeois, E. Lhuillier, and C. Thábaud. Valuing museum specimens: high-throughput DNA sequencing on historical collections of New Guinea crowned pigeons (Goura). *Biological Journal of the Linnean Society*, 117(1):71–82, 2016. ISSN 0024-4066. doi: 10.1111/bij.12494.

K. Bi, T. Linderoth, D. Vanderpool, J. M. Good, R. Nielsen, and C. Moritz. Unlocking the vault: next-generation museum population genomics. *Molecular Ecology*, 22(24):6018–6032, 2013. ISSN 1365-294X. doi: 10.1111/mec.12516.

A. M. Bolger, M. Lohse, and B. Usadel. Trimmomatic: a flexible trimmer for Illumina sequence data. *Bioinformatics*, 30(15):2114–2120, 2014. ISSN 1367-4811. doi: 10.1093/bioinformatics/btu170.

E. Bonaccorso, I. Koch, and A. T. Peterson. Pleistocene fragmentation of Amazon species

ranges. *Diversity and Distributions*, 12(2):157–164, 2006. ISSN 1472-4642. doi: 10.1111/j.1366-9516.2005.00212.x.

G. M. Boratyn, C. Camacho, P. S. Cooper, G. Coulouris, A. Fong, N. Ma, T. L. Madden, W. T. Matten, S. D. McGinnis, Y. Merezhuk, Y. Raytselis, E. W. Sayers, T. Tao, J. Ye, and I. Zaretskaya. BLAST: a more efficient report with usability improvements. *Nucleic Acids Research*, 41(Web Server issue):W29–33, 2013. ISSN 1362-4962. doi: 10.1093/nar/gkt282.

A. Brelsford, B. Milá, and D. E. Irwin. Hybrid origin of audubon's warbler. *Molecular Ecology*, 20(11):2380–2389, 2011. ISSN 1365-294X. doi: 10.1111/j.1365-294X.2011.05055.x.

A. W. Briggs, U. Stenzel, P. L. F. Johnson, R. E. Green, J. Kelso, K. Prfer, M. Meyer, J. Krause, M. T. Ronan, M. Lachmann, and S. Pääbo. Patterns of damage in genomic DNA sequences from a Neandertal. *Proceedings of the National Academy of Sciences*, 104 (37):14616–14621, 2007. ISSN 0027-8424. doi: 10.1073/pnas.0704665104.

D. Bryant and V. Moulton. Neighbor-Net: An Agglomerative Method for the Construction of Phylogenetic Networks. *Molecular Biology and Evolution*, 21(2):255–265, 2004. ISSN 0737-4038. doi: 10.1093/molbev/msh018.

H. A. Burbano, E. Hodges, R. E. Green, A. W. Briggs, J. Krause, M. Meyer, J. M. Good, T. Maricic, P. L. F. Johnson, Z. Xuan, M. Rooks, A. Bhattacharjee, L. Brizuela, F. W. Albert, M. de la Rasilla, J. Fortea, A. Rosas, M. Lachmann, G. J. Hannon, and S. Pääbo. Targeted investigation of the Neandertal genome by array-based sequence capture. *Science*, 328(5979):723–725, 2010. ISSN 1095-9203. doi: 10.1126/science.1188046.

R. Burri. Interpreting differentiation landscapes in the light of long-term linked selection. *Evolution Letters*, 1(3):118–131, 2017. ISSN 2056-3744. doi: 10.1002/evl3.14.

R. Butlin, J. Galindo, and J. W. Grahame. Sympatric, parapatric or allopatric: the most

important way to classify speciation? *Philosophical Transactions of the Royal Society B: Biological Sciences*, 363(1506):2997–3007, 2008. doi: 10.1098/rstb.2008.0076.

C. D. Cadena and L. N. Céspedes. Origin of elevational replacements in a clade of nearly flightless birds most diversity in tropical mountains accumulates via secondary contact following allopatric speciation.

C. D. Cadena, K. H. Kozak, J. P. Gómez, J. L. Parra, C. M. McCain, R. C. K. Bowie, A. C. Carnaval, C. Moritz, C. Rahbek, T. E. Roberts, N. J. Sanders, C. J. Schneider, J. VanDerWal, K. R. Zamudio, and C. H. Graham. Latitude, elevational climatic zonation and speciation in New World vertebrates. *Proceedings of the Royal Society B: Biological Sciences*, 279(1726):194–201, 2012. ISSN 1471-2954. doi: 10.1098/rspb.2011.0720.

C. D. Cadena, F. Zapata, and I. Jimnez. Issues and Perspectives in Species Delimitation using Phenotypic Data: Atlantean Evolution in Darwins Finches. *Systematic Biology*, 67 (2):181–194, 2018. ISSN 1063-5157. doi: 10.1093/sysbio/syx071.

L. M. Caro, P. C. Caycedo-Rosales, R. C. K. Bowie, H. Slabbekoorn, and C. D. Cadena. Ecological speciation along an elevational gradient in a tropical passerine bird? *Journal of Evolutionary Biology*, 26(2):357–374, 2013. ISSN 1420-9101. doi: 10.1111/jeb.12055.

M. A. Chapman, S. J. Hiscock, and D. A. Filatov. Genomic divergence during speciation driven by adaptation to altitude. *Molecular Biology and Evolution*, 30(12):2553–2567, 2013. ISSN 1537-1719. doi: 10.1093/molbev/mst168.

Z. A. Cheviron and R. T. Brumfield. Migration-selection balance and local adaptation of mitochondrial haplotypes in rufous-collared sparrows (Zonotrichia capensis) along an elevational gradient. *Evolution*, 63(6):1593–1605, 2009. ISSN 1558-5646. doi: 10.1111/j.1558-5646.2009.00644.x.

P. U. Clark, A. S. Dyke, J. D. Shakun, A. E. Carlson, J. Clark, B. Wohlfarth, J. X. Mitrovica,

S. W. Hostetler, and A. M. McCabe. The Last Glacial Maximum. *Science*, 325(5941): 710–714, 2009. ISSN 0036-8075, 1095-9203. doi: 10.1126/science.1172873.

A. Cooper, C. Mourer-Chauvir, G. K. Chambers, A. von Haeseler, A. C. Wilson, and S. Pääbo. Independent origins of New Zealand moas and kiwis. *Proceedings of the National Academy of Sciences*, 89(18):8741–8744, 1992. ISSN 0027-8424.

J. A. Coyne. Ernst mayr and the origin of species. *Evolution*, 48(1):19–30, 1994. ISSN 00143820. doi: 10.1111/j.1558-5646.1994.tb01290.x.

J. A. Coyne and H. A. Orr. *Speciation*. Sinauer, 2004. ISBN 978-0-87893-089-0.

T. E. Cruickshank and M. W. Hahn. Reanalysis suggests that genomic islands of speciation are due to reduced diversity, not reduced gene flow. *Molecular Ecology*, 23(13):3133–3157, 2014. ISSN 1365-294X. doi: 10.1111/mec.12796.

R. Cui, M. Schumer, K. Kruesi, R. Walter, P. Andolfatto, and G. G. Rosenthal. Phylogenomics Reveals Extensive Reticulate Evolution in Xiphophorus Fishes. *Evolution*, 67(8): 2166–2179, 2013. ISSN 1558-5646. doi: 10.1111/evo.12099.

J. Dabney and M. Meyer. Length and GC-biases during sequencing library amplification: a comparison of various polymerase-buffer systems with ancient and modern DNA sequencing libraries. *BioTechniques*, 52(2):87–94, 2012. ISSN 1940-9818. doi: 10.2144/000113809.

P. Danecek, A. Auton, G. Abecasis, C. A. Albers, E. Banks, M. A. DePristo, R. E. Handsaker, G. Lunter, G. T. Marth, S. T. Sherry, G. McVean, and R. Durbin. The variant call format and VCFtools. *Bioinformatics*, 27(15):2156–2158, 2011. ISSN 1367-4803. doi: 10.1093/bioinformatics/btr330.

C. Darwin. *On the origin of species by means of natural selection, or, the preservation of favoured races in the struggle for life*. John Murray, London, 1859.

K. De Queiroz. Species Concepts and Species Delimitation. *Systematic Biology*, 56(6): 879–886, 2007. ISSN 1063-5157. doi: 10.1080/10635150701701083.

K. Deiner, A. R. Lemmon, A. L. Mack, R. C. Fleischer, and J. P. Dumbacher. A Passerine Bird's evolution corroborates the geologic history of the island of New Guinea. *PloS One*, 6(5):e19479, 2011. ISSN 1932-6203. doi: 10.1371/journal.pone.0019479.

A. L. Delcher, S. Kasif, R. D. Fleischmann, J. Peterson, O. White, and S. L. Salzberg. Alignment of whole genomes. *Nucleic Acids Research*, 27(11):2369–2376, 1999. ISSN 0305-1048. doi: 10.1093/nar/27.11.2369.

K. E. Delmore, S. Hübner, N. C. Kane, R. Schuster, R. L. Andrew, F. Cámara, R. Guigá, and D. E. Irwin. Genomic analysis of a migratory divide reveals candidate genes for migration and implicates selective sweeps in generating islands of differentiation. *Molecular Ecology*, 24(8):1873–1888, 2015. ISSN 1365-294X. doi: 10.1111/mec.13150.

E. P. Derryberry, N. Seddon, G. E. Derryberry, S. Claramunt, G. F. Seeholzer, R. T. Brumfield, and J. A. Tobias. Ecological drivers of song evolution in birds: Disentangling the effects of habitat and morphology. *Ecology and Evolution*, 8(3):1890–1905, 2018. ISSN 2045-7758. doi: 10.1002/ece3.3760.

J. Diamond, S. L. Pimm, M. E. Gilpin, and M. LeCroy. Rapid Evolution of Character Displacement in Myzomelid Honeyeaters. *The American Naturalist*, 134(5):675–708, 1989. ISSN 0003-0147.

J. M. Diamond. *Avifauna of the Eastern Highlands of New Guinea*. Nuttall Ornithological Club, 1972a.

J. M. Diamond. Biogeographic Kinetics: Estimation of Relaxation Times for Avifaunas of Southwest Pacific Islands. *Proceedings of the National Academy of Sciences*, 69(11): 3199–3203, 1972b. ISSN 0027-8424, 1091-6490. doi: 10.1073/pnas.69.11.3199.

J. M. Diamond. Distributional Ecology of New Guinea Birds: Recent ecological and biogeographical theories can be tested on the bird communities of New Guinea. *Science*, 179 (4075):759–769, 1973. ISSN 0036-8075, 1095-9203. doi: 10.1126/science.179.4075.759.

T. Dobzhansky. Studies on Hybrid Sterility. II. Localization of Sterility Factors in Drosophila Pseudoobscura Hybrids. *Genetics*, 21(2):113–135, 1936. ISSN 0016-6731, 1943-2631.

T. Dobzhansky. *Genetics and the Origin of Species*. Columbia University Press, 1937. ISBN 978-0-231-05475-1.

M. Doebeli and U. Dieckmann. Speciation along environmental gradients. *Nature*, 421(6920): 259–264, 2003. ISSN 1476-4687. doi: 10.1038/nature01274.

M. Doebeli, U. Dieckmann, J. A. J. Metz, and D. Tautz. What We Have Also Learned: Adaptive Spectiation Is Theoretically Plausible. *Evolution*, 59(3):691–695, 2005. ISSN 1558-5646. doi: 10.1111/j.0014-3820.2005.tb01028.x.

S. G. DuBay and C. C. Witt. Differential high-altitude adaptation and restricted gene flow across a mid-elevation hybrid zone in Andean tit-tyrant flycatchers. *Molecular Ecology*, 23 (14):3551–3565, 2014. ISSN 1365-294X. doi: 10.1111/mec.12836.

R. A. Duckworth and G. A. Semenov. Hybridization Associated with Cycles of Ecological Succession in a Passerine Bird. *The American Naturalist*, 190(4):E94–E105, 2017. ISSN 0003-0147. doi: 10.1086/693160.

J. P. Dumbacher and R. C. Fleischer. Phylogenetic evidence for colour pattern convergence in toxic pitohuis: Mllerian mimicry in birds? *Proceedings of the Royal Society B: Biological Sciences*, 268(1480):1971–1976, 2001. ISSN 0962-8452, 1471-2954. doi: 10.1098/rspb.2001.1717.

D. A. R. Eaton. PyRAD: assembly of de novo RADseq loci for phylogenetic analyses. *Bioinformatics*, 30(13):1844–1849, 2014. ISSN 1367-4811. doi: 10.1093/bioinformatics/btu121.

N. B. Edelman, P. Frandsen, M. Miyagi, B. J. Clavijo, J. Davey, R. Dikow, G. G. Accinelli, S. V. Belleghem, N. J. Patterson, D. E. Neafsey, R. J. Challis, S. Kumar, G. Moreira, C. Salazar, M. Chouteau, B. Counterman, R. Papa, M. Blaxter, R. D. Reed, K. Dasmahapatra, M. Kronforst, M. Joron, C. D. Jiggins, W. O. McMillan, F. Di-Palma, A. J. Blumberg, J. Wakeley, D. Jaffe, and J. Mallet. Genomic architecture and introgression shape a butterfly radiation. *bioRxiv*, page 466292, 2018. doi: 10.1101/466292.

R. C. Edgar. MUSCLE: multiple sequence alignment with high accuracy and high throughput. *Nucleic Acids Research*, 32(5):1792–1797, 2004. ISSN 1362-4962. doi: 10.1093/nar/gkh340.

S. V. Edwards, S. B. Kingan, J. D. Calkins, C. N. Balakrishnan, W. B. Jennings, W. J. Swanson, and M. D. Sorenson. Speciation in birds: Genes, geography, and sexual selection. *Proceedings of the National Academy of Sciences*, 102(suppl 1):6550–6557, 2005. ISSN 0027-8424, 1091-6490. doi: 10.1073/pnas.0501846102.

F. Ehrendorfer. Differentiation-Hybridization Cycles and Polyploidy in Achillea. *Cold Spring Harbor Symposia on Quantitative Biology*, 24:141–152, 1959. ISSN 0091-7451, 1943-4456. doi: 10.1101/SQB.1959.024.01.014.

M. Elias, M. Joron, K. Willmott, K. L. SilvaBrando, V. Kaiser, C. F. Arias, L. M. G. Pierez, S. Uribe, A. V. Z. Brower, A. V. L. Freitas, and C. D. Jiggins. Out of the Andes: patterns of diversification in clearwing butterflies. *Molecular Ecology*, 18(8):1716–1729, 2009. ISSN 1365-294X. doi: 10.1111/j.1365-294X.2009.04149.x.

C. Elton and M. Nicholson. The Ten-Year Cycle in Numbers of the Lynx in Canada. *Journal of Animal Ecology*, 11(2):215–244, 1942. ISSN 0021-8790. doi: 10.2307/1358.

J. A. Endler. *Geographic Variation, Speciation, and Clines*. Princeton University Press, 1977. ISBN 978-0-691-08192-2.

B. C. Faircloth, J. E. McCormack, N. G. Crawford, M. G. Harvey, R. T. Brumfield, and T. C. Glenn. Ultraconserved elements anchor thousands of genetic markers spanning multiple evolutionary timescales. *Systematic Biology*, 61(5):717–726, 2012. ISSN 1076-836X. doi: 10.1093/sysbio/sys004.

J. Felsenstein. Skepticism Towards Santa Rosalia, or Why Are There so Few Kinds of Animals? *Evolution*, 35(1):124–138, 1981. ISSN 1558-5646. doi: 10.1111/j.1558-5646.1981.tb04864.x.

D. A. Filatov, O. G. Osborne, and A. S. T. Papadopulos. Demographic history of speciation in a Senecio altitudinal hybrid zone on Mt. Etna. *Molecular Ecology*, 25(11):2467–2481, 2016. ISSN 1365-294X. doi: 10.1111/mec.13618.

B. M. Fitzpatrick, J. A. Fordyce, and S. Gavrilets. What, if anything, is sympatric speciation? *Journal of Evolutionary Biology*, 21(6):1452–1459, 2008. ISSN 1420-9101. doi: 10.1111/j.1420-9101.2008.01611.x.

L. Flagel, Y. Brandvain, and D. R. Schrider. The Unreasonable Effectiveness of Convolutional Neural Networks in Population Genetic Inference. *Molecular Biology and Evolution*, 36 (2):220–238, 2019. ISSN 0737-4038. doi: 10.1093/molbev/msy224.

R. C. Fleischer, J. J. Kirchman, J. P. Dumbacher, L. Bevier, C. Dove, N. C. Rotzel, S. V. Edwards, M. Lammertink, K. J. Miglia, and W. S. Moore. Mid-Pleistocene divergence of Cuban and North American ivory-billed woodpeckers. *Biology Letters*, 2(3):466–469, 2006. ISSN 1744-9561. doi: 10.1098/rsbl.2006.0490.

B. Freeman and A. M. C. Freeman. The avifauna of Mt. Karimui, Chimbu Province, Papua New Guinea, including evidence for long-term population dynamics in undisturbed tropical forest. *Bulletin of the British Ornithologists' Club*, 134(1):30–51, 2014.

B. G. Freeman. Little evidence for Bergmann's rule body size clines in passerines along

tropical elevational gradients. *Journal of Biogeography*, 44(3):502–510, 2017. ISSN 1365-2699. doi: 10.1111/jbi.12812.

L. Fu, B. Niu, Z. Zhu, S. Wu, and W. Li. CD-HIT: accelerated for clustering the next-generation sequencing data. *Bioinformatics*, 28(23):3150–3152, 2012. ISSN 1367-4811. doi: 10.1093/bioinformatics/bts565.

W. C. Funk, M. A. Murphy, K. L. Hoke, E. Muths, S. M. Amburgey, E. M. Lemmon, and A. R. Lemmon. Elevational speciation in action? Restricted gene flow associated with adaptive divergence across an altitudinal gradient. *Journal of Evolutionary Biology*, 29 (2):241–252, 2016. ISSN 1420-9101. doi: 10.1111/jeb.12760.

C. R. Gadek, S. D. Newsome, E. J. Beckman, A. N. Chavez, S. C. Galen, E. Bautista, and C. C. Witt. Why are tropical mountain passes low for some species? Genetic and stable-isotope tests for differentiation, migration and expansion in elevational generalist songbirds. *Journal of Animal Ecology*, 87(3):741–753, 2018. ISSN 1365-2656. doi: 10.1111/1365-2656.12779.

C. Gamba, K. Hanghj, C. Gaunitz, A. H. Alfarhan, S. A. Alquraishi, K. A. S. Al-Rasheid, D. G. Bradley, and L. Orlando. Comparing the performance of three ancient DNA extraction methods for high-throughput sequencing. *Molecular Ecology Resources*, 16(2): 459–469, 2016. ISSN 1755-0998. doi: 10.1111/1755-0998.12470.

M. Gautier, K. Gharbi, T. Cezard, J. Foucaud, C. Kerdelhu, P. Pudlo, J.-M. Cornuet, and A. Estoup. The effect of RAD allele dropout on the estimation of genetic variation within and between populations. *Molecular Ecology*, 22(11):3165–3178, 2013. ISSN 1365-294X. doi: 10.1111/mec.12089.

S. Gavrilets. A Dynamical Theory of Speciation on Holey Adaptive Landscapes. *The American Naturalist*, 154(1):1–22, 1999. ISSN 0003-0147. doi: 10.1086/303217.

S. Gavrilets. Perspective: Models of Speciation: What Have We Learned in 40 Years? *Evolution*, 57(10):2197–2215, 2003. ISSN 1558-5646. doi: 10.1111/j.0014-3820.2003.tb00233.x.

S. Gavrilets, H. Li, and M. D. Vose. Rapid parapatric speciation on holey adaptive landscapes. *Proceedings of the Royal Society B: Biological Sciences*, 265(1405):1483–1489, 1998. ISSN 0962-8452.

Z. Gompert, J. A. Fordyce, M. L. Forister, A. M. Shapiro, and C. C. Nice. Homoploid Hybrid Speciation in an Extreme Habitat. *Science*, 314(5807):1923–1925, 2006. ISSN 0036-8075, 1095-9203. doi: 10.1126/science.1135875.

R. E. Green, J. Krause, A. W. Briggs, T. Maricic, U. Stenzel, M. Kircher, N. Patterson, H. Li, W. Zhai, M. H.-Y. Fritz, N. F. Hansen, E. Y. Durand, A.-S. Malaspinas, J. D. Jensen, T. Marques-Bonet, C. Alkan, K. Prüer, M. Meyer, H. A. Burbano, J. M. Good, R. Schultz, A. Aximu-Petri, A. Butthof, B. Höer, B. Höffner, M. Siegemund, A. Weihmann, C. Nusbaum, E. S. Lander, C. Russ, N. Novod, J. Affourtit, M. Egholm, C. Verna, P. Rudan, D. Brajkovic, Z. Kucan, I. Gusic, V. B. Doronichev, L. V. Golovanova, C. Lalueza-Fox, M. de la Rasilla, J. Fortea, A. Rosas, R. W. Schmitz, P. L. F. Johnson, E. E. Eichler, D. Falush, E. Birney, J. C. Mullikin, M. Slatkin, R. Nielsen, J. Kelso, M. Lachmann, D. Reich, and S. Pääbo. A Draft Sequence of the Neandertal Genome. *Science (New York, N.Y.)*, 328(5979):710–722, 2010. ISSN 0036-8075. doi: 10.1126/science.1188021.

P. Gregory. *Birds of New Guinea*. Lynx Edicions, Barcelona, 2017.

I. Gronau, M. J. Hubisz, B. Gulko, C. G. Danko, and A. Siepel. Bayesian inference of ancient human demography from individual genome sequences. *Nature Genetics*, 43(10): 1031–1034, 2011. ISSN 1546-1718. doi: 10.1038/ng.937.

K. Guschanski, J. Krause, S. Sawyer, L. M. Valente, S. Bailey, K. Finstermeier, R. Sabin, E. Gilissen, G. Sonet, Z. T. Nagy, G. Lenglet, F. Mayer, and V. Savolainen. Next-

generation museomics disentangles one of the largest primate radiations. *Systematic Biology*, 62(4):539–554, 2013. ISSN 1076-836X. doi: 10.1093/sysbio/syt018.

R. N. Gutenkunst, R. D. Hernandez, S. H. Williamson, and C. D. Bustamante. Inferring the Joint Demographic History of Multiple Populations from Multidimensional SNP Frequency Data. *PLOS Genetics*, 5(10):e1000695, 2009. ISSN 1553-7404. doi: 10.1371/journal.pgen.1000695.

J. C. Habel, M. Husemann, A. Finger, P. D. Danley, and F. E. Zachos. The relevance of time series in molecular ecology and conservation biology. *Biological Reviews of the Cambridge Philosophical Society*, 89(2):484–492, 2014. ISSN 1469-185X. doi: 10.1111/brv.12068.

C. Hahn, L. Bachmann, and B. Chevreux. Reconstructing mitochondrial genomes directly from genomic next-generation sequencing readsa baiting and iterative mapping approach. *Nucleic Acids Research*, 41(13):e129, 2013. ISSN 0305-1048. doi: 10.1093/nar/gkt371.

B. C. Haller and P. W. Messer. SLiM 3: Forward Genetic Simulations Beyond the Wright-Fisher Model. *Molecular Biology and Evolution*, 36(3):632–637, 2019. ISSN 0737-4038. doi: 10.1093/molbev/msy228.

Z. R. Hanna and A. B. Sellas. hyRADccg Version 1.0.0, 2017. URL `https://zenodo.org/record/268048#.XKi8w5NKgWo`. doi: 10.5281/zenodo.268048.

K. Harris and R. Nielsen. Inferring Demographic History from a Spectrum of Shared Haplotype Lengths. *PLOS Genetics*, 9(6):e1003521, 2013. ISSN 1553-7404. doi: 10.1371/journal.pgen.1003521.

R. G. Harrison. The Language of Speciation. *Evolution*, 66(12):3643–3657, 2012. ISSN 1558-5646. doi: 10.1111/j.1558-5646.2012.01785.x.

M. G. Harvey, A. Aleixo, C. C. Ribas, and R. T. Brumfield. Habitat Association Predicts Genetic Diversity and Population Divergence in Amazonian Birds. *The American Naturalist*, 190(5):631–648, 2017a. ISSN 0003-0147. doi: 10.1086/693856.

M. G. Harvey, G. F. Seeholzer, B. T. Smith, D. L. Rabosky, A. M. Cuervo, and R. T. Brumfield. Positive association between population genetic differentiation and speciation rates in New World birds. *Proceedings of the National Academy of Sciences*, 114(24): 6328–6333, 2017b. ISSN 0027-8424, 1091-6490. doi: 10.1073/pnas.1617397114.

Z. He, X. Li, M. Yang, X. Wang, C. Zhong, N. C. Duke, S. Shi, and C.-I. Wu. Speciation with gene flow via cycles of isolation and migration: Insights from multiple mangrove taxa. *National Science Review*, 6(2):275–288, 2019. doi: 10.1093/nsr/nwy078.

J. B. Henderson and Z. R. Hanna. GItaxidIsVert. Version 1.0.0, 2016. URL `https://zenodo.org/record/163737#.XKi83JNKgWo`. doi: 10.5281/zenodo.163737.

R. D. Hernandez. A flexible forward simulator for populations subject to selection and demography. *Bioinformatics*, 24(23):2786–2787, 2008. ISSN 1367-4811. doi: 10.1093/bioinformatics/btn522.

J. Hey. Isolation with Migration Models for More Than Two Populations. *Molecular Biology and Evolution*, 27(4):905–920, 2010. ISSN 0737-4038. doi: 10.1093/molbev/msp296.

J. Hey and R. Nielsen. Integration within the Felsenstein equation for improved Markov chain Monte Carlo methods in population genetics. *Proceedings of the National Academy of Sciences*, 104(8):2785–2790, 2007. ISSN 0027-8424, 1091-6490. doi: 10.1073/pnas.0611164104.

M. Hofreiter, V. Jaenicke, D. Serre, A. von Haeseler, and S. Pääbo. DNA sequences from multiple amplifications reveal artifacts induced by cytosine deamination in ancient DNA. *Nucleic Acids Research*, 29(23):4793–4799, 2001. ISSN 1362-4962.

G. Hope. The Sensitivity of the High Mountain Ecosystems of New Guinea to Climatic Change and Anthropogenic Impact. *Arctic, Antarctic, and Alpine Research*, 46(4):777–786, 2014. ISSN 1523-0430. doi: 10.1657/1938-4246-46.4.777.

Hua Xia. The impact of seasonality on niche breadth, distribution range and species richness: a theoretical exploration of Janzen's hypothesis. *Proceedings of the Royal Society B: Biological Sciences*, 283(1835):1–8, 2016. doi: 10.1098/rspb.2016.0349.

K. J. Hundertmark, G. F. Shields, I. G. Udina, R. T. Bowyer, A. A. Danilkin, and C. C. Schwartz. Mitochondrial Phylogeography of Moose (Alces alces): Late Pleistocene Divergence and Population Expansion. *Molecular Phylogenetics and Evolution*, 22(3):375–387, 2002. ISSN 1055-7903. doi: 10.1006/mpev.2001.1058.

D. H. Huson and D. Bryant. Application of Phylogenetic Networks in Evolutionary Studies. *Molecular Biology and Evolution*, 23(2):254–267, 2006. ISSN 0737-4038. doi: 10.1093/molbev/msj030.

D. E. Irwin. Sex chromosomes and speciation in birds and other ZW systems. *Molecular Ecology*, 27(19):3831–3851, 2018. ISSN 1365-294X. doi: 10.1111/mec.14537.

D. E. Irwin, B. Milá, D. P. L. Toews, A. Brelsford, H. L. Kenyon, A. N. Porter, C. Grossen, K. E. Delmore, M. Alcaide, and J. H. Irwin. A comparison of genomic islands of differentiation across three young avian species pairs. *Molecular Ecology*, 27(23):4839–4855, 2018. ISSN 1365-294X. doi: 10.1111/mec.14858.

J. E. Jankowski, A. L. Ciecka, N. Y. Meyer, and K. N. Rabenold. Beta diversity along environmental gradients: implications of habitat specialization in tropical montane landscapes. *Journal of Animal Ecology*, 78(2):315–327, 2009. ISSN 1365-2656. doi: 10.1111/j.1365-2656.2008.01487.x.

D. H. Janzen. Why Mountain Passes are Higher in the Tropics. *The American Naturalist*, 101(919):233–249, 1967. ISSN 0003-0147.

T. Jombart. adegenet: a R package for the multivariate analysis of genetic markers. *Bioinformatics*, 24(11):1403–1405, 2008. ISSN 1367-4811. doi: 10.1093/bioinformatics/btn129.

M. R. Jones and J. M. Good. Targeted capture in evolutionary and ecological genomics. *Molecular Ecology*, 25(1):185–202, 2016. ISSN 1365-294X. doi: 10.1111/mec.13304.

H. Jónsson, A. Ginolhac, M. Schubert, P. L. F. Johnson, and L. Orlando. mapDamage2.0: fast approximate Bayesian estimates of ancient DNA damage parameters. *Bioinformatics*, 29(13):1682–1684, 2013. ISSN 1367-4811. doi: 10.1093/bioinformatics/btt193.

J. Jouganous, W. Long, A. P. Ragsdale, and S. Gravel. Inferring the Joint Demographic History of Multiple Populations: Beyond the Diffusion Approximation. *Genetics*, 206(3): 1549–1567, 2017. ISSN 0016-6731, 1943-2631. doi: 10.1534/genetics.117.200493.

J. Kelleher, A. M. Etheridge, and G. McVean. Efficient Coalescent Simulation and Genealogical Analysis for Large Sample Sizes. *PLOS Computational Biology*, 12(5):e1004842, 2016. ISSN 1553-7358. doi: 10.1371/journal.pcbi.1004842.

M. Kirkpatrick and V. Ravigné. Speciation by Natural and Sexual Selection: Models and Experiments. *The American Naturalist*, 159(S3):S22–S35, 2002. ISSN 0003-0147. doi: 10.1086/338370.

J. Klicka and R. M. Zink. The Importance of Recent Ice Ages in Speciation: A Failed Paradigm. *Science*, 277(5332):1666–1669, 1997. ISSN 0036-8075, 1095-9203. doi: 10.1126/science.277.5332.1666.

J. Klicka and R. M. Zink. Pleistocene effects on North American songbird evolution. *Proceedings of the Royal Society of London. Series B: Biological Sciences*, 266(1420):695–700, 1999. doi: 10.1098/rspb.1999.0691.

L. L. Knowles. Tests of Pleistocene Speciation in Montane Grasshoppers (genus Melanoplus) from the Sky Islands of Western North America. *Evolution*, 54(4):1337–1348, 2000. ISSN 1558-5646. doi: 10.1111/j.0014-3820.2000.tb00566.x.

N. M. Kopelman, L. Stone, O. Gascuel, and N. A. Rosenberg. The behavior of admixed populations in neighbor-joining inference of population trees. *Pacific Symposium on Biocomputing*, pages 273–284, 2013. ISSN 2335-6936.

T. S. Korneliussen, A. Albrechtsen, and R. Nielsen. ANGSD: Analysis of Next Generation Sequencing Data. *BMC Bioinformatics*, 15(1):356, 2014. ISSN 1471-2105. doi: 10.1186/s12859-014-0356-4.

V. Kumar, F. Lammers, T. Bidon, M. Pfenninger, L. Kolter, M. A. Nilsson, and A. Janke. The evolutionary history of bears is characterized by gene flow across species. *Scientific Reports*, 7:46487, 2017. ISSN 2045-2322. doi: 10.1038/srep46487.

A. M. Lamb, A. G. d. S. Silva, L. Joseph, P. Sunnucks, and A. Pavlova. Pleistocene-dated biogeographic barriers drove divergence within the Australo-Papuan region in a sex-specific manner: an example in a widespread Australian songbird. *Heredity*, page 1, 2019. ISSN 1365-2540. doi: 10.1038/s41437-019-0206-2.

B. Langmead. Aligning short sequencing reads with Bowtie. *Current Protocols in Bioinformatics*, 11:11.7.1–11.7.14, 2010. ISSN 1934-340X. doi: 10.1002/0471250953.bi1107s32.

S. A. Levin and R. T. Paine. Disturbance, patch formation, and community structure. *Proceedings of the National Academy of Sciences*, 71(7):2744–2747, 1974. ISSN 0027-8424.

H. Li, B. Handsaker, A. Wysoker, T. Fennell, J. Ruan, N. Homer, G. Marth, G. Abecasis, R. Durbin, and 1000 Genome Project Data Processing Subgroup. The Sequence Alignment/Map format and SAMtools. *Bioinformatics*, 25(16):2078–2079, 2009. ISSN 1367-4811. doi: 10.1093/bioinformatics/btp352.

E. Linck, S. Schaack, and J. P. Dumbacher. Genetic differentiation within a widespread "supertramp" taxon: Molecular phylogenetics of the Louisiade White-eye (Zosterops griseotinctus). *Molecular Phylogenetics and Evolution*, 94(Pt A):113–121, 2016. ISSN 1095-9513. doi: 10.1016/j.ympev.2015.08.018.

E. Linck, B. G. Freeman, and J. P. Dumbacher. Speciation with gene flow across an elevational gradient in New Guinea kingfishers. *bioRxiv*, page 589044, 2019. doi: 10.1101/589044.

E. B. Linck, Z. R. Hanna, A. Sellas, and J. P. Dumbacher. Evaluating hybridization capture with RAD probes as a tool for museum genomics with historical bird specimens. *Ecology and Evolution*, 7(13):4755–4767, 2017. ISSN 2045-7758. doi: 10.1002/ece3.3065.

B. Liu, J. Yuan, S.-M. Yiu, Z. Li, Y. Xie, Y. Chen, Y. Shi, H. Zhang, Y. Li, T.-W. Lam, and R. Luo. COPE: an accurate k-mer-based pair-end reads connection tool to facilitate genome assembly. *Bioinformatics*, 28(22):2870–2874, 2012. ISSN 1367-4811. doi: 10.1093/bioinformatics/bts563.

J. B. Losos and R. E. Glor. Phylogenetic comparative methods and the geography of speciation. *Trends in Ecology & Evolution*, 18(5):220–227, 2003. ISSN 0169-5347. doi: 10.1016/S0169-5347(03)00037-5.

I. J. Lovette. Glacial cycles and the tempo of avian speciation. *Trends in Ecology & Evolution*, 20(2):57–59, 2005. ISSN 0169-5347. doi: 10.1016/j.tree.2004.11.011.

A. Mack and J. Dumbacher. Birds of Papua. *The Ecology of Papua Part*, 1:654–688, 2007.

T. Mago and S. L. Salzberg. FLASH: fast length adjustment of short reads to improve genome assemblies. *Bioinformatics*, 27(21):2957–2963, 2011. ISSN 1367-4811. doi: 10.1093/bioinformatics/btr507.

J. Mallet. Speciation in the 21st century. *Heredity*, 95:105–109, 2005. ISSN 1365-2540. doi: 10.1038/sj.hdy.6800686.

J. Mallet. Hybridization, ecological races and the nature of species: empirical evidence for the ease of speciation. *Philosophical Transactions of the Royal Society B: Biological Sciences*, 363(1506):2971–2986, 2008. ISSN 0962-8436, 1471-2970. doi: 10.1098/rstb.2008.0081.

J. Mallet. Why was Darwins view of species rejected by twentieth century biologists? *Biology & Philosophy*, 25(4):497–527, 2010. ISSN 1572-8404. doi: 10.1007/s10539-010-9213-7.

M. Martin. Cutadapt removes adapter sequences from high-throughput sequencing reads. *EMBnet.journal*, 17(1):10–12, 2011. ISSN 2226-6089. doi: 10.14806/ej.17.1.200.

S. H. Martin, K. K. Dasmahapatra, N. J. Nadeau, C. Salazar, J. R. Walters, F. Simpson, M. Blaxter, A. Manica, J. Mallet, and C. D. Jiggins. Genome-wide evidence for speciation with gene flow in Heliconius butterflies. *Genome Research*, 23(11):1817–1828, 2013. ISSN 1088-9051, 1549-5469. doi: 10.1101/gr.159426.113.

S. H. Martin, J. W. Davey, C. Salazar, and C. D. Jiggins. Recombination rate variation shapes barriers to introgression across butterfly genomes. *PLOS Biology*, 17(2):e2006288, 2019. ISSN 1545-7885. doi: 10.1371/journal.pbio.2006288.

E. Mayr. *Systematics and the Origin of Species, from the Viewpoint of a Zoologist*. Harvard University Press, 1942. ISBN 978-0-674-86250-0.

E. Mayr. *Animal species and evolution*. Harvard University Press, 1963.

J. E. McCormack and T. B. Smith. Niche expansion leads to small-scale adaptive divergence along an elevation gradient in a medium-sized passerine bird. *Proceedings of the Royal Society B: Biological Sciences*, 275(1647):2155–2164, 2008. doi: 10.1098/rspb.2008.0470.

J. E. McCormack, B. C. Faircloth, N. G. Crawford, P. A. Gowaty, R. T. Brumfield, and T. C. Glenn. Ultraconserved elements are novel phylogenomic markers that resolve placental mammal phylogeny when combined with species-tree analysis. *Genome Research*, 22(4): 746–754, 2012. ISSN 1549-5469. doi: 10.1101/gr.125864.111.

J. E. McCormack, W. L. E. Tsai, and B. C. Faircloth. Sequence capture of ultraconserved elements from bird museum specimens. *Molecular Ecology Resources*, 16(5):1189–1203, 2016. ISSN 1755-0998. doi: 10.1111/1755-0998.12466.

A. McKenna, M. Hanna, E. Banks, A. Sivachenko, K. Cibulskis, A. Kernytsky, K. Garimella, D. Altshuler, S. Gabriel, M. Daly, and M. A. DePristo. The Genome Analysis Toolkit: A MapReduce framework for analyzing next-generation DNA sequencing data. *Genome Research*, 20(9):1297–1303, 2010. ISSN 1088-9051, 1549-5469. doi: 10.1101/gr.107524.110.

A. Miles, P. Ralph, S. Rae, and R. Pisupati. scikit-allel: v1.2.0, 2019. doi: 10.5281/zenodo.2652508.

M. Miller, W. Pfeiffer, and T. Schwartz. Creating the CIPRES Science Gateway for Inference of Large Phylogenetic Trees. *Proceedings of the Gateway Computing Environments Workshop (GCE)*, pages 1–8, 2010.

R. G. Moyle, J. D. Manthey, P. A. Hosner, M. Rahman, M. Lakim, and F. H. Sheldon. A genome-wide assessment of stages of elevational parapatry in Bornean passerine birds reveals no introgression: implications for processes and patterns of speciation. *PeerJ*, 5: e3335, 2017. ISSN 2167-8359. doi: 10.7717/peerj.3335.

V. Narasimhan, P. Danecek, A. Scally, Y. Xue, C. Tyler-Smith, and R. Durbin. BCFtools/RoH: a hidden Markov model approach for detecting autozygosity from next-generation sequencing data. *Bioinformatics*, 32(11):1749–1751, 2016. ISSN 1367-4811. doi: 10.1093/bioinformatics/btw044.

M. Nei. Mathematical models of speciation and genetic distance. In *Population Genetics and Ecology*, pages 723–766. Academic Press, New York, 1976.

R. Nielsen and J. Wakeley. Distinguishing migration from isolation: a Markov chain Monte Carlo approach. *Genetics*, 158(2):885–896, 2001. ISSN 0016-6731.

L. C. Norris, B. J. Main, Y. Lee, T. C. Collier, A. Fofana, A. J. Cornel, and G. C. Lanzaro. Adaptive introgression in an African malaria mosquito coincident with the increased usage of insecticide-treated bed nets. *Proceedings of the National Academy of Sciences*, 112(3): 815–820, 2015. ISSN 0027-8424, 1091-6490. doi: 10.1073/pnas.1418892112.

P. Nosil. Ernst Mayr and the integration of geographic and ecological factors in speciation. *Biological Journal of the Linnean Society*, 95(1):26–46, 2008a. ISSN 0024-4066. doi: 10.1111/j.1095-8312.2008.01091.x.

P. Nosil. Speciation with gene flow could be common. *Molecular Ecology*, 17(9):2103–2106, 2008b. ISSN 1365-294X. doi: 10.1111/j.1365-294X.2008.03715.x.

P. Nosil. *Ecological Speciation*. Oxford Series in Ecology and Evolution. Oxford University Press, Oxford, New York, 2012. ISBN 978-0-19-958711-7.

O. G. Osborne, T. E. Batstone, S. J. Hiscock, and D. A. Filatov. Rapid Speciation with Gene Flow Following the Formation of Mt. Etna. *Genome Biology and Evolution*, 5(9): 1704–1715, 2013. doi: 10.1093/gbe/evt127.

E. Paradis, J. Claude, and K. Strimmer. APE: Analyses of Phylogenetics and Evolution in R language. *Bioinformatics*, 20(2):289–290, 2004. ISSN 1367-4803. doi: 10.1093/bioinformatics/btg412.

R. B. Payne and M. D. Sorenson. Museum Collections as Sources of Genetic Data. *Bonner zoologische Beitrge*, 51(3/4):97–104, 2002.

J. V. Penalba, L. Joseph, and C. Moritz. Current geography masks dynamic history of gene flow during speciation in northern Australian birds. *bioRxiv*, page 178475, 2017. doi: 10.1101/178475.

B. K. Peterson, J. N. Weber, E. H. Kay, H. S. Fisher, and H. E. Hoekstra. Double Digest RADseq: An Inexpensive Method for De Novo SNP Discovery and Genotyping in Model and Non-Model Species. *PLOS ONE*, 7(5):e37135, 2012. ISSN 1932-6203. doi: 10.1371/journal.pone.0037135.

J. R. Petit, J. Jouzel, D. Raynaud, N. I. Barkov, J.-M. Barnola, I. Basile, M. Bender, J. Chappellaz, M. Davis, G. Delaygue, M. Delmotte, V. M. Kotlyakov, M. Legrand, V. Y.

Lipenkov, C. Lorius, L. Ppin, C. Ritz, E. Saltzman, and M. Stievenard. Climate and atmospheric history of the past 420,000 years from the Vostok ice core, Antarctica. *Nature*, 399(6735):429, 1999. ISSN 1476-4687. doi: 10.1038/20859.

C. Pinho and J. Hey. Divergence with Gene Flow: Models and Data. *Annual Review of Ecology, Evolution, and Systematics*, 41(1):215–230, 2010. doi: 10.1146/annurev-ecolsys-102209-144644.

H. N. Poinar, C. Schwarz, J. Qi, B. Shapiro, R. D. E. Macphee, B. Buigues, A. Tikhonov, D. H. Huson, L. P. Tomsho, A. Auch, M. Rampp, W. Miller, and S. C. Schuster. Metagenomics to paleogenomics: large-scale sequencing of mammoth DNA. *Science (New York, N.Y.)*, 311(5759):392–394, 2006. ISSN 1095-9203. doi: 10.1126/science.1123360.

N. R. Polato, B. A. Gill, A. A. Shah, M. M. Gray, K. L. Casner, A. Barthelet, P. W. Messer, M. P. Simmons, J. M. Guayasamin, A. C. Encalada, B. C. Kondratieff, A. S. Flecker, S. A. Thomas, C. K. Ghalambor, N. L. Poff, W. C. Funk, and K. R. Zamudio. Narrow thermal tolerance and low dispersal drive higher speciation in tropical mountains. *Proceedings of the National Academy of Sciences*, 115(49):12471–12476, 2018. ISSN 0027-8424, 1091-6490. doi: 10.1073/pnas.1809326115.

D. M. Portik, A. D. Leach, D. Rivera, M. F. Barej, M. Burger, M. Hirschfeld, M.-O. Rdel, D. C. Blackburn, and M. K. Fujita. Evaluating mechanisms of diversification in a Guineo-Congolian tropical forest frog using demographic model selection. *Molecular Ecology*, 26 (19):5245–5263, 2017. ISSN 1365-294X. doi: 10.1111/mec.14266.

T. K. Pratt and B. M. Beehler. *Birds of New Guinea: Second Edition*. Princeton University Press, 2015. ISBN 978-0-691-09563-9.

T. Price. *Speciation in Birds*. Roberts and Company, 2008. ISBN 978-0-9747077-8-5.

W. B. Provine. Ernst Mayr: Genetics and Speciation. *Genetics*, 167(3):1041–1046, 2004. ISSN 0016-6731, 1943-2631.

S. J. Puechmaille. The program structure does not reliably recover the correct population structure when sampling is uneven: subsampling and new estimators alleviate the problem. *Molecular Ecology Resources*, 16(3):608–627, 2016. ISSN 1755-0998. doi: 10.1111/1755-0998.12512.

A. R. Quinlan and I. M. Hall. BEDTools: a flexible suite of utilities for comparing genomic features. *Bioinformatics*, 26(6):841–842, 2010. ISSN 1367-4803. doi: 10.1093/bioinformatics/btq033.

F. Racimo, S. Sankararaman, R. Nielsen, and E. Huerta-Sánchez. Evidence for archaic adaptive introgression in humans. *Nature Reviews Genetics*, 16(6):359–371, 2015. ISSN 1471-0064. doi: 10.1038/nrg3936.

A. L. Rand. Altitudinal variation in New Guinea birds. *American Museum Novitates*, (890), 1936.

J. A. Rattenbury. Cyclic Hybridization as a Survival Mechanism in the New Zealand Forest Flora. *Evolution*, 16(3):348–363, 1962. ISSN 1558-5646. doi: 10.1111/j.1558-5646.1962.tb03227.x.

R. Ricklefs and E. Bermingham. The Causes of Evolutionary Radiations in Archipelagoes: Passerine Birds in the Lesser Antilles. *The American Naturalist*, 169(3):285–297, 2007. ISSN 0003-0147. doi: 10.1086/510730.

E. Rizzi, M. Lari, E. Gigli, G. De Bellis, and D. Caramelli. Ancient DNA studies: new perspectives on old samples. *Genetics Selection Evolution*, 44(1):21, 2012. ISSN 1297-9686. doi: 10.1186/1297-9686-44-21.

T. Rognes, T. Flouri, B. Nichols, C. Quince, and F. Mah. VSEARCH: a versatile open source tool for metagenomics. *PeerJ*, 4:e2584, 2016. ISSN 2167-8359. doi: 10.7717/peerj.2584.

C. Rougeux, L. Bernatchez, and P.-A. Gagnaire. Modeling the Multiple Facets of Speciation-with-Gene-Flow toward Inferring the Divergence History of Lake Whitefish Species Pairs

(Coregonus clupeaformis). *Genome Biology and Evolution*, 9(8):2057–2074, 2017. ISSN 1759-6653.

K. Roy, J. W. Valentine, D. Jablonski, and S. M. Kidwell. Scales of climatic variability and time averaging in Pleistocene biotas: implications for ecology and evolution. *Trends in Ecology & Evolution*, 11(11):458–463, 1996. ISSN 0169-5347. doi: 10.1016/0169-5347(96)10054-9.

H. D. Rundle and P. Nosil. Ecological speciation. *Ecology Letters*, 8(3):336–352, 2005. ISSN 1461-0248. doi: 10.1111/j.1461-0248.2004.00715.x.

P. G. Ryan, P. Bloomer, C. L. Moloney, T. J. Grant, and W. Delport. Ecological Speciation in South Atlantic Island Finches. *Science*, 315(5817):1420–1423, 2007. ISSN 0036-8075, 1095-9203. doi: 10.1126/science.1138829.

K. Sam, B. Koane, and V. Novotny. New avian records along the elevational gradient of Mt. Wilhelm, Papua New Guinea. *Bulletin of the British Ornithologists' Club*, 134(2):116–133, 2014.

V. Savolainen, M.-C. Anstett, C. Lexer, I. Hutton, J. J. Clarkson, M. V. Norup, M. P. Powell, D. Springate, N. Salamin, and W. J. Baker. Sympatric speciation in palms on an oceanic island. *Nature*, 441(7090):210–213, 2006. ISSN 1476-4687. doi: 10.1038/nature04566.

U. K. Schliewen, D. Tautz, and S. Pbo. Sympatric speciation suggested by monophyly of crater lake cichlids. *Nature*, 368(6472):629–632, 1994. ISSN 1476-4687. doi: 10.1038/368629a0.

D. Schluter. Ecology and the origin of species. *Trends in Ecology & Evolution*, 16(7):372–380, 2001. ISSN 0169-5347. doi: 10.1016/S0169-5347(01)02198-X.

D. Schluter. Evidence for Ecological Speciation and Its Alternative. *Science*, 323(5915):737–741, 2009. ISSN 0036-8075, 1095-9203. doi: 10.1126/science.1160006.

D. Schluter and J. D. McPhail. Ecological character displacement and speciation in sticklebacks. *The American Naturalist*, 140(1):85–108, 1992. ISSN 0003-0147. doi: 10.1086/285404.

C. J. Schneider, T. B. Smith, B. Larison, and C. Moritz. A test of alternative models of diversification in tropical rainforests: Ecological gradients vs. rainforest refugia. *Proceedings of the National Academy of Sciences*, 96(24):13869–13873, 1999. ISSN 0027-8424, 1091-6490. doi: 10.1073/pnas.96.24.13869.

D. R. Schrider and A. D. Kern. Supervised Machine Learning for Population Genetics: A New Paradigm. *Trends in Genetics*, 34(4):301–312, 2018. ISSN 0168-9525. doi: 10.1016/j.tig.2017.12.005.

M. Schumer, G. G. Rosenthal, and P. Andolfatto. How Common Is Homoploid Hybrid Speciation? *Evolution*, 68(6):1553–1560, 2014. ISSN 1558-5646. doi: 10.1111/evo.12399.

M. Schumer, G. G. Rosenthal, and P. Andolfatto. What do we mean when we talk about hybrid speciation? *Heredity*, 120(4):379, 2018a. ISSN 1365-2540. doi: 10.1038/s41437-017-0036-z.

M. Schumer, C. Xu, D. L. Powell, A. Durvasula, L. Skov, C. Holland, J. C. Blazier, S. Sankararaman, P. Andolfatto, G. G. Rosenthal, and M. Przeworski. Natural selection interacts with recombination to shape the evolution of hybrid genomes. *Science*, 360 (6389):656–660, 2018b. ISSN 0036-8075, 1095-9203. doi: 10.1126/science.aar3684.

L. Scrucca, M. Fop, T. B. Murphy, and A. E. Raftery. mclust 5: Clustering, Classification and Density Estimation Using Gaussian Finite Mixture Models. *The R Journal*, 8(1): 289–317, 2016. ISSN 2073-4859.

O. Seehausen, G. Takimoto, D. Roy, and J. Jokela. Speciation reversal and biodiversity dynamics with hybridization in changing environments. *Molecular Ecology*, 17(1):30–44, 2008. ISSN 1365-294X. doi: 10.1111/j.1365-294X.2007.03529.x.

M. R. Servedio, G. S. V. Doorn, M. Kopp, A. M. Frame, and P. Nosil. Magic traits in speciation: magic but not rare? *Trends in Ecology & Evolution*, 26(8):389–397, 2011. ISSN 0169-5347. doi: 10.1016/j.tree.2011.04.005.

K. S. Sheldon, R. B. Huey, M. Kaspari, and N. J. Sanders. Fifty Years of Mountain Passes: A Perspective on Dan Janzens Classic Article. *The American Naturalist*, 191(5):553–565, 2018. ISSN 0003-0147. doi: 10.1086/697046.

A. J. Shultz, A. J. Baker, G. E. Hill, P. M. Nolan, and S. V. Edwards. SNPs across time and space: population genomic signatures of founder events and epizootics in the House Finch (Haemorhous mexicanus). *Ecology and Evolution*, 6(20):7475–7489, 2016. ISSN 2045-7758. doi: 10.1002/ece3.2444.

H. Slabbekoorn and T. B. Smith. Habitat-Dependent Song Divergence in the Little Greenbul: An Analysis of Environmental Selection Pressures on Acoustic Signals. *Evolution*, 56(9): 1849–1858, 2002. ISSN 0014-3820.

L. Smeds, A. Qvarnstrm, and H. Ellegren. Direct estimate of the rate of germline mutation in a bird. *Genome Research*, 26(9):1211–1218, 2016. ISSN 1088-9051. doi: 10.1101/gr.204669.116.

B. T. Smith, J. E. McCormack, A. M. Cuervo, M. J. Hickerson, A. Aleixo, C. D. Cadena, J. Prez-Emn, C. W. Burney, X. Xie, M. G. Harvey, B. C. Faircloth, T. C. Glenn, E. P. Derryberry, J. Prejean, S. Fields, and R. T. Brumfield. The drivers of tropical speciation. *Nature*, 515(7527):406–409, 2014. ISSN 1476-4687. doi: 10.1038/nature13687.

B. T. Smith, G. F. Seeholzer, M. G. Harvey, A. M. Cuervo, and R. T. Brumfield. A latitudinal phylogeographic diversity gradient in birds. *PLOS Biology*, 15(4):e2001073, 2017. ISSN 1545-7885. doi: 10.1371/journal.pbio.2001073.

J. M. Smith. Sympatric Speciation. *The American Naturalist*, 100(916):637–650, 1966. ISSN 0003-0147.

P. S. Soltis and D. E. Soltis. Ancient DNA: Prospects and limitations. *New Zealand Journal of Botany*, 31(3):203–209, 1993.

V. Sousa and J. Hey. Understanding the origin of species with genome-scale data: modelling gene flow. *Nature Reviews Genetics*, 14(6):404–414, 2013. ISSN 1471-0064. doi: 10.1038/nrg3446.

A. Stamatakis. RAxML version 8: a tool for phylogenetic analysis and post-analysis of large phylogenies. *Bioinformatics*, 30(9):1312–1313, 2014. ISSN 1367-4803. doi: 10.1093/bioinformatics/btu033.

J. L. Strasburg and L. H. Rieseberg. Molecular Demographic History of the Annual Sunflowers Helianthus Annuus and H. Petiolaris—Large Effective Population Sizes and Rates of Long-Term Gene Flow. *Evolution*, 62(8):1936–1950, 2008. ISSN 1558-5646. doi: 10.1111/j.1558-5646.2008.00415.x.

J. L. Strasburg and L. H. Rieseberg. Interpreting the estimated timing of migration events between hybridizing species. *Molecular Ecology*, 20(11):2353–2366, 2011. ISSN 1365-294X. doi: 10.1111/j.1365-294X.2011.05048.x.

K. F. Stryjewski and M. D. Sorenson. Mosaic genome evolution in a recent and rapid avian radiation. *Nature Ecology & Evolution*, 1(12):1912, 2017. ISSN 2397-334X. doi: 10.1038/s41559-017-0364-7.

T. Suchan, C. Pitteloud, N. S. Gerasimova, A. Kostikova, S. Schmid, N. Arrigo, M. Pajkovic, M. Ronikier, and N. Alvarez. Hybridization Capture Using RAD Probes (hyRAD), a New Tool for Performing Genomic Analyses on Collection Specimens. *PLOS ONE*, 11(3):e0151651, 2016. ISSN 1932-6203. doi: 10.1371/journal.pone.0151651.

R. C. Team. R: A language and environment for statistical computing., 2018. URL `https://www.R-project.org/`.

J. Terborgh and J. S. Weske. The Role of Competition in the Distribution of Andean Birds. *Ecology*, 56(3):562–576, 1975. ISSN 1939-9170. doi: 10.2307/1935491.

J. Terhorst, J. A. Kamm, and Y. S. Song. Robust and scalable inference of population history from hundreds of unphased whole-genomes. *Nature Genetics*, 49(2):303–309, 2017. ISSN 1061-4036. doi: 10.1038/ng.3748.

J. Thioulouse and S. Dray. Interactive Multivariate Data Analysis in R with the ade4 and ade4tkgui Packages. *Journal of Statistical Software*, 22(1):1–14, 2007. ISSN 1548-7660. doi: 10.18637/jss.v022.i05.

D. L. Toews, S. Taylor, R. Vallender, A. Brelsford, B. Butcher, P. Messer, and I. Lovette. Plumage Genes and Little Else Distinguish the Genomes of Hybridizing Warblers. *Current Biology*, 26(17):2313–2318, 2016. ISSN 0960-9822. doi: 10.1016/j.cub.2016.06.034.

D. P. L. Toews, L. Campagna, S. A. Taylor, C. N. Balakrishnan, D. T. Baldassarre, P. E. Deane-Coe, M. G. Harvey, D. M. Hooper, D. E. Irwin, C. D. Judy, N. A. Mason, J. E. McCormack, K. G. McCracken, C. H. Oliveros, R. J. Safran, E. S. C. Scordato, K. F. Stryjewski, A. Tigano, J. A. C. Uy, and B. M. Winger. Genomic approaches to understanding population divergence and speciation in birds. *The Auk*, 133(1):13–30, 2015. ISSN 0004-8038, 1938-4254. doi: 10.1642/AUK-15-51.1.

G. Turesson. The Plant Species in Relation to Habitat and Climate. *Hereditas*, 6(2):147–236, 1925. ISSN 1601-5223. doi: 10.1111/j.1601-5223.1925.tb03139.x.

S. Via. Natural selection in action during speciation. *Proceedings of the National Academy of Sciences*, 106(Supplement 1):9939–9946, 2009. ISSN 0027-8424, 1091-6490. doi: 10.1073/pnas.0901397106.

S. Via. Divergence hitchhiking and the spread of genomic isolation during ecological speciation-with-gene-flow. *Philosophical Transactions of the Royal Society B: Biological Sciences*, 367(1587):451–460, 2012. doi: 10.1098/rstb.2011.0260.

H. K. Voris. Maps of Pleistocene sea levels in Southeast Asia: shorelines, river systems and time durations. *Journal of Biogeography*, 27(5):1153–1167, 2000. ISSN 1365-2699. doi: 10.1046/j.1365-2699.2000.00489.x.

J. A. Vucetich, T. A. Waite, and L. Nunney. Fluctuating Population Size and the Ratio of Effective to Census Population Size. *Evolution*, 51(6):2017–2021, 1997. ISSN 1558-5646. doi: 10.1111/j.1558-5646.1997.tb05123.x.

B. S. Vuilleumier. Pleistocene changes in the fauna and flora of South america. *Science*, 173 (3999):771–780, 1971. ISSN 0036-8075. doi: 10.1126/science.173.3999.771.

M. Wagner. *The Darwinian theory and the law of the migration of organismus: Translated from the german of Moritz Wagner by James L. Laird*. Edward Stanford, 1873.

P. Wandeler, P. E. A. Hoeck, and L. F. Keller. Back to the future: museum specimens in population genetics. *Trends in Ecology & Evolution*, 22(12):634–642, 2007. ISSN 0169-5347. doi: 10.1016/j.tree.2007.08.017.

J. Wang. Application of the One-Migrant-per-Generation Rule to Conservation and Management. *Conservation Biology*, 18(2):332–343, 2004. ISSN 1523-1739. doi: 10.1111/j.1523-1739.2004.00440.x.

W. C. Warren, D. F. Clayton, H. Ellegren, A. P. Arnold, L. W. Hillier, A. Knstner, S. Searle, S. White, A. J. Vilella, S. Fairley, A. Heger, L. Kong, C. P. Ponting, E. D. Jarvis, C. V. Mello, P. Minx, P. Lovell, T. A. F. Velho, M. Ferris, C. N. Balakrishnan, S. Sinha, C. Blatti, S. E. London, Y. Li, Y.-C. Lin, J. George, J. Sweedler, B. Southey, P. Gunaratne, M. Watson, K. Nam, N. Backström, L. Smeds, B. Nabholz, Y. Itoh, O. Whitney, A. R. Pfenning, J. Howard, M. Völker, B. M. Skinner, D. K. Griffin, L. Ye, W. M. McLaren, P. Flicek, V. Quesada, G. Velasco, C. Lopez-Otin, X. S. Puente, T. Olender, D. Lancet, A. F. A. Smit, R. Hubley, M. K. Konkel, J. A. Walker, M. A. Batzer, W. Gu, D. D. Pollock, L. Chen, Z. Cheng, E. E. Eichler, J. Stapley, J. Slate, R. Ekblom, T. Birkhead, T. Burke,

D. Burt, C. Scharff, I. Adam, H. Richard, M. Sultan, A. Soldatov, H. Lehrach, S. V. Edwards, S.-P. Yang, X. Li, T. Graves, L. Fulton, J. Nelson, A. Chinwalla, S. Hou, E. R. Mardis, and R. K. Wilson. The genome of a songbird. *Nature*, 464(7289):757–762, 2010. ISSN 1476-4687. doi: 10.1038/nature08819.

D. S. Weber, B. S. Stewart, J. C. Garza, and N. Lehman. An empirical genetic assessment of the severity of the northern elephant seal population bottleneck. *Current Biology*, 10 (20):1287–1290, 2000. ISSN 0960-9822.

J. T. Weir and D. Schluter. Ice sheets promote speciation in boreal birds. *Proceedings of the Royal Society B: Biological Sciences*, 271(1551):1881–1887, 2004. doi: 10.1098/rspb.2004.2803.

P. Wiersma, A. Muoz-Garcia, A. Walker, and J. B. Williams. Tropical birds have a slow pace of life. *Proceedings of the National Academy of Sciences*, 104(22):9340–9345, 2007. ISSN 0027-8424, 1091-6490. doi: 10.1073/pnas.0702212104.

E. O. Wilson. Some Ecological Characteristics of Ants in New Guinea Rain Forests. *Ecology*, 40(3):437–447, 1959. ISSN 1939-9170. doi: 10.2307/1929761.

B. M. Winger and J. M. Bates. The tempo of trait divergence in geographic isolation: Avian speciation across the Maraon Valley of Peru. *Evolution*, 69(3):772–787, 2015. ISSN 1558-5646. doi: 10.1111/evo.12607.

J. M. Wójcik, A. Kawalko, S. Marková, J. B. Searle, and P. Kotlík. Phylogeographic signatures of northward post-glacial colonization from high-latitude refugia: a case study of bank voles using museum specimens. *Journal of Zoology*, 281(4):249–262, 2010. ISSN 1469-7998. doi: 10.1111/j.1469-7998.2010.00699.x.

Y. Zhen, R. J. Harrigan, K. C. Ruegg, E. C. Anderson, T. C. Ng, S. Lao, K. E. Lohmueller, and T. B. Smith. Genomic divergence across ecological gradients in the Central African

rainforest songbird (Andropadus virens). *Molecular Ecology*, 26(19):4966–4977, 2017. ISSN 1365-294X. doi: 10.1111/mec.14270.

VITA

Ethan Linck was born in Saratoga Springs, New York. Growing up, he lived primarily in Vermont, with stints elsewhere in upstate New York, in New Hampshire, and in Tucson, Arizona. His time in Tucson—where he was captivated to learn jaguars and trogons occasionally ranged in the nearby Santa Ritas—was a particular influence on his decision to become a biologist. He was also encouraged by his parents Bob and Leanne, their love of the outdoors, and their careers as conservationists. An independent trip to Papua New Guinea at 17 sealed the deal, and he decided to attend Reed College in Portland, OR on the basis of its strength in the sciences as much as its desireable location. Completing a B.A. in Biology, he completed fieldwork on avian population biology in Oregon, the Mariana Islands, and Costa Rica, and wrote his undergraduate thesis (supervised by Dr. Sarah Schaack) on the phylogeography of a species of white-eye found on small coral atolls across Melanesia. He continued this research with his external advisor Dr. Jack Dumbacher at the California Academia of Sciences after graduation, before moving to the town of Gothic, Colorado. There, he spent a winter snowbound as a caretaker at the Rocky Mountain Biological Laboratory, backcountry skiing every day and applying to graduate school. Joining John Klicka's lab at University of Washington, he fell in love with collecting and specimen preparation on long roadtrips across the inland Northwest, discovered a deep interest in population genetics, got married, and and skied off a few volcanoes. He also began writing about humans, science, and nature for a popular audience, with essays and hot takes appearing in *The Los Angeles Review of Books, High Country News*, and *Slate.* (Ask him about his assignment for that last magazine over beers.) He's heading to conduct postdoctoral work with Dr. Kimberly Sheldon and Dr. Chris Witt at University of Tennessee and University of New Mexico, respectively, and is grateful to continue working as a scientist.